TARGETED DRUG DELIVERY TO LEUKOCYTES WITH ICAM-1

DERIVED PEPTIDES

By

Sumit Majumdar

B.S. Pharmaceutical Technology, Jadavpur University, 2000
M.S. Industrial Pharmacy, the University of Toledo, 2003
M.S. Pharmaceutical Chemistry, the University of Kansas, 2006

Submitted to the Department of Pharmaceutical Chemistry and the Faculty of the Graduate School of the University of Kansas in partial fulfillment of the requirements for the degree of Doctor of Philosophy.

Dissertation Committee:

_____

Chairperson Teruna J. Siahaan

_____

Kenneth L. Audus

_____

Jeffrey P. Krise

_____

Cory J. Berkland

_____

Sunil A. David

Dissertation Defended on June 24, 2008

The Dissertation Committee for Sumit Majumdar certifies

that this is the approved version of the following dissertation:

TARGETED DRUG DELIVERY TO LEUKOCYTES WITH ICAM-1 DERIVED PEPTIDES

Dissertation Committee:

_____

Chairperson Teruna J. Siahaan

_____

Kenneth L. Audus

_____

Jeffrey P. Krise

_____

Cory J. Berkland

_____

Sunil A. David

Date approved: June 24, 2008

Targeted drug delivery to leukocytes with ICAM-1 derived peptides

Sumit Majumdar

The University of Kansas, 2008

Intercellular adhesion molecule-1 (ICAM-1) derived cyclic peptide cIBR [cyclo(1,12)PenPRGGSVLVTGC] showed high affinity for leukocyte function associated antigen-1 (LFA-1) receptor and was internalized into the MOLT-3 T-cells. Therefore, the objective of the dissertation was to explore the possibility of selectively delivering drugs to leukocytes using ICAM-1 derived peptides. Fluorescein isothiocyanate conjugated cIBR (FITC-cIBR) and doxorubicin conjugated cIBR (DOX-cIBR) entered the HL-60 cells by receptor mediated endocytosis and passive diffusion, respectively. High hydrophobicity of DOX-cIBR was proposed to be responsible for its energy-independent entry (chapter 2). To check the effect of hydrophobicity on internalization, two relatively more hydrophilic cIBR-derived peptides were conjugated to DOX. However, both the DOX-peptide conjugates were internalized passively (chapter 3). Degradation mechanism of methotrexate conjugate of cIBR (MTX-cIBR) was studied and suitable formulation conditions were developed. Stability of MTX-cIBR was assessed with *in vitro* biological matrices to determine optimum dosing regimen for *in vivo* studies (chapter 4).

Dedicated to:

My parents

Pratima Majumdar and Narayan Chandra Majumdar

My sister

Sudipa Majumdar

My brother

Sourav Majumdar

Acknowledgements

I would like to thank my advisor Dr. Teruna J. Siahaan for his tremendous support and guidance during the past five years. I have been inspired to watch his involvement with students. I always had access to his office to discuss any issue related to research. Most importantly, I had the freedom to make a decision regarding research and discuss with him. It helped me to become more independent as a researcher. He encouraged me to strive for perfection. I will always remember his contribution to help me grow as a person.

I want to express my gratitude to Dr. Jeffrey P. Krise. He helped me a lot in my research with his expertise. He was always helpful and allowed me to use his instruments whenever I needed. It has been a very good experience to get an opportunity to work with him.

I would like to thank my dissertation committee members Dr. Kenneth L Audus, Dr. Cory J. Berkland, Dr. Jeffrey P. Krise and Dr. Sunil A. David. I want to take this opportunity to thank Dr. Cory J. Berkland and Dr. Jeffrey P Krise for the comments and suggestions as readers of this dissertation.

I want convey my thanks to Dr. Naoki Kobayashi, a former post doctoral researcher in our group. Naoki was instrumental in teaching me a lot of different aspects of research. He helped me to think analytically and taught me to be patient. I will always remember the great experience of working with him.

I am thankful to Dr. Todd Williams for his help with mass spectrometric analysis experiments. I also want to thank Dr. David Moore for his help with the

microscopic observation studies. Dr. Debbie Galinis was my mentor during my internship at Cephalon, Inc. I want to thank her for her help with some of the mass spectrometric analysis studies. I want to thank the members of Krise group for their help with the instruments. They have always been very helpful. I want to thank Kwame for his help with stability studies.

I want to thank Dr. Bimo Tejo and Dr. Tatyana Yakovleva for their help in my research. It has been a wonderful experience to work with Prakash, Barlas, Maulik, Kai, Ahmed, Emma, Paul, and Kevin. I want to thank them all for creating a very good work environment in our group. We all have mutual respect and admiration for each other and that has helped me a lot to focus only on the research aspect without any distraction.

In Lawrence I have made new friends and few of my old friends moved here to pursue higher studies. Some of these friends have become very close and we have tried to look after each other through thick and thin. It would have been really difficult to spend these five years here without Sandipan, Vaswati, Rashida, Deb and Mrinal. They were there whenever I needed any help. I will cherish the memories of these days and look forward to many more years of friendship.

Finally, I want to thank my family members. I owe everything I am today to my mom, Mrs. Pratima Majumdar and my dad, Mr. Narayan Majumdar. They went through lots of hardship to send me to USA for higher studies. Without their support I could not do it. My siblings Sudipa Majumdar and Sourav Majumdar are my best friends. We share a strong bonding with each other and I want to thank them for their

support. Last, I want to thank Tania for her moral support and encouragement during the last few very stressful months. She has taught me to be positive in any circumstances and prevented me from giving up.

Table of Contents

Chapter 1

Chapter 2

Chapter 3

Chapter 4

Chapter 5

Chapter 1

Peptide-mediated targeted drug delivery

1.1 Introduction

Targeted drug delivery methods to improve drug efficacy and lower side effects by directing the drug to a specific cell type have been explored. To date, many strategies have been investigated to accomplish this goal, and some of these strategies rely on the differences between the cellular compositions of the targeted cells and those of the non-targeted cells. These differences could be in the expressed surface receptors (i.e., the absence or presence of certain receptors), the metabolism profiles (i.e., different enzyme expression or intracellular trafficking), the site/location of the cells (i.e., circulating in blood stream vs. organ), and the nature of the cells (i.e., normal vs. cancerous). For example, tumor cells have certain upregulated receptors, enzymes, and other metabolic features that are not present in normal cells in the body. These differences can be used to discriminate the delivery of a drug to diseased cells rather than to normal cells. Furthermore, the differences in cellular trafficking profiles and the pH of endosomes between normal and cancer cells have also been exploited for selective drug delivery to a specific compartment in the intracellular space of cancer vs. normal cells.[1]

Peptides (e.g., Arg-Gly-Asp (RGD) peptides,[2] poly-Arg peptides,[3,4] proteins (e.g., antibodies,[5] transport proteins, and transferrin[6]), and small molecules (e.g., folate[7]) have been used to selectively direct drugs to cancer cells with upregulated receptors by forming drug-carrier conjugates (Figure 1.1). However, none of the drug-peptide

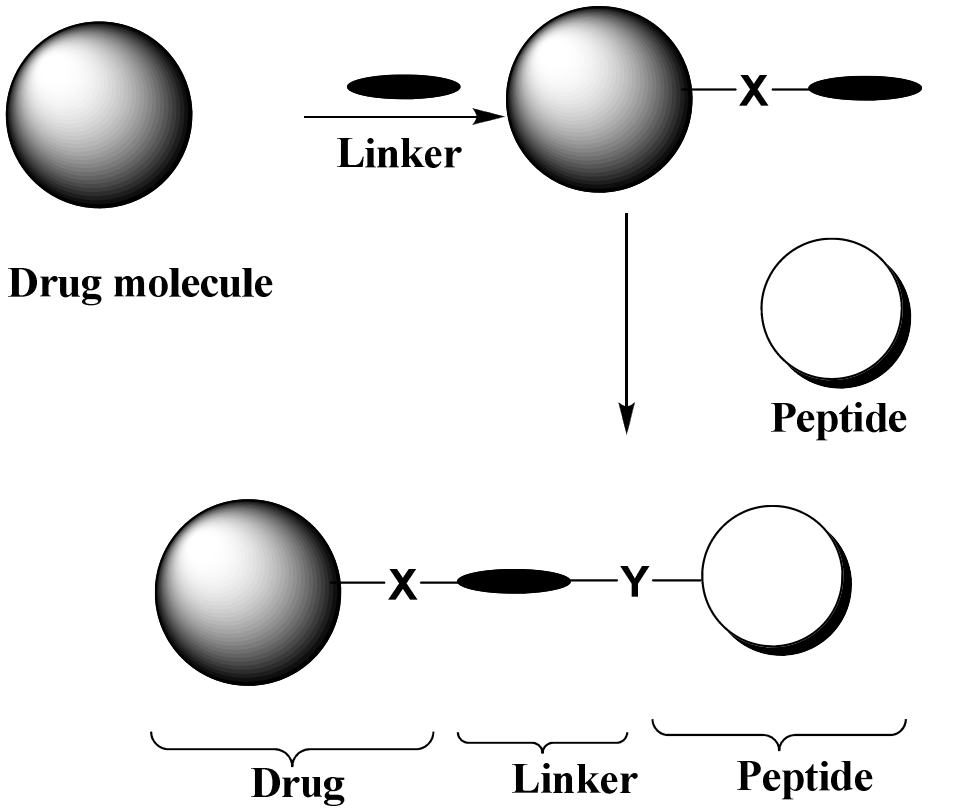

X and Y can be similar or different functionalities
Some possibilities for X or Y can be

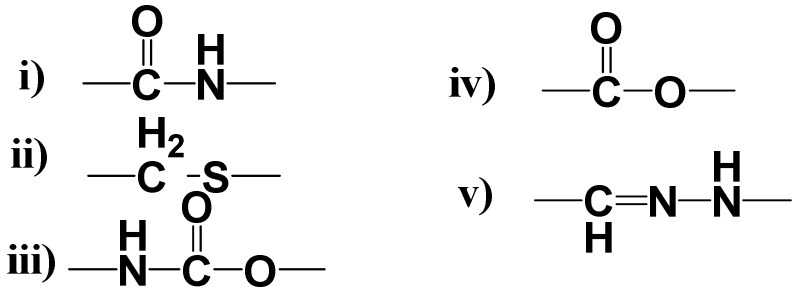

Figure 1.1 The structure of a drug-linker-peptide conjugate. X and Y represent the common functional groups used to connect either the drug or the peptide to the linker. X may be similar to or different than Y. Here, the primary focus is on the nature of the X bond, and the drug peptide conjugation chemistry has been classified according to the nature of the X bond: i) amide, ii) thioether, iii) carbamate ester, iv) carboxylic acid ester, and v) hydrazone bond.

conjugates has successfully reached the market; this may be due to various factors, including (a) the difficulty in developing the appropriate ligand for the targeted receptor(s) on the cell surface, (b) the lack of understanding of the receptor recycling and trafficking mechanisms, (c) insufficient information on the mechanisms of uptake and disposition of the ligand inside the cells, (d) a lack of understanding of the pharmacokinetic and pharmacodynamic profiles of the drug-peptide conjugate, and (e) the limited number of systematic studies on the relationships between the physicochemical and transport properties of the conjugates. Thus, there is a need to study these aspects of the drug-peptide conjugates to increase the probability of success of these molecules in clinical settings. Ideally, conjugation of the drug to the targeting peptide should not interfere with the recognition of the peptide by its receptor(s). In addition, the pharmacologic or cytotoxic property of the drug should be maintained when the drug is conjugated to the carrier molecules.

This review illustrates the chemistry, biology, and utilization of small drug-peptide conjugates for selectively delivering the drugs to a specific group of cells (Figure 1.1). The first section discusses the attributes of an ideal peptide carrier and the drug. Emphasis will be placed on cyclic peptides and their possible conjugation sites. The second section explores the chemistry behind the drug-peptide conjugation via different types of chemical bonds, including carboxylic acid ester, amide, carbamate ester, hydrazone, and enzymatically-cleavable bonds. The presence of a spacer between the drug and the peptide carrier may be necessary to ensure recognition of the carrier by the receptor. The third section focuses on the families of

peptides that have been conjugated to drugs and their evaluation in *in vitro* and *in vivo* biological systems.

Drug-peptide conjugates are most often administered via the parenteral route because they cannot be efficiently delivered orally. The physicochemical properties of peptides (i.e., size, hydrophilicity, and hydrogen-bonding potential) make it difficult for them to cross the intestinal mucosal barriers. In addition, proteases on the surface of intestinal mucosa brush border membranes rapidly metabolize the peptide carrier into fragments. In parenteral delivery, the conjugates travel through the systemic circulation and are distributed to the small capillaries that carry them to the target cells. Upon peptide-receptor interaction, the conjugate can potentially undergo receptor-mediated endocytosis, in which the conjugate may move through the early and late endosomes and finally into the lysosome (Figure 1.2). The receptors are either separated from the conjugates in the early sorting endosomes or move to the lysosomes along with the conjugate. After separation from the conjugates, the receptors may be recycled onto the cell surface for the next round of transport. There is a significant drop in pH in the lysosome that may affect the binding between the conjugate and the receptor. It can also affect the linkage between the drug and the peptide (Figure 1.2). As an example, the transferrin receptors bind and carry the transferrin protein to transport iron into the cells and, after pH change in the endosomes, the transferrin releases iron and the receptor is recycled back to the cell surface.[8] The mechanisms of receptor uptake can occur via clathrin coat-[9] or caveolin-mediated endocytosis (i.e., CD11a/CD18).[10]

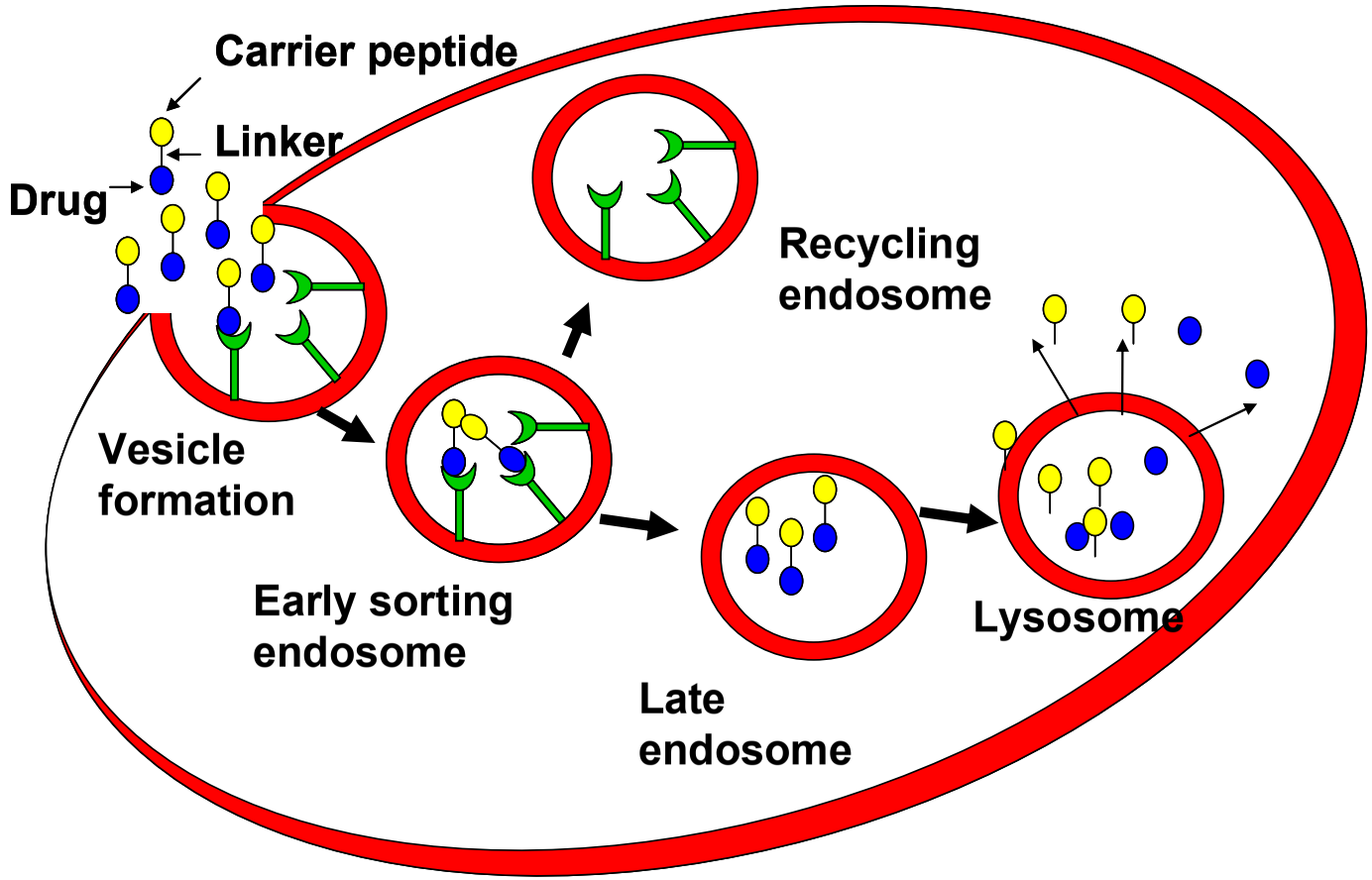

Figure 1.2 Hypothetical schematic of one possible cellular-internalization process for a drug-peptide conjugate. Drug-linker-peptide interacts with the cell surface receptor for internalization via receptor-mediated endocytosis. Early sorting endosomes may separate the receptor from the conjugate and recycle receptors to cell surface. The conjugate moves to cellular compartments with progressively lower acidity leading to separation of the drug from the carrier. The drug is then released into the cytoplasm to reach the target site for the drug

1.2 Drug-Peptide Conjugates

1.2.1 Peptide Carrier

There are several important requirements for using peptides as carrier molecules. First, the peptide should selectively bind to the cell surface receptors on the target cells. Second, the receptor should be expressed only on the target cells or the expression should be higher in the target cells than in the non-targeted cells. Third, the peptide carrier should be sufficiently stable in the systemic circulation to reach the target cells at an effective concentration. Fourth, selection of the site of conjugation on the peptide is critical for retaining its binding properties to the receptor because drug conjugation may impose a steric hindrance that interferes with receptor recognition.

Peptides as carriers may offer some advantages over proteins because peptides are relatively easy to modify for generating derivatives and to produce in large quantities. The drug-peptide conjugate is easier to analyze than a drug-protein conjugate. Due to the absence of tertiary structure in peptides, they often do not undergo physical degradation as do proteins. In addition, the number of drug molecules and their conjugation regioselectivity can be controlled; in contrast, it is difficult to control the number and regioselectivity of the conjugated drugs on a protein. Because the drugs are often conjugated to the side chains of reactive residues (e.g. Lys or Asp), the conjugates consist of a distribution of products with various numbers of drugs attached to various sites of individual protein molecules. Thus, the formation of the conjugates may be difficult to reproduce, and the resulting products

can also be difficult to analyze. In addition, peptide-drug conjugates may have lower immunogenicity than protein-drug conjugates.[11] The immunogenicity of protein-drug conjugates may arise from the presence of non-native protein conformers or protein aggregates upon drug conjugation.

1.2.1.1 Cyclic Peptides and Different Sites of Conjugation

In many cases, cyclic peptides have higher selectivity for the receptor than do the parent linear peptides because cyclic peptides have more restricted conformations. However, it is still possible that the formation of the cyclic peptide may force the adoption of an unfavorable conformation for binding to the receptor. Cyclic peptides are prepared by three different cyclization methods: (1) backbone-to-backbone, (2) backbone-to-side chain, and (3) side chain-to-side chain (Figure 1.3). The backbone-to-backbone cyclization is formed using an amide bond between the N- and C-termini (Conjugates 1 and 2). In this case, the side chain of Lys, Asp, or Glu is utilized as the conjugation point between the drug and the peptide (Conjugates 1 and 2). It is preferable that the amino acid for conjugation site should not be part of the receptor recognition sequence. The backbone-to-side chain cyclization is formed by connecting the N-terminus with the carboxylic acid side chain of Asp or Glu residue by an amide bond, and the drug is conjugated to the C-terminus of the peptide (Conjugate 3). Alternatively, the peptide C-terminus is linked to the side chain of the Lys residue, while the drug is conjugated to the N-terminus of the peptide (Conjugate 4). Finally, the side chain-to-side chain cyclization can be formed by using an amide

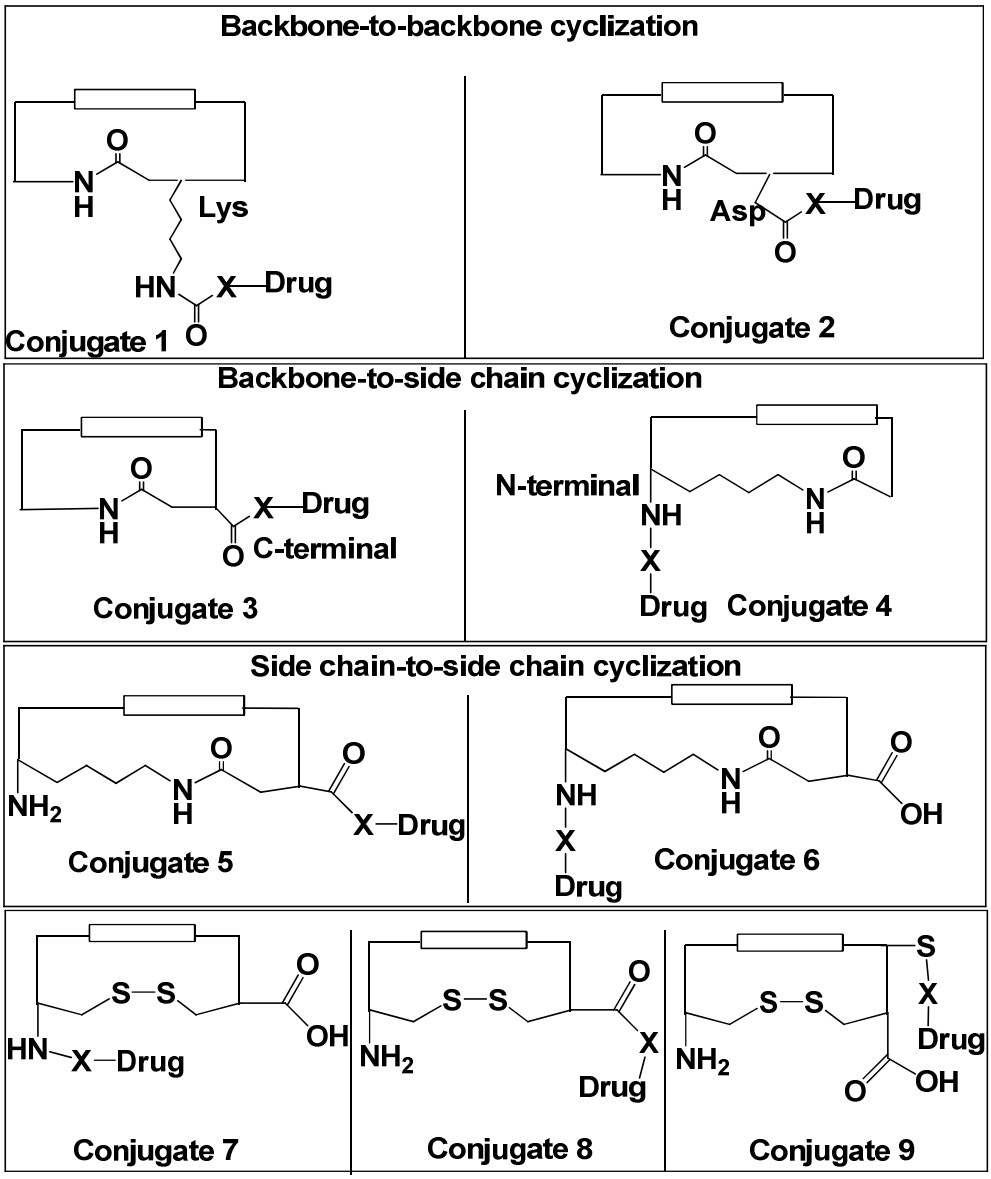

Figure 1.3 (a) Conjugates **1** and **2**: Cyclic peptides formed by backbone-to-backbone cyclization with side chains of Lys and Asp available for drug conjugation. **(b)** Conjugates **3** and **4**: Cyclic peptides formed by backbone-to-side chain cyclization. N- and C- termini of the peptide can be conjugated to the Asp and Lys side chains, respectively. Free C- and N-termini can then be conjugated to the drug. **(c)** Conjugates **5** and **6**: Cyclic peptides formed by side chain-to-side chain cyclization via amide bond. Side chains of Lys and Asp can be conjugated, and the free C- and N-termini can be used for drug conjugation. **(d)** Conjugates **7**, **8**, and **9**: Cyclic peptides formed by side chain-to-side chain cyclization. Cysteine side chains can be conjugated via disulfide bond. Free N-terminal, C-terminal and free Cys present in the sequence can be used for drug conjugation.

bond or a disulfide bond. A peptide bond between the Asp side chain and the amino group of a Lys residue produces a cyclic peptide with an open C- or N-terminus that can be utilized to conjugate the drug (Conjugates 5 and 6). A cyclic peptide is also made by linking the side chains of two Cys residues to make a disulfide bond and the drug is conjugated to either the N- (Conjugate 7) or C-terminus (Conjugate 8). A Cys residue can be inserted within the sequence of a cyclic peptide, and the thiol group of the Cys residue can be utilized for linking the drug to the peptide (Conjugate 9).

1.2.2 Examples of Drug Molecules

The drug molecules described here are classified as cytotoxic small molecules such as doxorubicin (DOX), methotrexate (MTX), and camptothecin (CPT). These molecules have side effects because they are taken up by both cancerous and normal cells. Due to the physicochemical properties of DOX and CPT, these drugs enter the cells via a passive diffusion mechanism by readily partitioning into the cell membranes. On the other hand, methotrexate (MTX) enters the cell using uptake transporters such as reduced folate carrier (RFC) and membrane folate binding protein (MFBP).[12] The selectivity of MTX for cancer cells over normal cells occurs because cancer cells have upregulated expression of MFBP. Nonetheless, MTX can still be internalized by normal cells to produce side effects. Thus, conjugation of any of these drugs (i.e., DOX, CPT, or MTX) to a peptide carrier may direct them to a specific population of cells and lower the drug side effects. As in peptides, the site of conjugation on the drug molecule is an important consideration for maintaining the

drug activity. If the conjugation has to be done at the active functional group, a cleavable prodrug moiety may be used to link the drug to the peptide so that the free drug can be released from the carrier. One potential drawback of using a labile linker is that the drug may be released prematurely before reaching the target cells.

1.2.2.1 Doxorubicin (DOX)

DOX is widely used as a model drug for conjugation to different carriers such as peptides, antibodies,[13,14] polymers,[15,16] proteins,[17,18] and polymer beads.[19] The primary mechanism of action of DOX is DNA-intercalation and inhibition of topoisomerase II during DNA synthesis.[20] DOX can also exert cell toxicity through the generation of hydrogen peroxide, which damages the membranes of mitochondria.[21] For its activity as a DNA intercalator, it is necessary for the DOX molecule to enter the nucleus; ideally, the targeting system should carry the drug into the nucleus. However, conjugation of DOX to the carrier peptide may prevent DOX from entering the nucleus.[22] To overcome this problem, DOX has been conjugated to the carrier through a cleavable linker, which allows the drug to be released from the conjugate.

Several functional groups on the DOX molecule have been used for conjugation to the carrier molecules. The primary amine of the sugar moiety can be directly linked to a carboxylic acid group of the C-terminal or the Asp side chain on the peptide carrier. To provide a spacer between the DOX and the peptide carrier, the amino group is reacted with succinic or glutaric anhydride to give a product with a free

carboxylic acid group, which can be linked to a free amino group on the peptide. The primary alcohol at the C14 of DOX has been linked to a carboxylic acid group on the carrier molecule via an ester bond. The C13 ketone group on DOX is also reacted to hydrazine to form a hydrazone spacer that is linked to the peptide carrier.

1.2.2.2 Methotrexate (MTX)

Many studies have been done to conjugate MTX to different carriers for improving its delivery and efficacy. This drug is used for the treatment of rheumatoid arthritis and several different carcinomas, including acute lymphocytic leukemia, lymphomas, and choriocarcinoma. The effectiveness of this drug depends on the efficiency of the active transporters on the target cell. One of the mechanisms of action of MTX is inhibition of the activity of dihydrofolate reductase (DHFR) enzyme that subsequently blocks thymidine synthase for DNA synthesis. In addition, the MTX is trapped inside the cell by forming MTX polyglutamate adducts. In many cases of cancer therapy, MTX therapy is ineffective at low doses; at high doses this drug is effective but generates side effects due to its cytotoxicity to normal cells.

Targeting of MTX using antibodies and peptides has been explored to increase its effectiveness.[23] The MTX molecule is conjugated to the carrier molecule through the γ-carboxylic acid group of the glutamic acid residue to maintain its activity.[24] The α-carboxylic acid of MTX is necessary for binding to DHFR; thus, conjugation via the α-carboxylic acid is not desirable. To conjugate MTX to the carrier molecule, the α-carboxylic acid of the Glu residue is protected to give MTX-α-OtBu. After coupling

of the γ-carboxylic acid with the N-terminal of the peptide carrier, the tertiary-butyl protecting group can be removed to give the desired conjugate. [24]

1.3 Chemistry of Drug-Peptide Conjugation

Different approaches have been used to conjugate carrier peptides to cytotoxic drugs. The chemistry of conjugation has a profound impact on the stability of the conjugate. Each functional group to link the peptide and the drug has both advantages and disadvantages. Thus, this section explores common conjugation methods that have been used to make drug-peptide conjugates. The chemical bonds between the drug and the spacer will be discussed. The same chemical bonds are normally used to link the spacer and the peptide carrier or to link the drug directly to the peptide without a spacer.

1.3.1 Amide Bond

Drug-peptide conjugation via an amide bond is carried out by linking the carboxylic acid of the drug and primary amine of the spacer/peptide. The chemistry of the amide bond formation is straightforward, and the bond has relatively high chemical stability. Because the enzymatic cleavage of the amide bond between the drug and the peptide may be slow, there is a high probability that the conjugate will reach the target site with minor degradation. In this case, the drug portion of the conjugate may be active while it is attached to the peptide carrier. If the drug is attached through a functional group that is necessary for its activity, a cleavable

promoiety can be incorporated between the drug and the peptide, by which the drug can be released from the carrier peptide by pH change or enzymatic reaction (i.e., esterase). For amide bond formation, the carboxylic acid on the spacer, peptide, or the drug can be activated with O-benzotriazole-N,N,N′,N′-tetramethyl-uronium-hexafluoro-phosphate (HBTU) or a mixture of 1-ethyl-3-(3-dimethylaminopropyl) carbodiimide hydrochloride (EDC) and N-hydroxybenzotriazole (HOBT). The activated carboxylic acid is then reacted with an amine group of the counterpart (i.e., drug or peptide) in the presence of strong base (i.e., diisopropylethylamine or triethylamine) in different solvents, including dimethylformamide (DMF) or dimethylsulfoxide (DMSO) to give the desired conjugate.

DOX has been conjugated to different peptides, including cIBR [cyclo(1,12)PenPRGGSVLVTGC],[25] human calcitonin (hCT)-derived peptides,[26] and Vectocell peptides using an amide bond.[27] For conjugation to cIBR peptide, the DOX was modified to DOX-hemisuccinate by reacting the amino group of DOX with succinic anhydride to generate free carboxylic acid (Figure 1.4, pathway a). The free carboxylic acid of DOX-hemisuccinate was activated and reacted with the N-terminus of cIBR peptide to produce DOX-cIBR conjugate. The *in-vitro* stability of DOX-cIBR in human promyelocytic HL-60 cells showed that DOX-cIBR conjugate was stable; only 15% degradation was observed over a 24-h period, indicating the high stability of the amide conjugation method.[25] DOX was also conjugated to human calcitonin (hCT(9–32); **C**LGTYTQDFNKFHTFPQTAIGVGAP-NH_2) through a

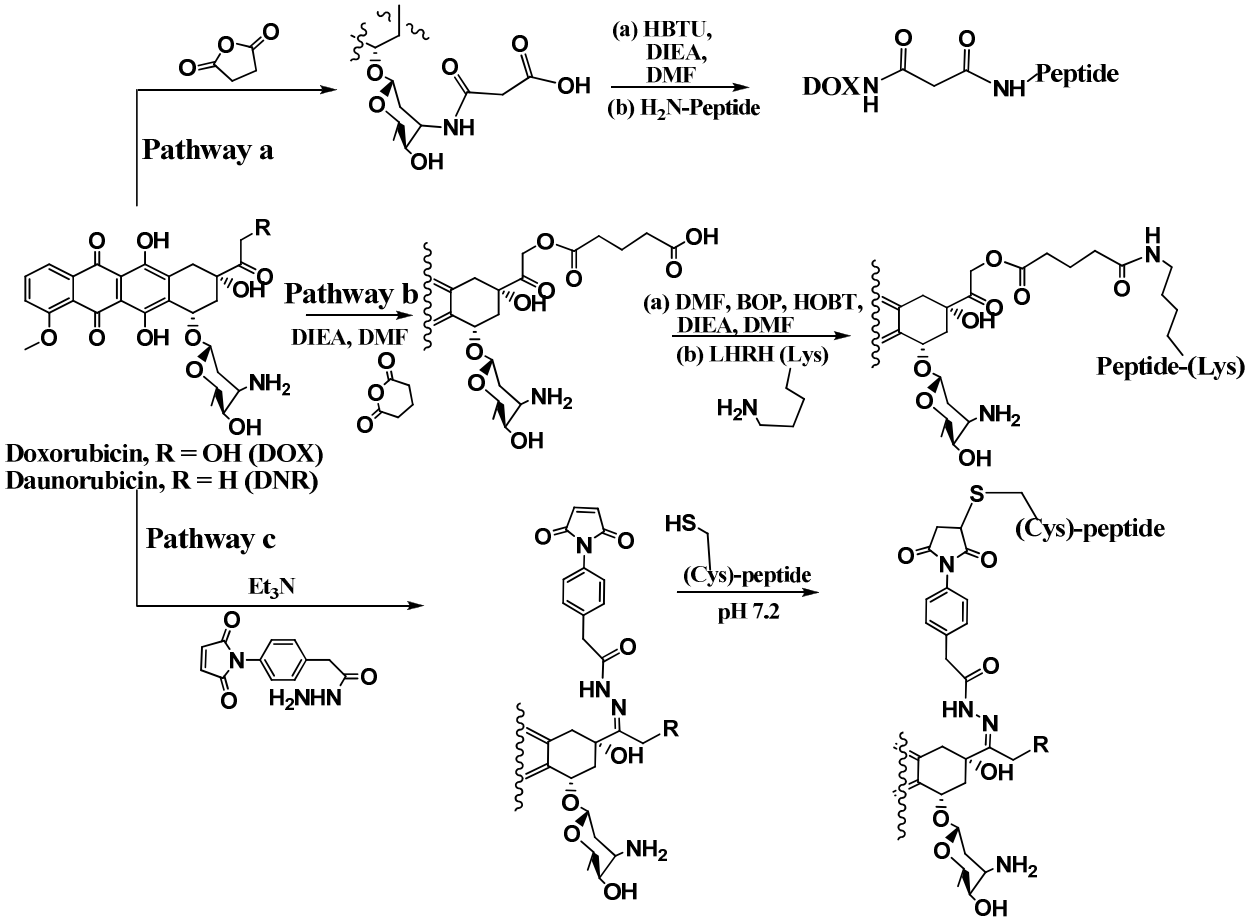

Figure 1.4 Different conjugation strategies are used to attach drug to peptide via linker. DOX and DNR are selected here as the drugs of choice. Pathway **(a)** shows the amide bond formation approach between the drug and the linker-peptide (ref 23). Pathway **(b)** depicts the carboxylic acid ester bond formation strategy between the drug and the linker-peptide (ref 27). Pathway **(c)** shows the hydrazone bond formation approach between the drug and the linker-peptide (ref 32)

maleimido-benzoic acid spacer. The amino group of DOX formed an amide bond with the carboxyl group of the maleimido-benzoic acid spacer. Then, nucleophilic attack of the double bond of the maleimide group by the thiol of the Cys1 residue on hCT(9–32) peptide produced the desired conjugate.[26] A similar approach was used for conjugation of DOX to Vectocell peptides (i.e., CVKRGLKLRHVRPRVTRMDV and SRRARRSPRHLGSGC) by amide bond formation with the carboxylic acid group of maleimidobutyric acid.[27]

1.3.2 Carboxylic Acid Ester Bond

The ester linkage is commonly used to conjugate drug to peptide because it can be hydrolyzed chemically or enzymatically (i.e., esterase) to release the drug. However, due to the instability of the ester bond, the drug may be released before reaching the target tissues. Different analogs of luteinizing hormone-releasing hormone (LHRH) peptide were conjugated via an ester bond to various cytotoxic agents, including DOX and its derivatives. To conjugate DOX to LHRH peptide (Glp-HWSYkLRPG-NH_2), C14 of DOX was modified with glutaric ester and the other carboxylic acid of the glutarate was linked to the side-chain amino group of D-Lys on LHRH peptide to give DOX-LHRH conjugate (Figure 1.4, pathway b).[28,29] The DOX-LHRH was quite stable in biological media and retained the cytotoxic property of DOX while maintaining its binding affinity to pituitary LHRH receptors.[30,31] The C14 position of DOX was also conjugated via a glutaric acid spacer to the cyclic peptide CNGRC using an ester bond to target the aminopeptidase N/CD13 receptor on the cell

surface.[28] In this case, the stability of DOX-CNGRC conjugate was dependent on the incubation matrix, which suggests that the DOX might be released before reaching the target tissue.[32] Thus, it is necessary to evaluate the stability of the ester drug-peptide conjugate in different biological matrices to ensure that the conjugate will reach the target tissue before releasing the drug component.

1.3.3 Hydrazone Bond

A hydrazone linkage can be utilized as an acid-labile bond for releasing the drug molecule from the conjugate upon a decrease in pH in tumor extracellular environments and in the lysosomes. Daunorubicin (DNR) and DOX with a ketone functional group at C-13 were derivatized with hydrazine maleimido spacers (i.e., *m*-maleimidobenzoic acid hydrazine or *p*-maleimidophenylacetic acid hydrazine) to give hydrazide intermediates (Figure 1.4 pathway c). These maleimide intermediates were reacted with the thiol group of the Cys residue in neuropeptide Y (YPSKPDNPGEDAPA**C**DLARYYSALRHYINLITRQRY-NH_2 or NPY) to give the respective conjugates.[33] The presence of an aromatic ring on the spacer provided the possibility to regulate the stability of the hydrazone bond.[33] This hydrazone linker released less than 10% of the free drug at pH 7.4 compared to 35–40% at pH 5.0 over a 24-h period. In contrast, the amide bond linkage showed very little drug released at either pH value.[34] Using the hydrazide bond, DOX was also conjugated to thermally responsive elastin-like-polypeptide (ELP) in an effort to utilize the enhanced

permeability and retention (EPR) effect;[35] the optimum release kinetics were controlled by changing the length and hydrophobicity of the spacer.[36]

1.3.4 Enzymatically Cleavable Bond

For enzymatic release of the drug, a specific peptide sequence may be utilized as a cleavable spacer between the drug and the carrier. One of the most widely used spacer sequences is a specific peptide substrate for the prostate-specific-antigen (PSA), a serine protease enzyme that is expressed at high levels by prostate tumors.[37] PSA is known to mediate hydrolysis of semenogelin-I with high specificity by cleaving the peptide bond between Gln349 and Ser350.[38-40] After mutation studies, several peptide sequences were specifically cleaved by PSA at the Gln-Ser or Gln-Leu peptide bond; thus, two peptide spacers (Glutaryl-Hyp-Ala-Ser-Chg-Gln-Ser-Leu-OH[40] and Mu-His-Ser-Ser-Lys-Leu-Gln[41]) were used to link between DOX and the carrier peptide (Figure 1.5, pathways a and b). These conjugates were highly toxic due to the release of Leu-DOX and DOX (Figure 1.5, pathways a and b).[40,41] Leu-DOX had cytotoxicity against cancer cell lines with fewer side effects such as cardiac toxicity.[42] It is noted that the direct conjugation of the amino group of DOX to Gln carboxylic acid (i.e., without the Ser or Lue residue at the C-terminal) failed to release free DOX by hydrolysis. It was also suggested that the presence of the carrier peptide might affect the specificity of the spacer for the proteolytic enzymes.

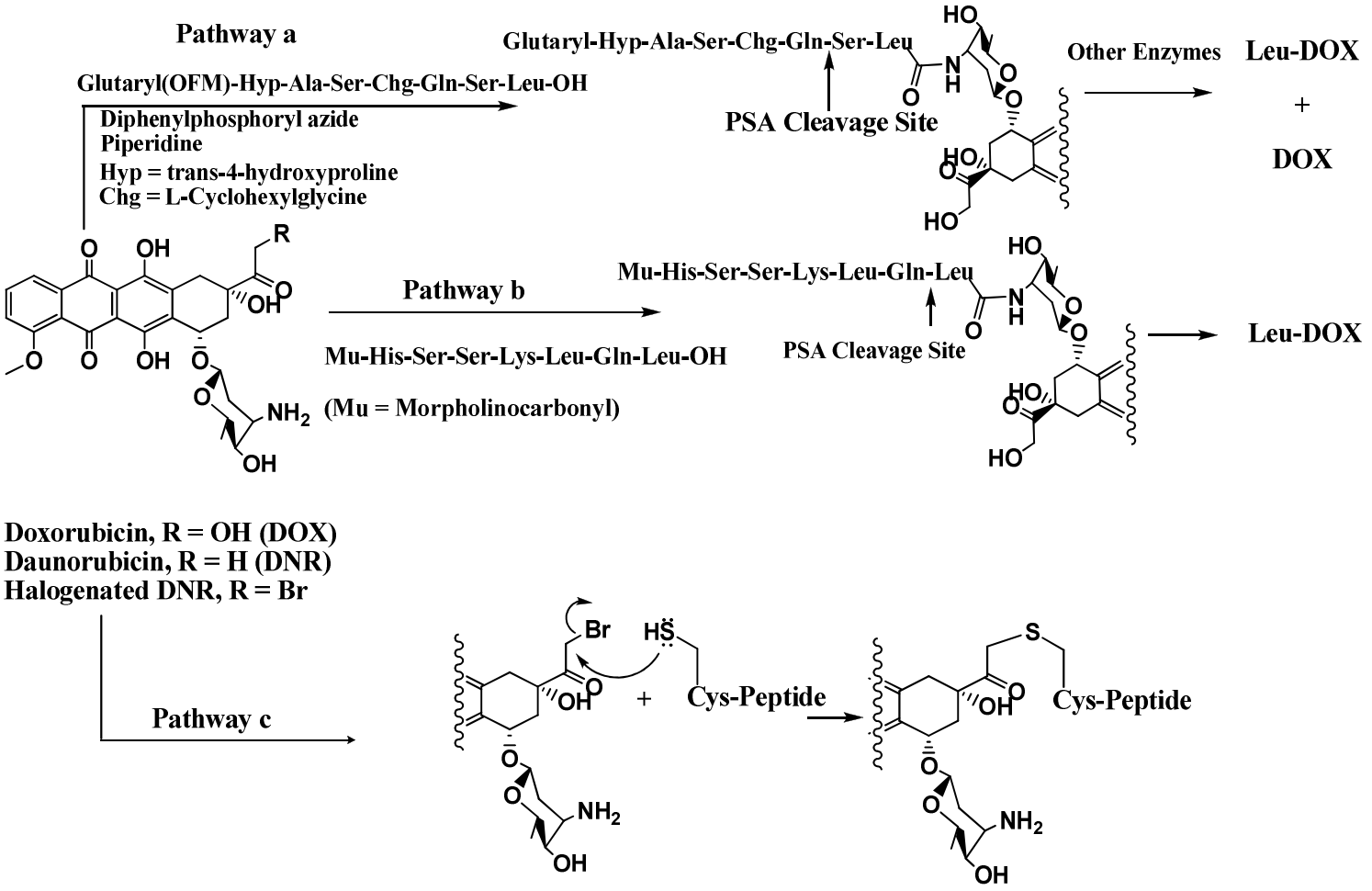

Figure 1.5 Different conjugation strategies are used to attach drug to peptide. DOX, DNR and halogenated DNR are selected here as the drugs of choice. Pathway **(a)** and **(b)** show the enzymatically cleavable [prostate specific antigen (PSA) cleavable] bond formation approach between the drug and the carrier peptide (refs 39, 40). Pathway **(c)** shows the thioether bond formation strategy between the drug and the carrier peptide (ref 26).

1.3.5 Thioether Bond

The thioether bond is chemically stable like the amide bond and, as a result, the release of free drug is impeded by this conjugation process. Peptides containing a free thiol group such as Vectocell peptides (i.e., CVKRGLKLRHVRPRVTRMDV and SRRARRSPRHLGSGC) have been conjugated with drugs using a thioether linkage because these peptides are translocated across the cell membranes in an energy-dependent manner. Vectocell peptides were conjugated to DNR through nucleophilic displacement of the halogen on DNR to make a thioether link (Figure 1.5, pathway c). These conjugates have been found to be significantly less cytotoxic than the free drug.[27] This may be due to several factors. First, the presence of the peptide carrier may prevent the recognition of DOX. Second, the DOX-Vectocell bond is very stable; therefore, DOX cannot be released from the carrier. It is also possible that the peptide cannot be effectively digested in the lysosomes to release all the delivered DOX. Third, although the DOX is structurally exposed for activity, the intact conjugate may not be able to enter the nucleus.

A thioether bond was used to conjugate oligodeoxynucleotides (ODNs) to peptide carriers to improve their cellular uptake. In this case, 5′-thiol-derivatized phosphorothioate-ODNs against the protooncogene *bcl-2* was conjugated to a cyclic somatostatin analog with a maleimide group at the N-terminus (maleimide-cyclo(2,7)-fCYwKTCT)) to form the thioether conjugate.[43] A thioether linkage was used to conjugate hydroxymethylacylfulvene (HMAF), an alkylating antitumor agent, to a cysteine-containing peptide (Figure 1.6a). Through a thiol-displacement reaction,

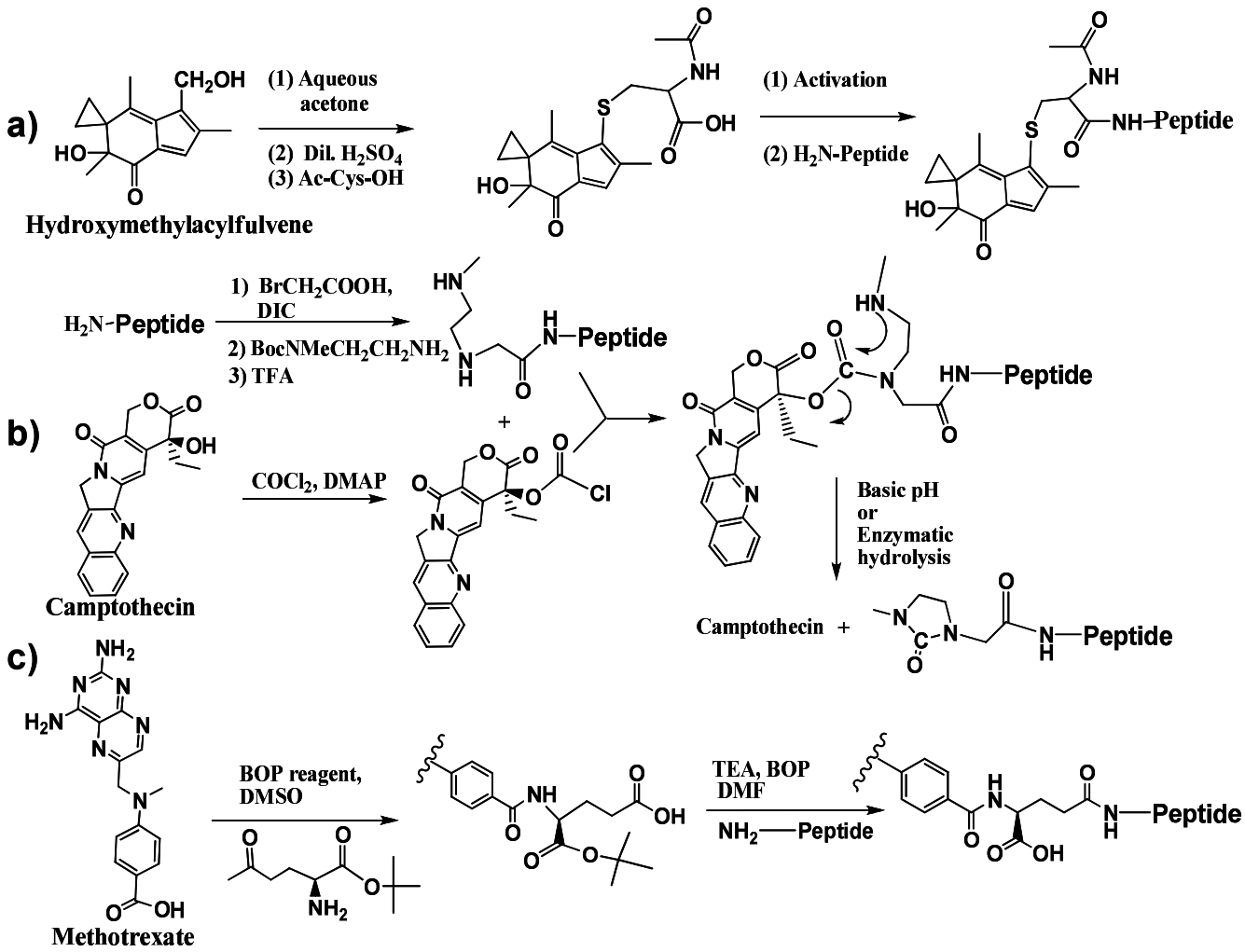

Figure 1.6 (a) Hydroxymethylacylfulvene is conjugated with Cys-containing peptides using thioether linking strategy (ref 43). **(b)** Camptothecin is conjugated with peptides using a carbamate ester bond to ensure release of the drug from the conjugate in a controlled manner (ref 45). **(c)** Methotrexate was conjugated with peptides using the γ-carboxylic acid of the glutamic acid residue of the drug (refs 22, 28) .

HMAF was first conjugated to N-acetylcysteine, and then the carboxylic acid of the N-acetylcysteine was activated and reacted with the N-terminus of the carrier peptide for targeting tumor cells.[44]

1.3.6 Carbamate Ester Bond

A carbamate bond has higher stability in plasma than an ester bond, providing a higher probability of the conjugate reaching the target site.[45] Camptothecin (CPT), and combretastatin (CBT) were conjugated to somatostatin analog peptides using a carbamate bond between the drug and the spacer (Figure 1.6b for CPT).[46] The spacer contained a methyl-aminoethyl moiety that was attached to the carbamate nitrogen as a "built-in-nucleophile assisted releasing" (BINAR) moiety, which acted as a nucleophile to release CPT. This secondary amine of the BINAR moiety attacked the carbonyl carbon of the carbamate group to form a five-membered ring urea on the spacer; this was followed by the release the drug into the medium. In this case, the pKa value of the hydroxyl group of the drug influenced the rate of drug release from this conjugate. For example, CBT conjugate was highly unstable compared to CPT conjugate due to the pKa of the alcohol in each drug. The CPT conjugate (Figure 1.6b) was highly cytotoxic to the human neuroblastoma cell line IMR32 with a high expression of somatostatin receptor and the conjugate had half-lives about 123 h and 18 h in phosphate buffer and rat serum, respectively. Modification of the length of the spacer influenced the stability of the conjugate. Although this approach has promise

for selective delivery with adjustable rate of release, it can only be used for drugs with a hydroxyl group.[46,47]

1.4 In vitro and in vivo Biology of Drug-Peptide Conjugates

1.4.1 Drug-Bombesin Analog Peptide Conjugates

Among the bombesin (BN) receptor subtypes, bombesin receptor type 2 (also known as gastrin-releasing peptide (GRP) receptor) may be the best choice for cancer cell targeted delivery because it is upregulated in breast, prostate, small cell lung, and pancreatic cancers[48]. Bombesin peptides have been conjugated to different drugs for targeting cancer cells. Receptor antagonist (RC-3095) and agonist (RC-3094) of bombesin receptors have been conjugated to DOX and 2-pyrrolino-DOX via a glutaric acid spacer (Figure 1.7 a,b). RC-3095 had higher binding affinity to the target receptor than RC-3094 on Swiss 3T3 cells; this is due to the presence of a hydrophobic D-Tpi residue on RC-3095 peptidomimetic. Conjugation of DOX or 2-pyrrolino-DOX to the less hydrophobic RC-3094 increased the conjugate binding affinity to the receptor about 1000 times. In contrast, conjugation of DOX to the hydrophobic antagonist RC-3095 lowered its binding affinity to the receptor about two times. Nonetheless, DOX-RC-3095 conjugate preserved the DOX activity to inhibit cell growth of several human cancer cells, including human pancreatic cancer (CFPAC-1), human SCLC (DMS-53), human prostate cancer (PC-3), and the human gastric cancer cell line (MKN-45).[49] The conjugate between RC-3094 and 2-pyrrolino-DOX showed significant antitumor activity with reduced toxicity in *in vivo*

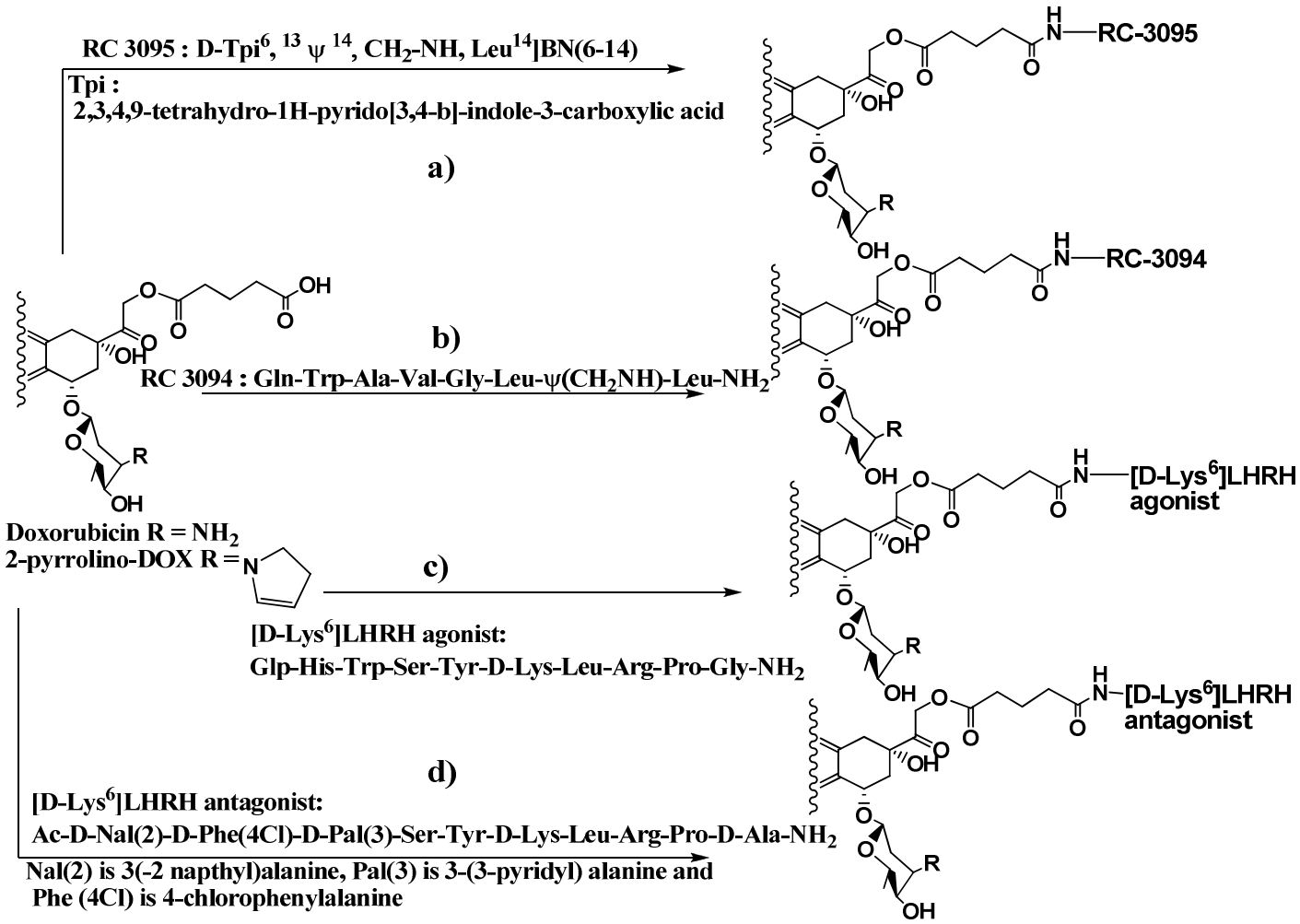

Figure 1.7 (a) and **(b)** show the conjugation of the N-termini of the bombesin antagonist peptide RC-3095 and RC-3094, respectively, to the C14 position of DOX and 2-pyrrolino-DOX using a glutaric acid spacer (ref 48). **(c)** and **(d)** show conjugation of D-Lys side chain of LHRH agonist and antagonist peptides, respectively, to the C14 position of DOX and 2-pyrrolino-DOX using a glutaric acid spacer (ref 27).

hamster nitrosamine-induced pancreatic cancer.[49] The conjugate activity could be inhibited by the parent peptide/peptidomimetic, suggesting that the conjugate bound to bombesin receptor. However, the selectivity of the conjugate for cells that express bombesin receptor over the cells that do not express the receptor has not been evaluated. This study suggests that peptide-drug conjugation may influence the receptor-binding properties of the conjugate.

1.4.2 Drug- LHRH (GnRH) Analog Peptide Conjugates

Overexpression of LHRH receptors in breast, ovarian, endometrial, and prostate cancers provides an excellent opportunity to target drugs to these cancer cells using LHRH peptides.[50,51] Short LHRH peptides have been designed as receptor agonists and antagonists for releasing luteinizing hormone.[52,53] DOX and 2-pyrrolino-DOX have also been conjugated to LHRH agonist and antagonist peptides for selectively targeting cancer cells (Figure 1.7c,d).[28] The presence of D-Lys at position 6 in LHRH peptide was necessary for high receptor binding affinity and agonistic activity (Figure 1.7c); on the other hand, the hydrophobic tripeptide sequence at the N-terminal region of LHRH was necessary for the antagonist activity (Figure 1.7d).[52,53] Conjugation of DOX and 2-pyrrolino-DOX to the agonist maintained the binding affinity to the LHRH receptors. However, conjugation of the same drugs to the antagonist peptide lowered the binding affinity to the receptor about four fold, suggesting that the drug moiety might interfere with the recognition of the peptide by the receptor. Nonetheless, the ability of LHRH-DOX conjugate to inhibit cancer cell growth (i.e.,

breast, prostate, mammary, and ovarian cancer cells) was comparable to that of the corresponding individual drugs.[28] In vivo studies indicated that the drug-agonist conjugates are less toxic and more potent than the corresponding individual drugs (i.e., DOX and 2-pyrrolino-DOX); this may be due to the selectivity of the conjugate to target cancer cells.

Polyethylene glycol (PEG; M_w ~5000) has been utilized to link LHRH peptides and camptothecin (CPT) to give CPT-PEG-LHRH for increasing conjugate solubility and retention in the systemic circulation.[54] CPT-PEG-LHRH conjugate was prepared by reacting the side chain of the Lys residue of LHRH peptide with N-hydroxysuccinimide-activated PEG containing vinylsulfone (NHS-PEG-VS) (Figure 1.8). To conjugate the drug, CPT was converted to CPT-Cys, and the thiol group on the Cys residue was reacted to the vinylsulfone to form the desired conjugate (Figure 1.8). The CPT-PEG-LHRH conjugate had a lower IC_{50} than the CPT-PEG conjugate without LHRH peptide against A7280 human ovarian carcinoma cells.[54]

1.4.3 Drug-Somatostatin Analog Peptide Conjugates

Somatostatin peptides (RC 121 and RC 160) were conjugated to DOX and 2-pyrrolino-DOX at the C14 position via a glutaric acid spacer (Figure 1.9a,b). Through a series of substitution studies, it was established that the C- and N-termini residues are important for their binding affinity by stabilizing the peptide conformation. Both RC 121 and RC 160 peptides showed binding affinities to the somatostatin receptor on rat pituitary membrane homogenates in the nanomolar (below 2 nM) range.

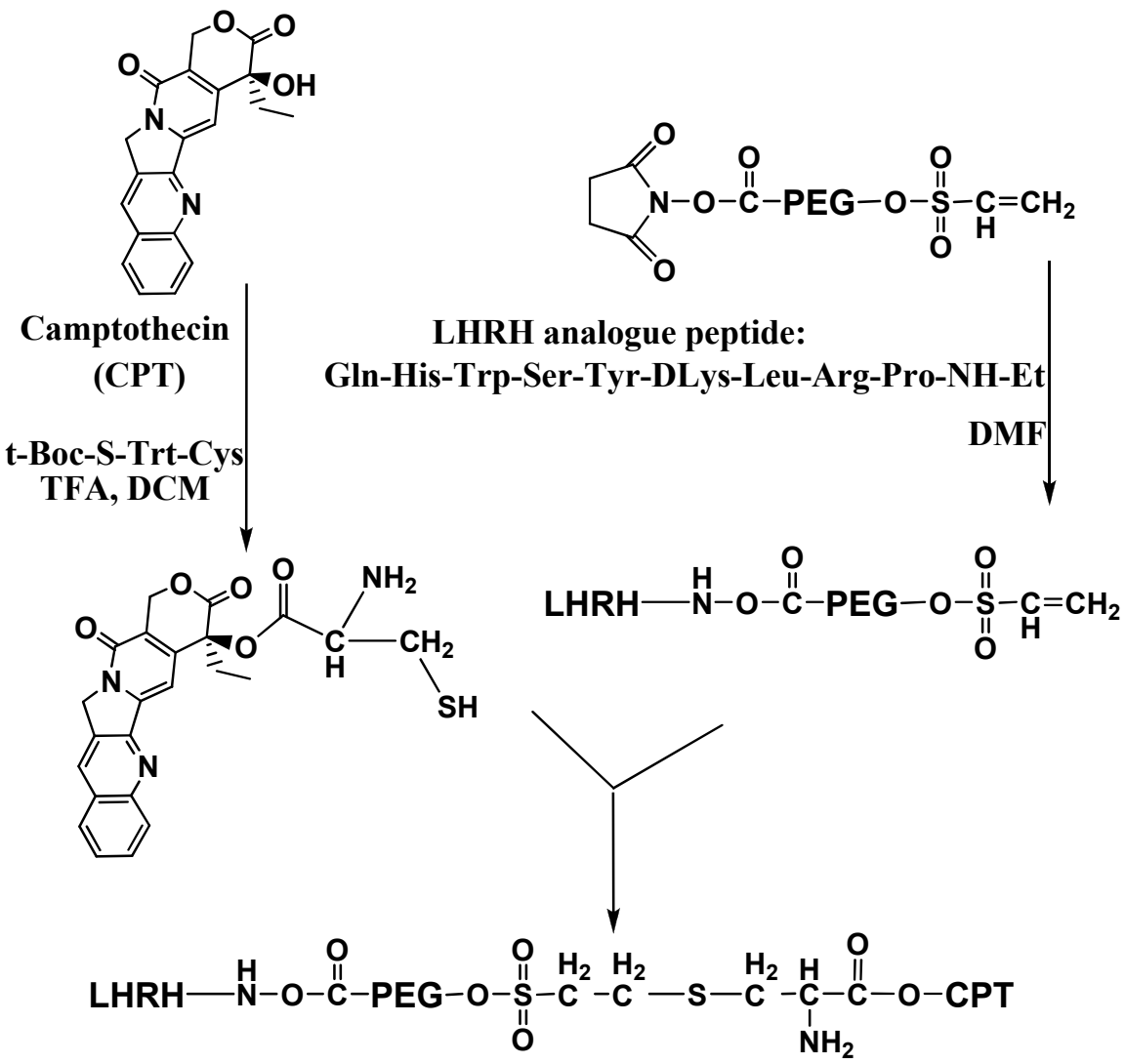

Figure 1.8 Camptothecin (CPT) was conjugated to an LHRH analog peptide using a polyethylene glycol (PEG) linker. CPT was conjugated to Cys to generate CPT-Cys. LHRH analog peptide was separately conjugated to NHS-PEG-VS (VS: vinylsulfone). CPT-Cys was then conjugated to LHRH-PEG-VS using thioether linking strategy (ref 53).

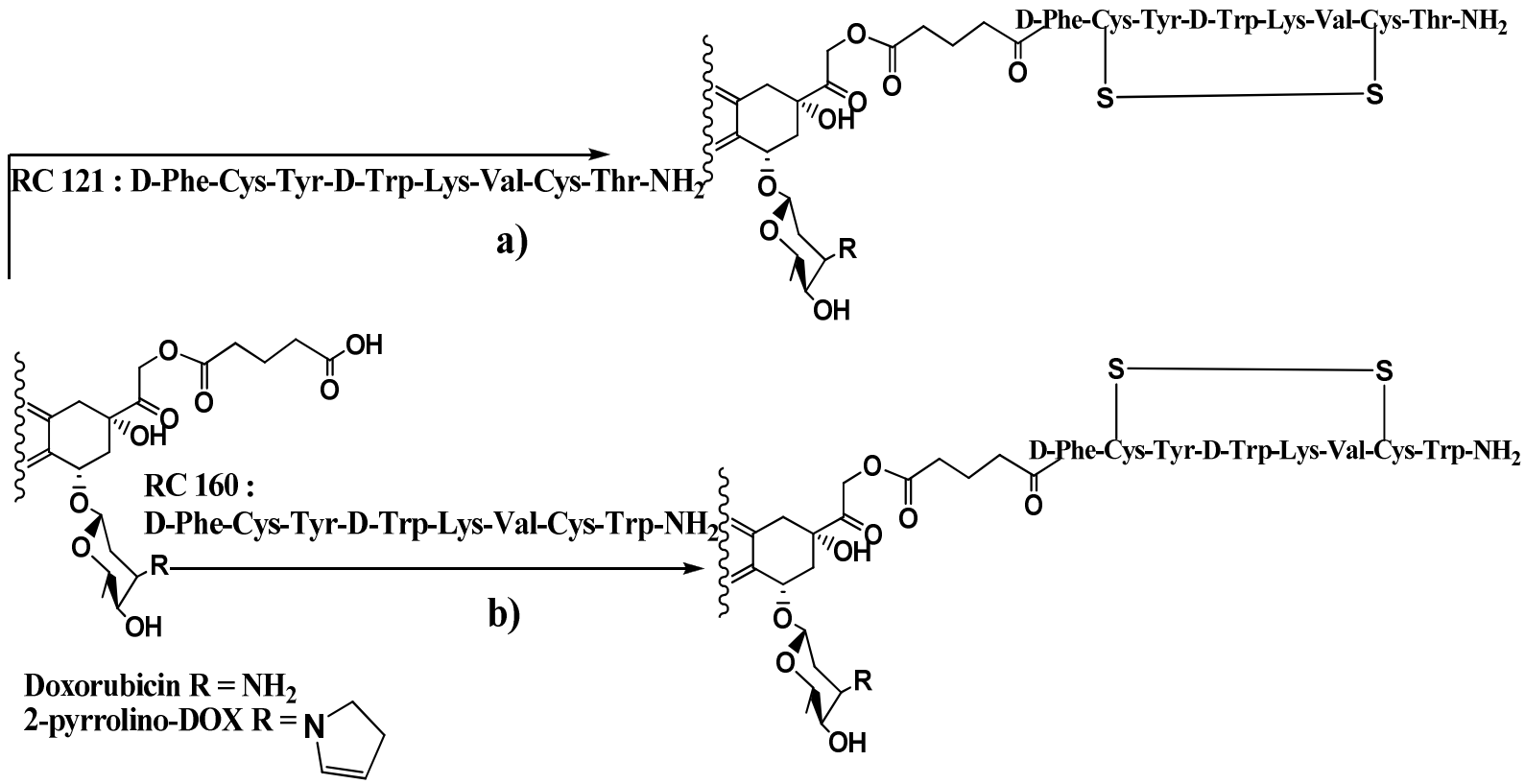

Figure 1.9 Somatostatin analog cyclic peptides were conjugated to DOX or 2-pyrrolino-DOX. **(a)** and **(b)** show the conjugation of N-termini of RC 121 and RC 160 to the C14 position of DOX and 2-pyrrolino-DOX using a glutaric acid spacer (ref 54).

However, conjugation to DOX lowered the binding affinity to the target receptors. The effect on binding affinity may be due to interference with the peptide binding site by the drug. In *in vivo* studies, the conjugate of 2-pyrrolino-DOX to RC-121 had better activity and less toxicity than the drug itself in inhibiting the growth of mouse and human mammary cancers in nude mice.[55] MTX was also conjugated via its γ-carboxylic acid to the N-terminal of RC-121 to give MTX-RC-121 (Figure 1.6c) with retained binding affinity to somatostatin receptors on rat cortex.[24,29,56] Furthermore, MTX-RC-121 conjugate inhibited the growth of MIA PaCa-2 human pancreatic cancer in nude mice. By contrast, neither the drug nor the peptide had an effect on inhibiting *in vivo* cancer growth.

1.4.4 Drug-RGD Peptide Conjugates

Arg-Gly-Asp (RGD) peptides are the best studied peptides for targeting a specific type of cell. The RGD sequence is found in many extracellular matrix (ECM) proteins, including fibronectin, collagen, laminin, and fibrinogen. The RGD sequence is responsible for the binding of ECM proteins to the integrin family of receptors, including $\alpha_v\beta_3$, $\alpha_v\beta_5$, $\alpha_v\beta_6$, $\alpha_v\beta_8$, $\alpha_5\beta_1$, $\alpha_{IIB}\beta_3$, $\alpha_8\beta_1$ receptors on the cell surface.[57-60] Cyclic RGD peptides, CDCRGDCFC (RGD-4C) and cyclo-(N-Me-VRGDf), selectively bind to $\alpha_v\beta_3$ and $\alpha_v\beta_5$ integrins, which are upregulated in tumors during angiogenesis. These cyclic peptides were conjugated to a formaldehyde adduct of DOX called doxsaliform via a short hydroxylamine ether linker, which acts as a prodrug linker that can release the drug via N-Mannich base hydrolysis (Figure 1.10).

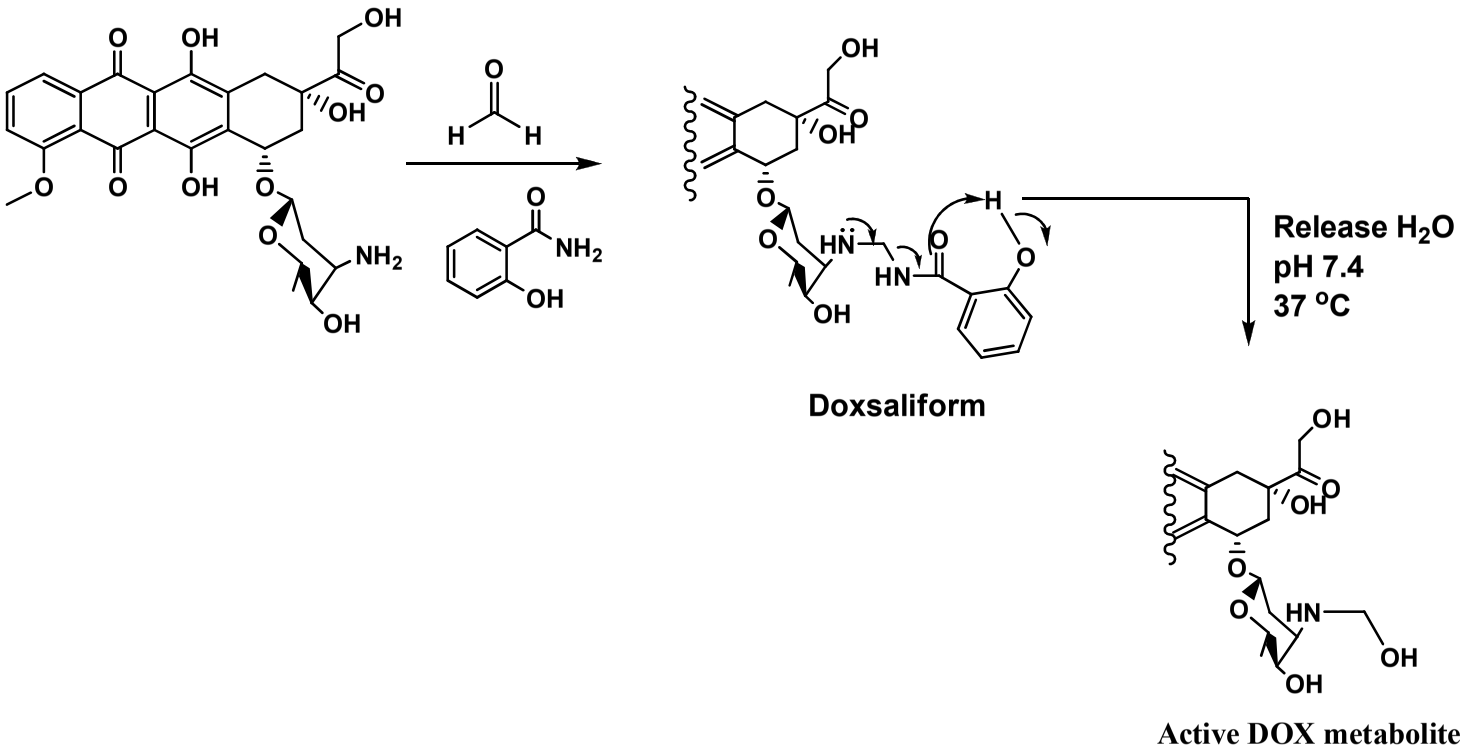

Figure 1.10 DOX was conjugated with formaldehyde and salicylamide to generate doxsaliform. Doxsaliform undergoes N-mannich base hydrolysis to generate the proposed active cytotoxic agent (ref 2).

The half-life of the drug release process was about 60 min, which allowed the conjugate sufficient time to accumulate in the tumors. Both drug-RGD peptide conjugates showed high binding affinity to integrin receptors in a vitronectin cell adhesion assay, and they also inhibited the growth of MDA-MB435 breast cancer *in vivo*.[2] In addition, paclitaxel was conjugated to a bicyclic RGD peptide ($c(RGDyK)]_2$), and the conjugate inhibited proliferation of MDA-MB435 cells. Although the conjugate had slightly lower binding affinity than the peptide itself, it had integrin-specific accumulation *in vivo*.[61] These results suggest that RGD peptides have promise in delivering drugs to cells with upregulated integrin receptors.

1.4.5 Drug-ICAM-1 Peptide Conjugates

Peptides derived from intercellular adhesion molecule-1 (ICAM-1) constitute a separate class of promising cell adhesion peptides that have the potential to target drugs to leukocytes. These peptides inhibited homotypic and heterotypic leukocyte adhesion mediated by leukocyte function-associated antigen-1 (LFA-1)/ICAM-1 interactions. The LFA-1/ICAM-1-mediated leukocyte adhesion can be modulated by anti-CD11a antibodies.[62] An ICAM-1-derived cyclic peptide called cIBR (cyclo(1,12)PenPRGGSVLVTGC) binds LFA-1 via the I-domain of the α-subunit of LFA-1 and can be internalized by LFA-1-expressing leukocytes. The entry of fluorescence isothiocyanate- (FITC)-labeled cIBR peptide into T-cells was followed by confocal microscopy and flow cytometry.[63-65] Therefore, cIBR peptide is an attractive molecule for targeting cytotoxic drugs to leukocytes.

To utilize cIBR peptide to target leukocytes, it was conjugated to MTX and DOX to give MTX-cIBR and DOX-cIBR respectively. MTX-cIBR retained its binding affinity for LFA-1 receptors on MOLT-3 T-cells. The conjugate also showed concentration-dependent inhibition of binding of anti-LFA-1 antibody to PMA-activated MOLT-3 T-cells.[66] The MTX-cIBR conjugate was effective in inhibiting the progression of rheumatoid arthritis in the rat adjuvant model and collagen-induced arthritis (CIA) mouse model. Efforts are underway to develop a stable formulation of the MTX-cIBR conjugate and to understand the *in vivo* stability of the conjugate.

The mechanism of entry of DOX-cIBR conjugate in to human leukemic cell HL-60 is via the energy-independent pathway instead of the receptor-mediated endocytosis pathway. The lack of receptor-mediated entry of DOX-cIBR conjugate is presumably due to its high hydrophobicity.[25] Recently, a new derivative called cIBR7 (cyclo(1,8)CPRGGSVC) has been developed that is more hydrophilic than cIBR and has higher binding affinity to the I-domain of LFA-1. However, although the DOX-cIBR7 conjugate is more hydrophilic than DOX-cIBR, the new DOX-cIBR7 conjugate still enters HL-60 cells by passive diffusion. To further increase the hydrophilicity of the conjugate, 11-amino-3,6,9-trioxaundecanoic was used to link DOX molecule to cIBR7 to form the DOX-PEG-cIBR7 conjugate, which is more hydrophilic than DOX-cIBR7. Despite the increase in hydrophilicity of DOX-PEG-cIBR7, this conjugate enters HL-60 cells via passive diffusion. Thus, it is necessary to re-investigate the mechanisms of cellular entry of conjugates of peptides with DOX. Recently, the general applicability of ICAM-1 peptides to deliver different drug

molecules with various hydrophilicities are being investigated for their selective delivery to leukocytes.

1.5 Conclusion

There has been increasing interest in using peptides to selectively deliver drugs to cancer cells, and promising results have been shown in both *in vitro* and *in vivo* studies. However, many aspects of drug-peptide conjugates have not been systematically elucidated, including (a) the effect of physicochemical properties of the drug on the uptake properties of the conjugate, (b) the mechanism of trafficking of the conjugate inside the cell, (c) the role of the spacer on receptor recognition and uptake of the conjugate, and (d) structural and binding properties of the conjugate vs. the peptide carrier to the cell surface receptors. There is also increasing success in targeting liposomes and nanoparticles to a specific type of cell by decorating the surface with peptides. Paclitaxel-peptide conjugates are currently undergoing phase I clinical trials for effective delivery to treat brain tumors. In the future, more data on drug-peptide conjugates will emerge to show the utility of carrier peptides in lowering the side effects of toxic drugs.

1.6 References

1. Kaufmann AM, Krise JP 2007.Lysosomal sequestration of amine-containing drugs: Analysis and therapeutic implications. J Pharm Sci 96(4):729-746.

2. Burkhart DJ, Kalet BT, Coleman MP, Post GC, Koch TH 2004.Doxorubicin-formaldehyde conjugates targeting {alpha}v{beta}3 integrin. Mol Cancer Ther 3(12):1593-1604.

3. Hudecz F, Banoczi Z, Csik G 2005.Medium-sized peptides as built in carriers for biologically active compounds. Med Res Rev 25(6):679-736.

4. Deshayes S, Morris MC, Divita G, Heitz F 2005.Cell-penetrating peptides: tools for intracellular delivery of therapeutics. Cell Mol Life Sci 62(16):1839-1849.

5. Garnett MC 2001.Targeted drug conjugates: principles and progress. Adv Drug Del Rev 53(2):171-216.

6. Widera A, Norouziyan F, Shen WC 2003.Mechanisms of TfR-mediated transcytosis and sorting in epithelial cells and applications toward drug delivery. Adv Drug Del Rev 55(11):1439-1466.

7. Leamon CP, Low PS 2001.Folate-mediated targeting: from diagnostics to drug and gene delivery. Drug Discovery Today 6(1):44-51.

8. Li H, Qian ZM 2002.Transferrin/transferrin receptor-mediated drug delivery. Med Res Rev 22(3):225-250.

9. Ungewickell EJ, Hinrichsen L 2007.Endocytosis: clathrin-mediated membrane budding. Curr Opin Cell Biol 19(4):417-425.

10. Fabbri M, Di Meglio S, Gagliani MC, Consonni E, Molteni R, Bender JR, Tacchetti C, Pardi R 2005.Dynamic partitioning into lipid rafts controls the endo-exocytic cycle of the alphaL/beta2 integrin, LFA-1, during leukocyte chemotaxis. Mol Biol Cell 16(12):5793-5803.

11. Yeung JH, Coleman JW, Park BK 1985.Drug-protein conjugates--IX. Immunogenicity of captopril-protein conjugates. Biochem Pharmacol 34(22):4005-4012.

12. Westerhof GR, Rijnboutt S, Schornagel JH, Pinedo HM, Peters GJ, Jansen G 1995.Functional activity of the reduced folate carrier in KB, MA104, and IGROV-I cells expressing folate-binding protein. Cancer Res 55(17):3795-3802.

13. Kaneko T, Willner D, Monkovic I, Knipe JO, Braslawsky GR, Greenfield RS, Vyas DM 1991.New hydrazone derivatives of adriamycin and their immunoconjugates--a correlation between acid stability and cytotoxicity. Bioconj Chem 2(3):133-141.

14. Froesch BA, Stahel RA, Zangemeister-Wittke U 1996.Preparation and functional evaluation of new doxorubicin immunoconjugates containing an acid-

sensitive linker on small-cell lung cancer cells. Cancer Immunol, Immunother 42(1):55-63.

15. Andersson L, Davies J, Duncan R, Ferruti P, Ford J, Kneller S, Mendichi R, Pasut G, Schiavon O, Summerford C, Tirk A, Veronese FM, Vincenzi V, Wu G 2005.Poly(ethylene glycol)-poly(ester-carbonate) block copolymers carrying PEG-peptidyl-doxorubicin pendant side chains: synthesis and evaluation as anticancer conjugates. Biomacromolecules 6(2):914-926.

16. Rodrigues PC, Beyer U, Schumacher P, Roth T, Fiebig HH, Unger C, Messori L, Orioli P, Paper DH, Mulhaupt R, Kratz F 1999.Acid-sensitive polyethylene glycol conjugates of doxorubicin: preparation, in vitro efficacy and intracellular distribution. Bioorg Med Chem 7(11):2517-2524.

17. Gabor F, Wollmann K, Theyer G, Haberl I, Hamilton G 1994.In vitro antiproliferative effects of albumin-doxorubicin conjugates against Ewing's sarcoma and peripheral neuroectodermal tumor cells. Anticancer Res 14(5A):1943-1950.

18. Kratz F, Beyer U, Roth T, Tarasova N, Collery P, Lechenault F, Cazabat A, Schumacher P, Unger C, Falken U 1998.Transferrin conjugates of doxorubicin: synthesis, characterization, cellular uptake, and in vitro efficacy. J Pharm Sci 87(3):338-346.

19. Triton TR, Yee G 1982.The anticancer agent adriamycin can be actively cytotoxic without entering cells. Science 217(4556):248-250.

20. Chaires JB, Satyanarayana S, Suh D, Fokt I, Przewloka T, Priebe W 1996.Parsing the Free Energy of Anthracycline Antibiotic Binding to DNA. Biochemistry (Mosc) 35(7):2047-2053.

21. Mizutani H, Tada-Oikawa S, Hiraku Y, Kojima M, Kawanishi S 2005.Mechanism of apoptosis induced by doxorubicin through the generation of hydrogen peroxide. Life Sci 76(13):1439-1453.

22. Duvvuri M, Konkar S, Funk RS, Krise JM, Krise JP 2005.A Chemical Strategy To Manipulate the Intracellular Localization of Drugs in Resistant Cancer Cells. Biochemistry (Mosc) 44(48):15743-15749.

23. Fitzpatrick JJ, Garnett MC 1995.Design, synthesis and in vitro testing of methotrexate carrier conjugates linked via oligopeptide spacers. Anti-Cancer Drug Des 10(1):1-9.

24. Nagy A, Szoke B, Schally AV 1993.Selective coupling of methotrexate to peptide hormone carriers through a gamma-carboxamide linkage of its glutamic acid moiety: benzotriazol-1-yloxytris(dimethylamino)phosphonium hexafluorophosphate activation in salt coupling. Proc Natl Acad Sci USA 90(13):6373-6376.

25. Majumdar S, Kobayashi N, Krise JP, Siahaan TJ 2007.Mechanism of internalization of an ICAM-1-derived peptide by human leukemic cell line HL-60: influence of physicochemical properties on targeted drug delivery. Mol Pharm 4(5):749-758.

26. Krauss U, Kratz F, Beck-Sickinger AG 2003.Novel daunorubicin-carrier peptide conjugates derived from human calcitonin segments. J Mol Recognit 16(5):280-287.

27. Meyer-Losic F, Quinonero J, Dubois V, Alluis B, Dechambre M, Michel M, Cailler F, Fernandez AM, Trouet A, Kearsey J 2006.Improved Therapeutic Efficacy of Doxorubicin through Conjugation with a Novel Peptide Drug Delivery Technology (Vectocell). J Med Chem 49(23):6908-6916.

28. Nagy A, Schally AV, Armatis P, Szepeshazi K, Halmos G, Kovacs M, Zarandi M, Groot K, Miyazaki M, Jungwirth A, Horvath J 1996.Cytotoxic analogs of luteinizing hormone-releasing hormone containing doxorubicin or 2-pyrrolinodoxorubicin, a derivative 500-1000 times more potent. Proc Natl Acad Sci USA 93(14):7269-7273.

29. Schally AV, Nagy A 1999.Cancer chemotherapy based on targeting of cytotoxic peptide conjugates to their receptors on tumors. European Journal of Endocrinology 141(1):1-14.

30. Halmos G, Nagy A, Lamharzi N, Schally AV 1999.Cytotoxic analogs of luteinizing hormone-releasing hormone bind with high affinity to human breast cancers. Cancer Lett 136(2):129-136.

31. Nagy A, Armatis P, Schally AV 1996.High yield conversion of doxorubicin to 2-pyrrolinodoxorubicin, an analog 500-1000 times more potent: structure-activity

relationship of daunosamine-modified derivatives of doxorubicin. Proc Natl Acad Sci USA 93(6):2464-2469.

32. van Hensbergen Y, Broxterman HJ, Elderkamp YW, Lankelma J, Beers JC, Heijn M, Boven E, Hoekman K, Pinedo HM 2002.A doxorubicin-CNGRC-peptide conjugate with prodrug properties. Biochem Pharmacol 63(5):897-908.

33. Langer M, Kratz F, Rothen-Rutishauser B, Wunderli-Allenspach H, Beck-Sickinger AG 2001.Novel Peptide Conjugates for Tumor-Specific Chemotherapy. J Med Chem 44(9):1341-1348.

34. Kruger M, Beyer U, Schumacher P, Unger C, Zahn H, Kratz F 1997.Synthesis and Stability of Four Maleimide Derivatives of the Anticancer Drug Doxorubicin for the Preparation of Chemoimmunoconjugates. Chem Pharm Bull 45(2):399-401.

35. Matsumura Y, Maeda H 1986.A new concept for macromolecular therapeutics in cancer chemotherapy: mechanism of tumoritropic accumulation of proteins and the antitumor agent smancs. Cancer Res 46(12 Pt 1):6387-6392.

36. Furgeson DY, Dreher MR, Chilkoti A 2006.Structural optimization of a "smart" doxorubicin-polypeptide conjugate for thermally targeted delivery to solid tumors. J Controlled Release 110(2):362-369.

37. Lilja H, Abrahamsson PA, Lundwall A 1989.Semenogelin, the predominant protein in human semen. Primary structure and identification of closely related

proteins in the male accessory sex glands and on the spermatozoa. J Biol Chem 264(3):1894-1900.

38. DeFeo-Jones D, Garsky VM, Wong BK, Feng DM, Bolyar T, Haskell K, Kiefer DM, Leander K, McAvoy E, Lumma P, Wai J, Senderak ET, Motzel SL, Keenan K, Van Zwieten M, Lin JH, Freidinger R, Huff J, Oliff A, Jones RE 2000.A peptide-doxorubicin 'prodrug' activated by prostate-specific antigen selectively kills prostate tumor cells positive for prostate-specific antigen in vivo. Nat Med 6(11):1248-1252.

39. Wong BK, DeFeo-Jones D, Jones RE, Garsky VM, Feng DM, Oliff A, Chiba M, Ellis JD, Lin JH 2001.PSA-specific and non-PSA-specific conversion of a PSA-targeted peptide conjugate of doxorubicin to its active metabolites. Drug Metab Disposition 29(3):313-318.

40. Garsky VM, Lumma PK, Feng DM, Wai J, Ramjit HG, Sardana MK, Oliff A, Jones RE, DeFeo-Jones D, Freidinger RM 2001.The Synthesis of a Prodrug of Doxorubicin Designed to Provide Reduced Systemic Toxicity and Greater Target Efficacy. J Med Chem 44(24):4216-4224.

41. Denmeade SR, Lou W, Lovgren J, Malm J, Lilja H, Isaacs JT 1997.Specific and Efficient Peptide Substrates for Assaying the Proteolytic Activity of Prostate-specific Antigen. Cancer Res 57(21):4924-4930.

42. Denmeade SR, Nagy A, Gao J, Lilja H, Schally AV, Isaacs JT 1998.Enzymatic Activation of a Doxorubicin-Peptide Prodrug by Prostate-Specific Antigen. Cancer Res 58(12):2537-2540.

43. Mier W, Eritja R, Mohammed A, Haberkorn U, Eisenhut M 2000.Preparation and evaluation of tumor-targeting peptide-oligonucleotide conjugates. Bioconj Chem 11(6):855-860.

44. McMorris TC, Yu J, Ngo HT, Wang H, Kelner MJ 2000.Preparation and Biological Activity of Amino Acid and Peptide Conjugates of Antitumor Hydroxymethylacylfulvene. J Med Chem 43(19):3577-3580.

45. Hansen KT, Faarup P, Bundgaard H 1991.Carbamate ester prodrugs of dopaminergic compounds: synthesis, stability, and bioconversion. J Pharm Sci 80(8):793-798.

46. Fuselier JA, Sun L, Woltering SN, Murphy WA, Vasilevich N, Coy DH 2003.An adjustable release rate linking strategy for cytotoxin-Peptide conjugates. Bioorg Med Chem Lett 13(5):799-803.

47. Cha SW, Gu HK, Lee KP, Lee MH, Han SS, Jeong TC 2000.Immunotoxicity of ethyl carbamate in female BALB/c mice: role of esterase and cytochrome P450. Toxicol Lett 115(3):173-181.

48. Smith CJ, Sieckman GL, Owen NK, Hayes DL, Mazuru DG, Kannan R, Volkert WA, Hoffman TJ 2003.Radiochemical investigations of gastrin-releasing

peptide receptor-specific [(99m)Tc(X)(CO)3-Dpr-Ser-Ser-Ser-Gln-Trp-Ala-Val-Gly-His-Leu-Met-(NH2)] in PC-3, tumor-bearing, rodent models: syntheses, radiolabeling, and in vitro/in vivo studies where Dpr = 2,3-diaminopropionic acid and X = H2O or P(CH2OH)3. Cancer Res 63(14):4082-4088.

49. Nagy A, Armatis P, Cai RZ, Szepeshazi K, Halmos G, Schally AV 1997.Design, synthesis, and in vitro evaluation of cytotoxic analogs of bombesin-like peptides containing doxorubicin or its intensely potent derivative, 2-pyrrolinodoxorubicin. Proc Natl Acad Sci USA 94(2):652-656.

50. Eaveri R, Ben-Yehudah A, Lorberboum-Galski H 2004.Surface antigens/receptors for targeted cancer treatment: the GnRH receptor/binding site for targeted adenocarcinoma therapy. Curr Cancer Drug Targets 4(8):673-687.

51. Limonta P, Moretti RM, Marelli MM, Motta M 2003.The biology of gonadotropin hormone-releasing hormone: role in the control of tumor growth and progression in humans. Front Neuroendocrinol 24(4):279-295.

52. Bajusz S, Janaky T, Csernus VJ, Bokser L, Fekete M, Srkalovic G, Redding TW, Schally AV 1989.Highly potent analogues of luteinizing hormone-releasing hormone containing D-phenylalanine nitrogen mustard in position 6. Proc Natl Acad Sci USA 86(16):6318-6322.

53. Bajusz S, Janaky T, Csernus VJ, Bokser L, Fekete M, Srkalovic G, Redding TW, Schally AV 1989.Highly potent metallopeptide analogues of luteinizing hormone-releasing hormone. Proc Natl Acad Sci USA 86(16):6313-6317.

54. Dharap SS, Qiu B, Williams GC, Sinko P, Stein S, Minko T 2003.Molecular targeting of drug delivery systems to ovarian cancer by BH3 and LHRH peptides. J Controlled Release 91(1-2):61-73.

55. Nagy A, Schally AV, Halmos G, Armatis P, Cai RZ, Csernus V, Kovacs M, Koppan M, Szepeshazi K, Kahan Z 1998.Synthesis and biological evaluation of cytotoxic analogs of somatostatin containing doxorubicin or its intensely potent derivative, 2-pyrrolinodoxorubicin. Proc Natl Acad Sci USA 95(4):1794-1799.

56. Radulovic S, Nagy A, Szoke B, Schally AV 1992.Cytotoxic analog of somatostatin containing methotrexate inhibits growth of MIA PaCa-2 human pancreatic cancer xenografts in nude mice. Cancer Lett 62(3):263-271.

57. Ruoslahti E, Pierschbacher MD 1986.Arg-Gly-Asp: A versatile cell recognition signal. Cell 44(4):517-518.

58. Hayman EG, Pierschbacher MD, Ruoslahti E 1985.Detachment of cells from culture substrate by soluble fibronectin peptides. J Cell Biol 100(6):1948-1954.

59. Pierschbacher MD, Ruoslahti E 1984.Variants of the Cell Recognition Site of Fibronectin That Retain Attachment-Promoting Activity. Proc Natl Acad Sci USA 81(19):5985-5988.

60. Dunehoo AL, Anderson ME, Majumdar S, Kobayashi N, Berkland C, Siahaan TJ 2006.Cell adhesion molecules for targeted drug delivery. J Pharm Sci 95(9):1856-1872.

61. Chen X, Plasencia C, Hou Y, Neamati N 2005.Synthesis and Biological Evaluation of Dimeric RGD Peptide-Paclitaxel Conjugate as a Model for Integrin-Targeted Drug Delivery. J Med Chem 48(4):1098-1106.

62. Tibbetts SA, Chirathaworn C, Nakashima M, Jois DS, Siahaan TJ, Chan MA, Benedict SH 1999.Peptides derived from ICAM-1 and LFA-1 modulate T cell adhesion and immune function in a mixed lymphocyte culture. Transplantation 68(5):685-692.

63. Gursoy RN, Jois DS, Siahaan TJ 1999.Structural recognition of an ICAM-1 peptide by its receptor on the surface of T cells: conformational studies of cyclo (1, 12)-Pen-Pro-Arg-Gly-Gly-Ser-Val-Leu-Val-Thr-Gly-Cys-OH. J Pept Res 53(4):422-431.

64. Gursoy RN, Siahaan TJ 1999.Binding and internalization of an ICAM-1 peptide by the surface receptors of T cells. J Pept Res 53(4):414-421.

65. Jois DS, Pal D, Tibbetts SA, Chan MA, Benedict SH, Siahaan TJ 1997.Inhibition of homotypic adhesion of T-cells: secondary structure of an ICAM-1-derived cyclic peptide. J Pept Res 49(6):517-526.

66. Anderson ME. 2003. Utilization of ICAM-1 derived peptides for targeted drug delivery to T-cells. Pharmaceutical Chemistry, ed., Lawrence: University of Kansas.

Chapter 2

Mechanism of internalization of an ICAM-1-derived peptide by human leukemic cell line HL-60: influence of physicochemical properties on targeted drug delivery

2.1 Introduction

Most chemotherapeutic agents are cytotoxic to cells; they eliminate tumor cells based on the rapid growth of these cells compared to normal cells. Unfortunately, it is difficult to avoid drug toxicity against normal cells, which leads to drug side effects. Thus, any method that lowers the side effects of antitumor agents can be of benefit to cancer patients during chemotherapy. One way to lower drug side effects is to selectively target the drug to tumor cells by utilizing the upregulated and/or activated receptors on the surface of tumor cells. In this case, the ligand for the upregulated receptor is used to selectively direct and carry the drug into tumor cells by covalently conjugating the drug to the ligand.[1-3] For example, the increased expression of folate receptors in tumor cells has been successfully used to target antitumor agents to tumor cells using drug-folate conjugates.[3-5] Due to the higher expression of transferrin receptors in tumor cells than in normal cells, transferrin protein and transferrin-receptor-antibody have been conjugated to cytotoxic molecules (*i.e.*, ricin, doxorubicin) for selectively eliminating tumor cells.[6-10] Other methods for selectively delivering drugs to tumor cells have been investigated, including the use of biodegradable polymers, nanoparticles, peptides, and carbohydrates.

In recent years, cell surface adhesion molecules have been investigated for targeting drugs to tumor cells.[2] Integrins have been shown to undergo endocytosis from the cell surface, and they have been utilized by viruses for infecting the host cells.[11] In cancer cells, there is a selective upregulation of certain integrin receptors.

Upregulation of $\alpha_v\beta_3$ and $\alpha_v\beta_5$ integrins on the vascular endothelial cells of solid tumors during angiogenesis has been exploited to halt angiogenesis or for tumor diagnosis.[2,12] In this case, RGD sequence containing cyclic peptides (CDCRGDCFC[12] and E[c(RGDyK)]$_2$[13]) that are selective for $\alpha_v\beta_3$ and $\alpha_v\beta_5$ receptors were conjugated to a cytotoxic agent such as doxorubicin (DOX) or taxol for selectively eliminating tumor cells.[12,13] For example, a conjugate between CDCRGDCFC peptide and DOX (DOX-RGD) was shown to improve the survival of mice bearing human breast carcinoma cells (MDA-MB-435).[12] At equivalent doses the DOX-RGD conjugate is more selective towards the tumor and less toxic than free DOX in this mouse model, suggesting that the conjugate targets the upregulated $\alpha_v\beta_3$ and $\alpha_v\beta_5$ in tumor cells. However, the internalization and localization processes of RGD peptide conjugates by integrins have not been fully characterized; understanding these processes will provide a better method of selecting a more effective drug to conjugate to the peptide.

In this work, we studied the internalization and localization of an ICAM-1-derived peptide called cIBR [cyclo(1,12)PenPRGGSVLVTGC] that has been shown to bind to isolated $\alpha_L\beta_2$ integrin (LFA-1) on the surface of T cells.[14,15] Because LFA-1 is expressed only on leukocytes and not on other types of cells (*i.e.*, epithelial and endothelial), this peptide could be used to target drugs to leukocytes for treating leukocyte-related disorders such as leukemia and autoimmune diseases. To follow the mechanism of binding and internalization of cIBR peptide, its N-terminus was conjugated with fluorescein isothiocyanate (FITC) and DOX to give FITC-cIBR and DOX-cIBR conjugates, respectively. For the synthesis of DOX-cIBR conjugate

primary amine of DOX was conjugated to succinic anhydride linker by amide bond. Amide bond linking strategy was chosen as it is a stable bond. For understanding the internalization mechanism of DOX-cIBR, stability of the conjugate was an important factor. The mechanisms of internalization of these conjugates were compared in LFA-1-expressing leukemic cells (*i.e.*, HL-60) and LFA-1-deficient cells (*i.e.*, HUVEC). Results from this study may be used to select a better drug-cIBR conjugate to selectively target leukocytes.

2.2 Experimental

2.2.1 Cells and Chemicals

The human acute promyeloid leukemic cell line HL-60 was kindly provided by Dr. Yueshang Zhang (Arizona Cancer Center, University of Arizona). Cells were grown in RPMI 1640 medium supplemented with 10% fetal bovine serum, 100 units/ml of penicillin G sodium, 100 μg/ml of streptomycin sulfate, and 2.0 g/l $NaHCO_3$. Cells were maintained at a density of 1×10^6 cells/ml to 2×10^6 cells/ml at 37 °C in a humidified 5% CO_2 atmosphere. HUVEC was purchased from ATCC (Manassas, VA) and grown in DMEM supplemented with 10% fetal bovine serum, 100 units/ml of penicillin G sodium, 100 μg/ml of streptomycin sulfate, 2.0 g/l $NaHCO_3$, 1.42 g/l HEPES-Na, 1% glutamine, and 1% nonessential amino acids. Doxorubicin hydrochloride, succinic anhydride, and diisopropylethyl amine were obtained from Sigma Chemicals, Inc. (St. Louis, MO). Solvents used in peptide synthesis were of pure analytical grade. All reagents, resins, and Fmoc-protected

amino acids for peptide syntheses were purchased from Peptides International, Inc. (Louisville, KY), Advanced ChemTech (Louisville, KY), and Applied Biosystems (Foster City, CA).

2.2.2 Peptide Synthesis

Synthesis of linear IBR peptide (PenPRGGSVLVTGC) was performed on a Pioneer peptide synthesizer (PerSeptive Biosystems, CA) using the standard Fmoc solid-phase strategy with O-(7-azabenzotriazole-1-yl)-N,N,N',N'-tetramethyluronium hexafluorophosphate (HATU) as the activating agent. Extended coupling cycles were employed. The resin-containing peptide was washed several times with methylene chloride and then with methanol followed by vacuum drying. A cleavage cocktail containing trifluoroacetic acid (TFA, 90%), 1,2-ethane dithiol (3%), anisole (2%), and thioanisole (5%) was used during peptide cleavage from the solid support followed by precipitation in ice-cold diethyl ether. Diethyl ether solution was allowed to stand overnight at 4 °C for maturation of the precipitate. Subsequently, the precipitate of peptide was separated from ether-containing scavengers by centrifugation. The crude linear peptide was purified by semi-preparative C18 reversed-phase HPLC. The cyclization of the linear peptide to give cIBR peptide was carried out by bubbling air for 2 h into the peptide solution (0.06 mM) containing ammonium bicarbonate (0.05 M) and ammonium hydroxide at pH 8.5. The solution was lyophilized and crude cIBR was purified by semi-preparative C18 reversed-phase HPLC. The molecular weight of cIBR peptide was determined by electrospray

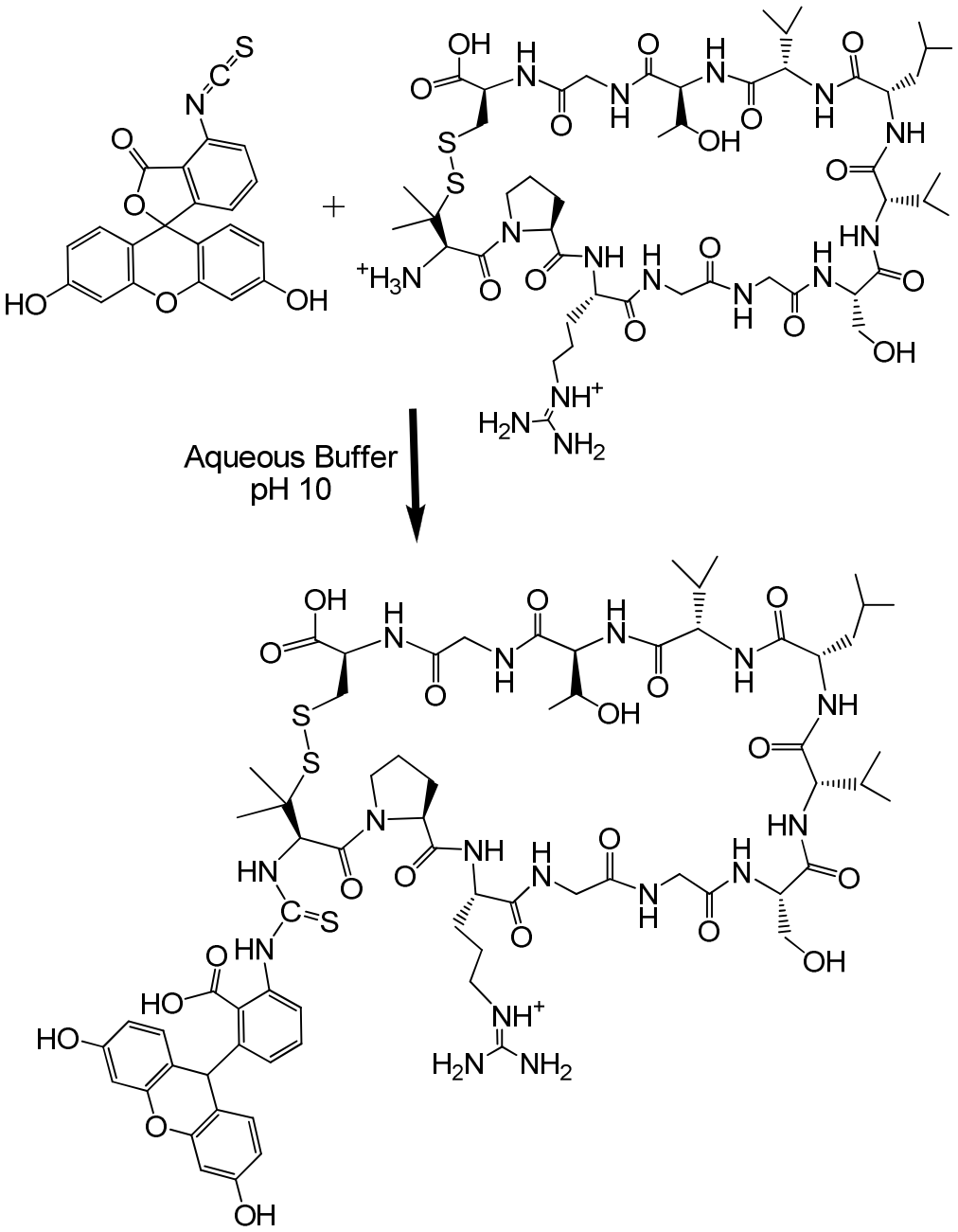

Figure 2.1(a) Structure and synthetic steps to make FITC-cIBR

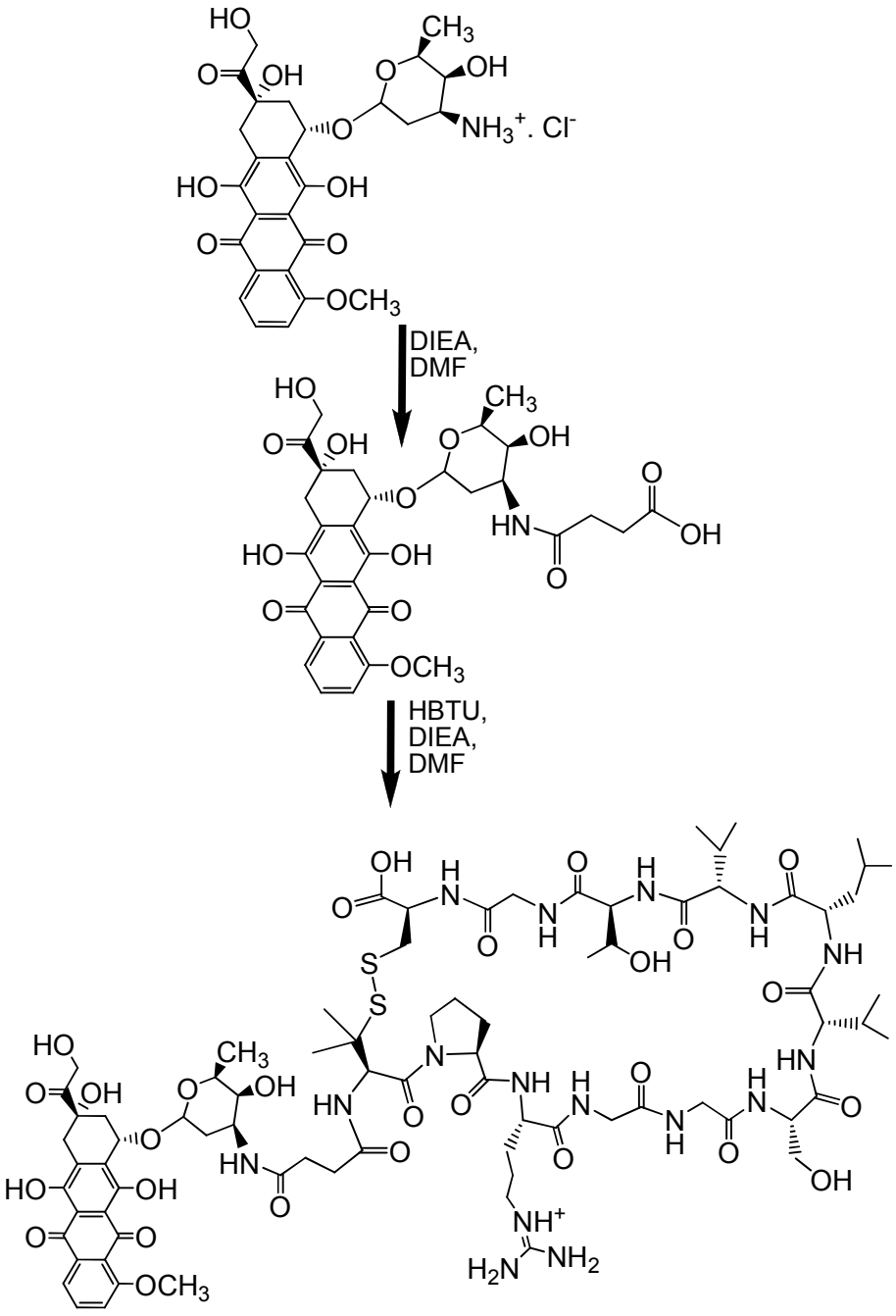

Figure 2.1(b) Structure and synthetic steps to make DOX-cIBR.

ionization mass spectrometry (M+1 = 1174.5 amu).

2.2.3 Conjugation of FITC with cIBR Peptide

Conjugation of FITC with cIBR was done according to our previously published method (Figure 2.1a).[16] Briefly, pure cIBR peptide (0.04 mmol) was dissolved in 5 ml of Nanopure water; 0.08 mmol fluorescein-5-isothiocyanate (Sigma) was added to the peptide solution and the pH was adjusted to 10 by addition of 1.0 N NaOH solution. After stirring for 1 h with a magnetic stirrer, the reaction mixture was neutralized by the addition of 10% v/v acetic acid solution. The solution was lyophilized and the resulting crude product of FITC-cIBR was purified by semi-preparative C18 reversed-phase HPLC. The pure FITC-cIBR was analyzed by analytical C18 reversed-phase HPLC and identified by electrospray ionization mass spectrometry (M+1 = 1563.4 amu).

2.2.4 Conjugation of Doxorubicin (DOX) with cIBR Peptide

In this case, the amino group in the sugar moiety of DOX was reacted with succinic anhydride in dimethyl formamide (DMF) in the presence of diisopropylethyl amine to give DOX-hemisuccinate (M+1 = 643 amu) (Figure 2.1b). Subsequently, DOX-hemisuccinate was reacted with the N-terminus of cIBR in the presence of HBTU in DMF to give the DOX-cIBR. The progress of the reaction was monitored with C18 reversed-phase analytical HPLC. The DOX-cIBR was purified using semi-

preparative HPLC with a C18 column; the molecular weight of the final product was confirmed by mass spectrometry (M+1 = 1799 amu).

2.2.5 Internalization Studies of FITC-cIBR, DOX-cIBR and DOX using HL-60 Cells

2.2.5.1 Temperature-dependent Internalization Studies

HL-60 cells were centrifuged and re-suspended in RPMI-1640 at a concentration of 1×10^6 cells/ml. 250 µl of the cell suspension was plated in two different tissue culture plates; then, 250 µl of a solution of FITC-cIBR (100 µM), DOX-cIBR (5 µM), DOX (5 µM), and FITC-dextran (200 µM, MW 10,000, Molecular Probes™, Eugene, OR) was added to the respective wells. The cells were incubated at 37 °C and 4 °C for 1 h while protected from light, and were then transferred into 1.5 ml Eppendorf tubes and centrifuged at 1000 rpm for 2 min. The cells were washed three times with ice-cold phosphate buffered saline (PBS) and finally suspended in 20 µl of PBS. Final cell density used for the microscopic observation was 12.5 x 10^6 cells/ml. 10 µl of that suspension was put on the slide for observation. Control cells without any compound added were treated the same way. A Nikon Eclipse 80*i* microscope equipped for epifluoroscence was used to view the cells, and the fluorescence emissions of DOX and FITC were observed using rhodamine and FITC filter sets, respectively. Untreated cells were viewed with both set of filters to check for their autofluorescence. The images were captured using an Orca ER camera (Hamamatsu,

Inc., Bridgewater, NJ) controlled by the Metamorph program (Version 6.2, Universal Imaging Corp., West Chester, PA).

2.2.5.2 ATP Requirement for Internalization Studies

Cells were centrifuged and resuspended in 250 µl solution of either RPMI 1640 or PBS containing 50 mM 2-deoxy-D-glucose and 25 mM sodium azide and were incubated for 45 min at 37 °C in 5% CO_2.[17] Next, the cells were incubated for 1 h with 250 µl solutions of FITC-cIBR (100 µM), DOX-cIBR (5 µM), DOX (5 µM), and FITC-dextran (MW. 10,000, 200 µM). The cells were then washed three times with ice-cold PBS and finally suspended in 20 µl of PBS for microscopic observation.

2.2.5.3 Microtubule Disruption Studies

Cells were plated as indicated above and were incubated with 50 µM Nocodazole in DMSO (0.5% in PBS) for 4 h prior to addition of 250 µl of FITC-cIBR (100 µM), DOX-cIBR (5 µM), DOX (5 µM), FITC-dextran (MW. 10,000), and Oregon Green (5 µM, Molecular Probes™, Eugene, OR) into the wells.[18] Cells were treated with 250 µl of solution of 0.5% DMSO in PBS to check the effect of DMSO on the cells. Washing and microscopic observations were carried out in the same manner as described above.

2.2.6 Stability Study of DOX-cIBR Conjugate using HL-60 Cells

Exponentially growing HL-60 cells were centrifuged and resuspended in RPMI 1640 at a concentration of 2×10^6 cells/ml. 250 µl of cell suspension was distributed into a 48-well tissue culture plate (BD Biosciences, San Jose, CA). Then, 250 µl of 100 µM DOX-cIBR solution in PBS at pH 7.4 was added to each of the wells over different time periods (0, 1, 2, 14, 18, and 24 h) and the cells were incubated in a humidified atmosphere with 5% CO_2. Three samples of cell suspension along with the compound solution at each time point were transferred to 1.5 ml Eppendorf tubes and 500 µl of acetonitrile was added. Samples were vortexed for 2 min followed by sonication at 37 °C for 30 min. After sonication, the samples were vortexed again for 2 min and centrifuged at 14,000 rpm for 10 min. Aliquots from the supernatant (20 µl) were mixed with 20 µl of solvent (52:48 ratio of acetonitrile and water in the presence of 0.05% TFA). Each sample (20 µl) was injected into the analytical reversed-phase HPLC with a C18 column and detected at 480 nm absorption wavelength. The elution system was performed using a gradient program involving solvent A (95% water containing 0.1% TFA and 5% acetonitrile) and solvent B (acetonitrile). A linear gradient program from 100% A to 100% B over a period of 18 min was used with a flow rate of 1 ml/min.

2.2.7 Determination of Octanol/Aqueous Buffer Distribution Ratio

1.0 ml of *n*-octanol (Fisher) was added to 10 ml of PBS (pH 7.4) containing 2.0 µM of DOX-cIBR or FITC-cIBR in a separatory funnel and shaken for 30 min. The two phases were allowed to equilibrate for 24 h while protected from light. The

concentration of DOX-cIBR or FITC-cIBR in each phase was determined using a fluorescence spectrophotometer (RF5000U, Shimadzu Inc., Kyoto, Japan). The fluorescence intensity of DOX-cIBR or FITC-cIBR in aqueous buffer solutions was measured at different concentrations, and a calibration curve was generated using Microcal Origin version 6.0.

2.2.8 Internalization Studies with HUVEC

HUVECs were grown to confluency in 75 cm^2 tissue culture flask. Confluent cells were trypsinized and resuspended in 20 ml of fresh DMEM. Sterile coverslips were placed in 6-well plates and 2 ml of the cell suspension were added to each of the wells. Cells were allowed to grow for 24 hours. Before the experiment, coverslips were checked for cell attachment and each coverslip was washed three times to remove the unattached cells. Coverslips with relatively similar cell attachment were used for the experiment. 500 µl of fresh DMEM was added to each well followed by 500 µl of FITC-cIBR (100 µM), DOX-cIBR (5 µM), FITC-dextran (MW. 10,000, 200 µM). Cells were incubated with the compounds for 1 h, washed 3 times with ice-cold PBS and observed under a microscope.

2.3 Results

2.3.1 Evaluation of the Mechanism of the Cellular Entry of FITC-cIBR using HL-60 Cells

The mechanism of endocytosis of FITC-cIBR was compared to that of FITC-

dextran using HL-60 cells under different conditions (Figure 2.2). FITC-dextran, which has been used as a marker for fluid phase endocytosis, was used as a positive control.[19-21] To evaluate the effect of cellular metabolism on the internalization of FITC-cIBR, it was incubated at two different temperatures, 37 °C (Figure 2.2a) and 4 °C (Figure 2.2b). At 37 °C, punctate fluorescence stains of FITC-cIBR (Figure 2.2a) were found in the HL-60 cells suggesting that FITC-cIBR was localized in the endocytic compartments similar to FITC-dextran (Figure 2.2c). In contrast, there was no fluorescence stain when the cells were incubated with FITC-cIBR (Figure 2.2b) and FITC-dextran (Figure 2.2d) at 4 °C. This suggests the possibility of receptor-mediated uptake of FITC-cIBR. Incubation at 4 °C knocks out the endocytic uptake pathway and therefore molecules taken up by this process (e.g. dextran) can not enter the cell. However, molecules that interact with the cell surface receptors may still bind without internalization. However, FITC-cIBR binding was not observed at 4 °C suggesting that the target receptor in this cell line was not in high affinity conformation for binding the ligand at this temperature.

Sodium azide is an inhibitor of mitochondrial ATPase.[22] 2-deoxy-D-glucose inhibits glucose meatolism.[23] Incubation of the cells with these compounds inhibits the energy dependent uptake mechanism. To evaluate whether there was a difference between the mechanisms of endocytosis of FITC-cIBR and FITC-dextran, HL-60 cells were incubated with these ATP synthesis inhibitors prior to incubation with FITC-cIBR and FITC-dextran. In absence of the inhibitors, FITC-cIBR (Figure 2.2e)

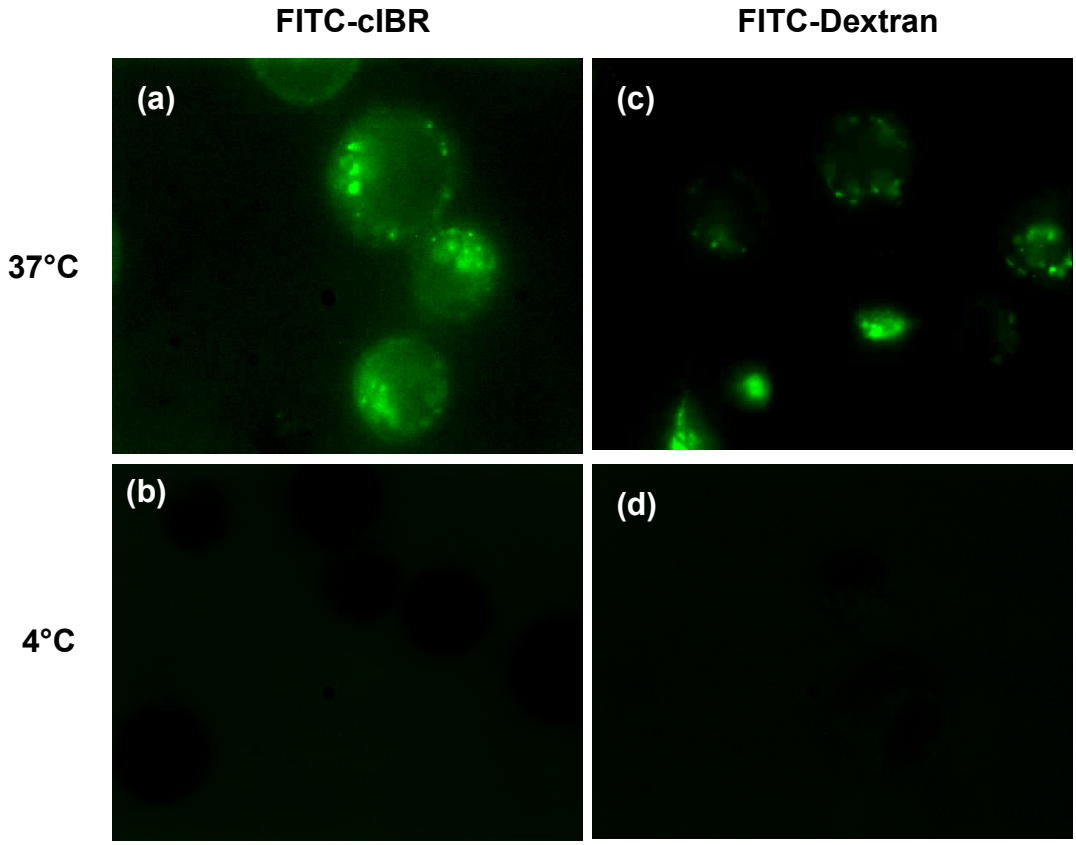

Figure 2.2(a-d) FITC-cIBR showed temperature dependent entry into HL-60 cell line and was localized into distinct endocytic compartments inside the cells. Panel **(a)** shows internalization and intracellular distribution profile of FITC-cIBR at 37 °C. Panel **(b)** shows the cells incubated with FITC-cIBR at 4 °C. The lack of energy of the cells at 4 °C prevented the receptor binding and cellular entry of FITC-cIBR. Internalization and intracellular distribution profiles of a fluid phase endocytosis marker, FITC-dextran were compared at **(c)** 37 °C and **(d)** 4 °C as control.

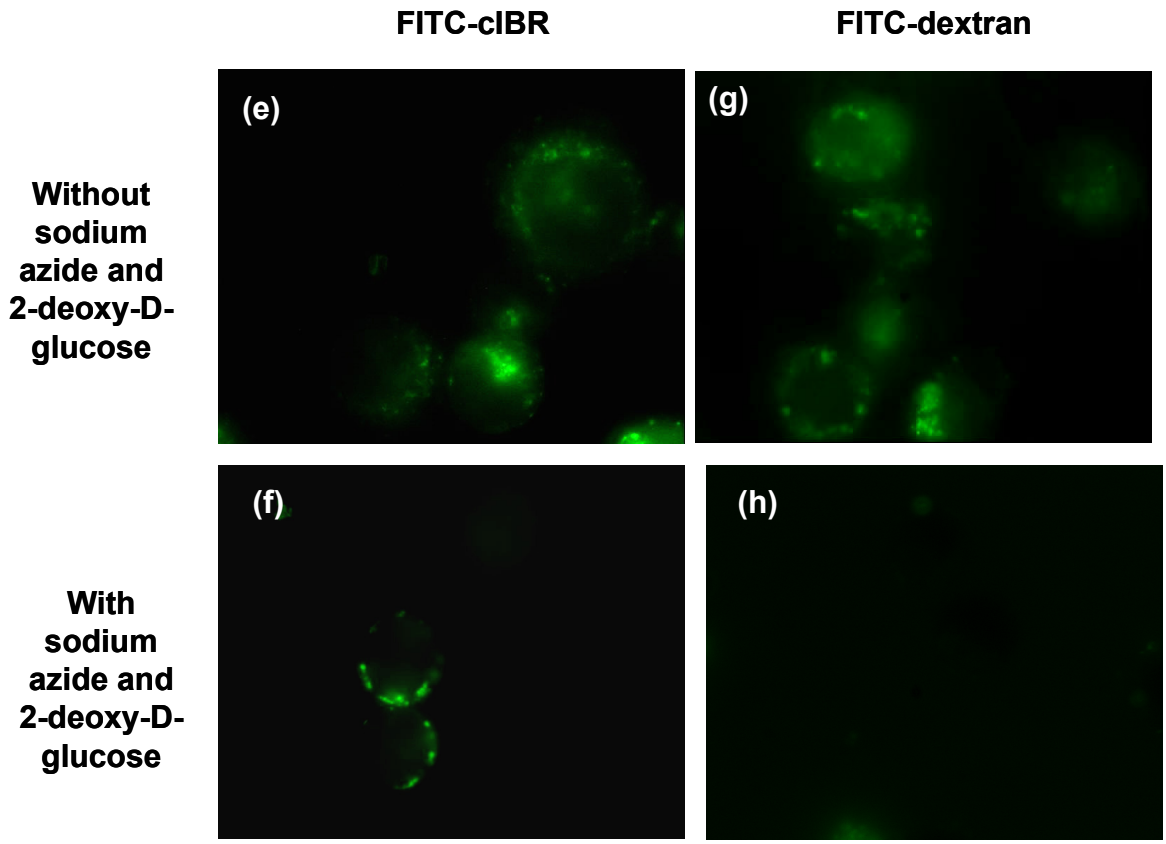

Figure 2.2(e-h) FITC-cIBR entry into the HL-60 cells was affected by ATP synthesis inhibitors sodium azide and 2-deoxy-D-glucose. Panel **(e)** shows FITC-cIBR internalization and intracellular distribution without the inhibitors. Panel **(f)** shows the FITC-cIBR internalization profile for the cells treated with the inhibitors. FITC-cIBR entry into the cells was inhibited by these compounds with the punctate stains localized possibly in the early endocytic compartments closer to the cell membrane. As a control FITC-dextran internalization profiles were compared in the **(g)** absence and **(h)** presence of sodium azide and 2-deoxy-D-glucose. These compounds completely blocked the entry of this fluid phase endocytosis marker into the HL-60 cells. There was difference between the internalization mechanisms of FITC-cIBR and FITC-dextran.

and FITC-dextran (Figure 2.2g) followed endocytic uptake pathway. The presence of ATP synthesis inhibitors affected the endocytosis of both FITC-cIBR (Figure 2.2f) and FITC-dextran (Figure 2.2h). However, the cells treated with FITC-cIBR in the presence of the inhibitors showed punctate staining possibly in the early endosomal compartments nearer to the cell membranes (Figure 2.2f) and FITC-dextran-treated cells did not (Figure 2.2h). The localization of cluster of dots in the early endosomal compartments suggested the possibility of receptor mediated entry as the marker for fluid phase endocytosis did not enter the cells. There was a clear difference between the internalization of FITC-cIBR and FITC-dextran, which implied that FITC-cIBR was internalized by a receptor-mediated process and not via fluid phase endocytosis.

Next, the effect of a microtubule disrupting agent, nocodazole, on the cellular uptake of FITC-cIBR was compared to its effect on the uptake of FITC-dextran and Oregon Green (Figure 2.3). Nocodazole blocked the cellular entry of FITC-cIBR (Figures 2.3a,b) as well as FITC-dextran (Figures 2.3c,d); however, it did not block the entry of Oregon Green (Figures 2.3e,f). Nocodazole depolymerizes the microtubule network and affects the cellular entry of compounds taken up by both receptor mediated endocytosis and fluid phase endocytosis. However, the effect of nocodazole on endocytic uptake pathway depends on the cell type.[21] Inhibition of uptake of FITC-cIBR and FITC-dextran by this compound suggested that the intact microtubule network was necessary for the receptor-mediated uptake of FITC-cIBR

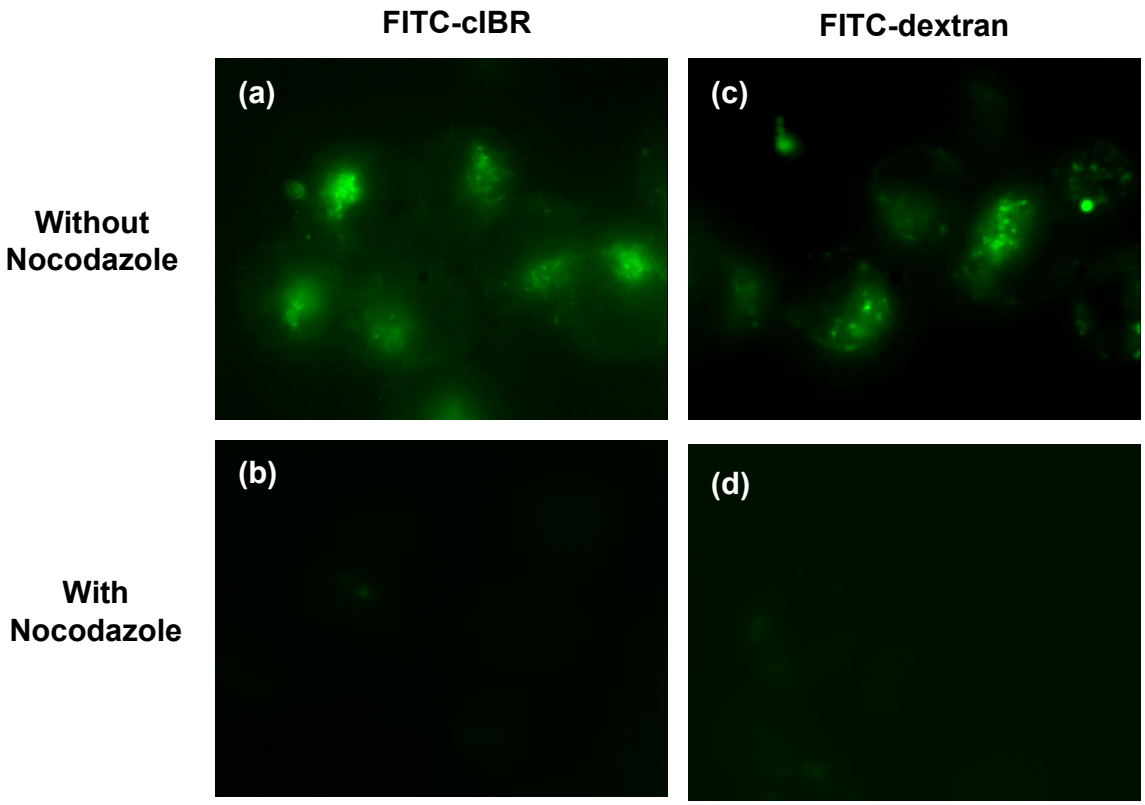

Figure 2.3(a-d) FITC-cIBR entry into HL-60 cells was blocked by a microtubule disrupting agent, nocodazole. Panel **(a)** represents the internalization of FITC-cIBR into HL-60 cells without nocodazole. Panel **(b)** shows that FITC-cIBR entry into the cells was blocked by the disruption of microtubules by nocodazole. Internalization profiles of FITC-dextran in the **(c)** absence and **(d)** presence of nocodazole were compared as control.

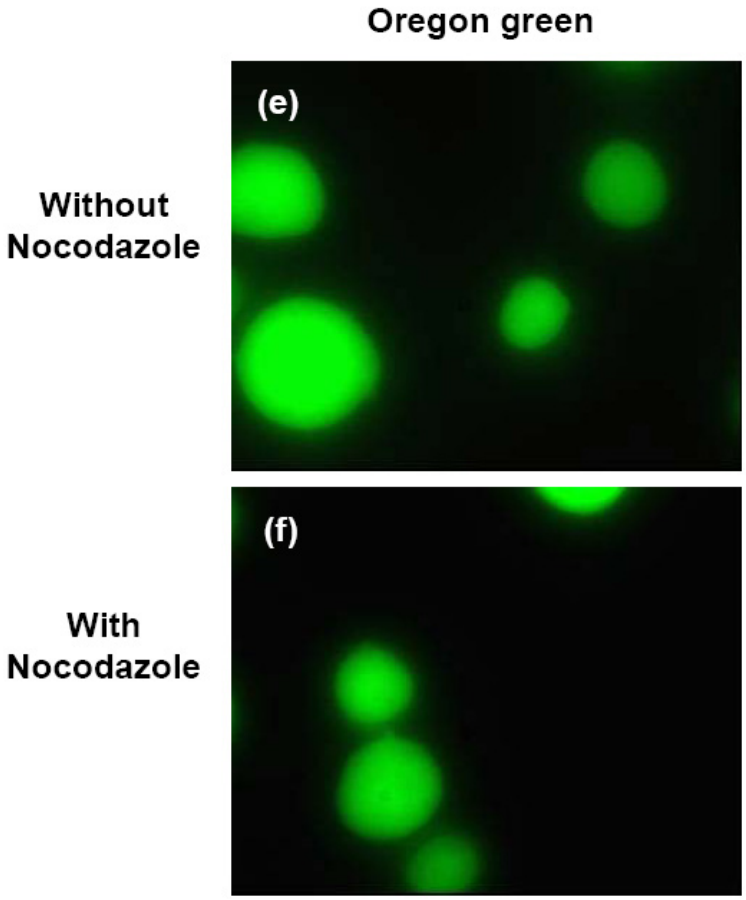

Figure 2.3(e-f) Entry of Oregon Green in HL-60 cells was not affected by the disruption of microtubule network by nocodazole. Panel **(e)** shows the uptake of Oregon Green in absence of nocodazole. Panel **(f)** shows the fluorescence intensity and distribution pattern of Oregon Green inside the cells were not affected by nocodazole.

as well as the fluid phase uptake of FITC-dextran by HL-60 cells.

2.3.2 Comparison of Intracellular Distribution of DOX and DOX-cIBR using HL-60 Cells

The possibility of utilizing cIBR peptide to target DOX to HL-60 cells was evaluated using DOX-cIBR conjugate. The intracellular distributions of DOX-cIBR were compared to those of DOX alone by observing the fluorescence of DOX at emission λ of 540 nm after excitation at λ of 480 nm. Because DOX is toxic, the viability of cells at the concentration used for uptake studies was evaluated using Trypan blue staining to ensure that DOX did not induce cell death during the study. Neither DOX nor DOX-cIBR killed HL-60 cells under the conditions used for the uptake studies (data not shown). At 37 °C, DOX-cIBR was found primarily in the cytoplasm, and there was no apparent distribution of the molecules in the endosomes or nucleus (Figure 2.4a). Although there was a decrease in the intensity of DOX-cIBR in the cytoplasm of HL-60 cells when cells were incubated at 4 °C, there was no inhibition of uptake of DOX-cIBR (Figure 2.4b). This suggests that conjugation of DOX to cIBR altered the receptor-mediated endocytic uptake of cIBR (see above). DOX incubated at 37 °C showed a high distribution in the nucleus with lower distribution in the cytoplasm (Figure 2.4c). Migration of DOX into the nucleus has been shown to be time- and concentration-dependent.[24] Lowering the incubation temperature from 37 °C to 4 °C inhibited the uptake of DOX to some degree, and its distribution was shown in the nucleus as well as the cytoplasm (Figure 2.4d). The

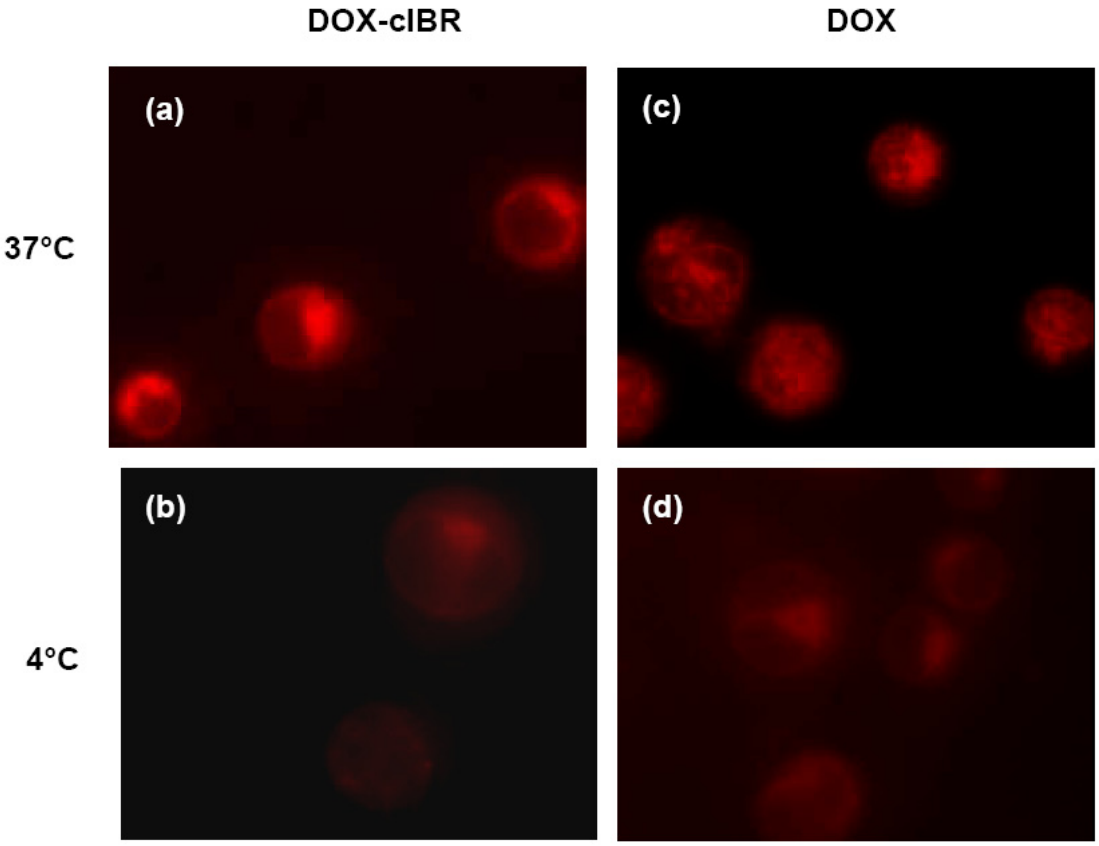

Figure 2.4(a-d) DOX-cIBR entry into the HL-60 cells was not affected by temperature. Panel **(a)** shows the diffuse cytoplasmic fluorescence distribution pattern of DOX-cIBR at 37 °C inside HL-60 cells. Absence of punctate fluorescence pattern was indicative of non-endocytic uptake pathway. Panel **(b)** shows uptake of DOX-cIBR by the cells when incubated at 4 °C. Incubation at 4 °C did not prevent the conjugate entry or change its intracellular distribution pattern. As a control DOX uptake profiles were compared at **(c)** 37 °C and **(d)** 4 °C

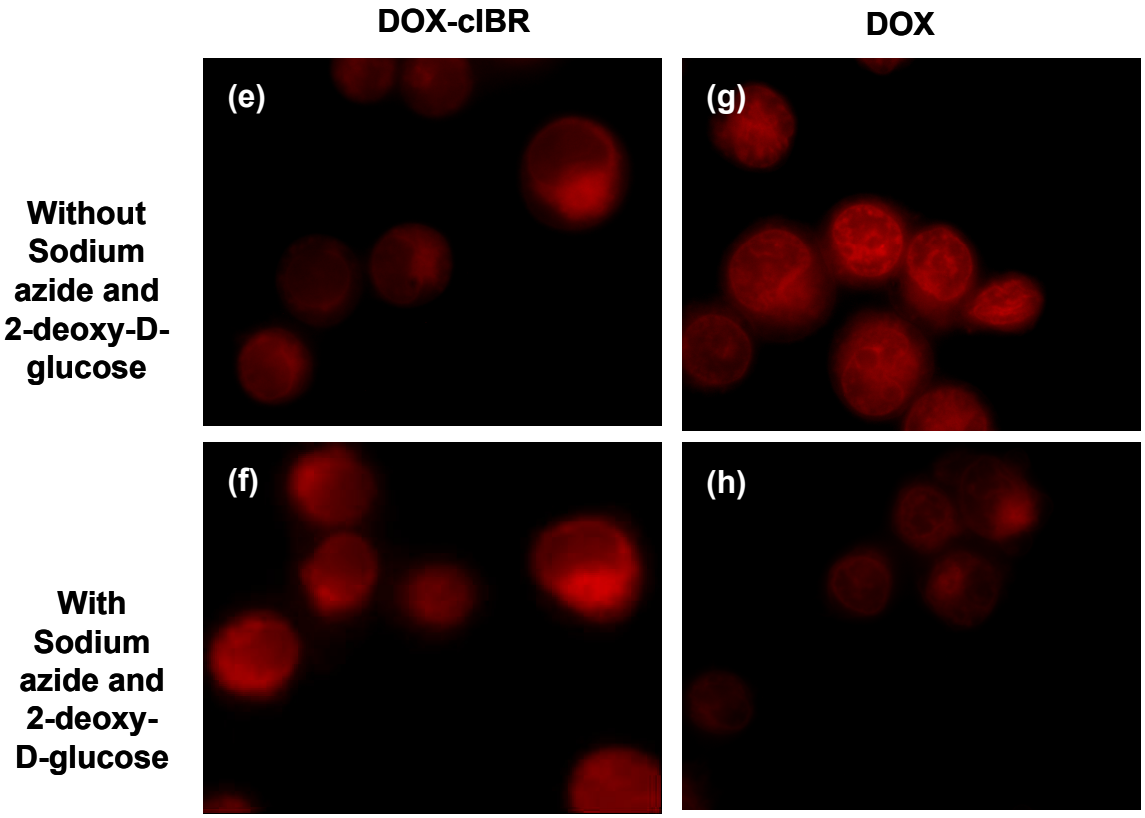

Figure 2.4(e-h) DOX-cIBR entry into HL-60 cells was not affected by the ATP synthesis inhibitors sodium azide and 2-deoxy-D-glucose. Panel **(e)** shows the diffuse cytoplasmic distribution profile of DOX-cIBR in absence of these compounds. In presence of the inhibitors there was no change in the distribution profile or the intensity of fluorescence of DOX-cIBR inside the cell as shown in Panel **(f)**. For comparison, DOX internalization profiles are shown in **(g)** absence and **(h)** presence of sodium azide and 2-deoxy-D-glucose.

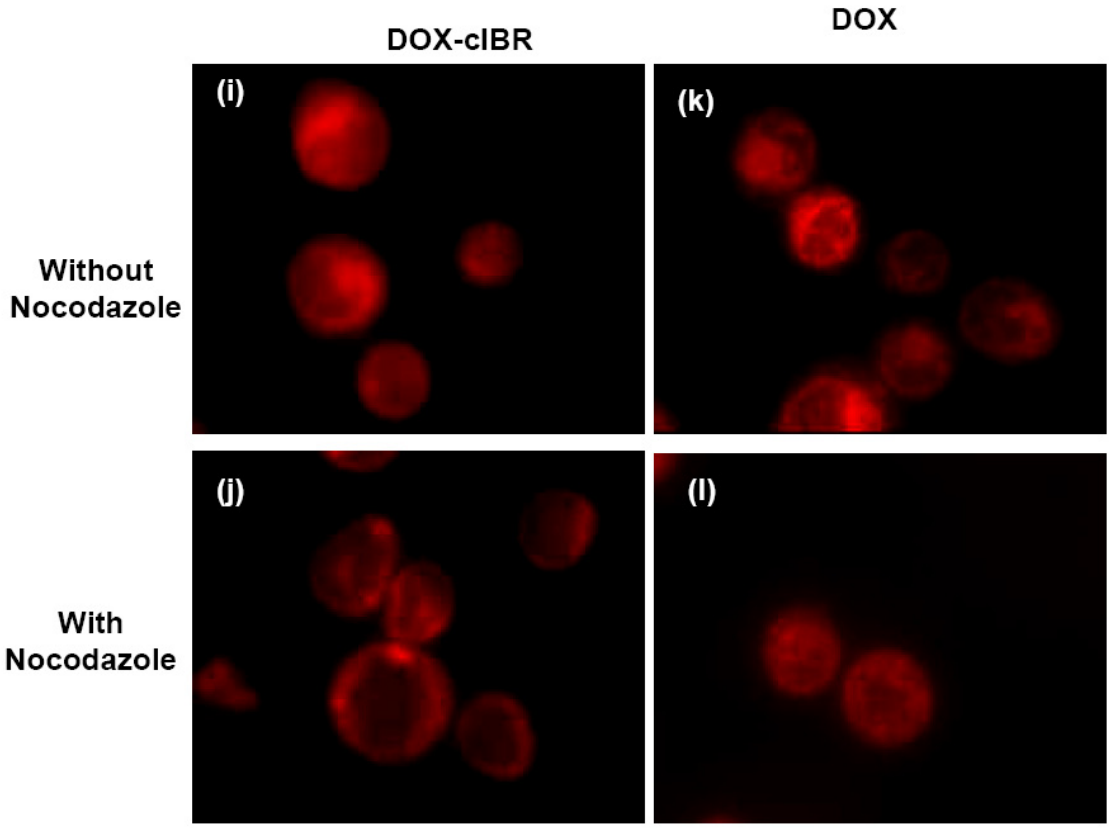

Figure 2.4(i-l) Depolymerization of microtubule assembly by nocodazole did not inhibit the entry of DOX-cIBR into the HL-60 cells. Panel **(i)** shows the fluorescence micrograph of the cells incubated with DOX-cIBR conjugate in absence of nocodazole. Panel **(j)** shows that the cells incubated with nocodazole did not show any change in fluorescence distribution pattern or intensity. Nocodazole did not have any effect on the internalization of the passively permeating DOX as shown in Panels **(k)** and **(l)**.

effect of the energy-dependent process on DOX-cIBR uptake was evaluated by incubating the HL-60 cells with sodium azide and 2-deoxy-D-glucose for 1 h prior to incubation with DOX-cIBR. The results showed that there was no difference in the cell cytoplasmic fluorescence from DOX-cIBR on untreated (Figure 2.4e) and treated (Figure 2.4f) cells. This suggests that DOX-cIBR could still enter the cell cytosol in the absence of ATP. Similarly, DOX alone was also not affected by the inhibition of energy-dependent processes (Figures 2.4g,h). As shown previously, FITC-dextran cell entry was blocked by the inhibitors. These results may suggest that the major route of DOX-cIBR entry into HL-60 cells was via passive diffusion rather than the receptor-mediated endocytosis process.

HL-60 cells were also incubated with nocodazole to evaluate the effect of microtubule disruption on the entry of DOX-cIBR compared to that of DOX. The fluorescence intensity of DOX-cIBR in the cell cytoplasm was not distinguishable in the absence (Figure 2.4i) and presence (Figure 2.4j) of nocodazole, suggesting that DOX-cIBR internalization did not involve microtubule formation. Similarly, the fluorescence intensity in the cells incubated with DOX appeared to be similar in the presence (Figure 2.4l) and absence (Figure 2.4k) of nocodazole. Taken together, these results suggested that the major route of cellular uptake of DOX-cIBR and DOX was not via a receptor-mediated endocytic process but via passive diffusion.

2.3.3 Comparison of Uptake of FITC-cIBR and DOX-cIBR using HUVEC

LFA-1 receptor deficient cell line HUVEC was used as a model system in order to further explore the internalization profiles of FITC-cIBR and DOX-cIBR. It was expected that HUVEC might show difference in internalization profiles for the two conjugates as it lacks the target receptor that recognizes the cIBR peptide. DOX-cIBR entered the HL-60 cells by passive diffusion and as such its entry into the cell would not be inhibited by the lack of LFA-1 receptor in a cell line. FITC-dextran would be able to enter these cells as it enters by fluid phase endocytosis. Comparison of the panels (a) and (c) of Figure 2.5 shows that FITC-cIBR entry in HUVEC was inhibited compared to that of FITC-dextran. The reduced fluorescence intensity of FITC-cIBR inside the cell possibly reflected the requirement of LFA-1 receptor for its internalization. Ideally, FITC-cIBR should also be taken up by the HUVEC by non specific endocytosis like FITC-dextran. It was possible that some fraction of FITC-cIBR entered into these cells by non-specific endocytosis. However, it was difficult to observe the fluorescence from intracellular FITC-cIBR possibly because of the association of FITC with external cell adhering glass surface which produced high background fluorescence. DOX-cIBR was found inside the HUVECs (Figure 2.5b) with high fluorescence intensity.

2.3.4 Physicochemical Properties of DOX-cIBR and FITC-cIBR

The stability of DOX-cIBR was evaluated in the presence of HL-60 cells using the same conditions as those in the experiments for endocytic uptake process. This was done to make sure that the presence of fluorescence in the cytoplasm of HL-

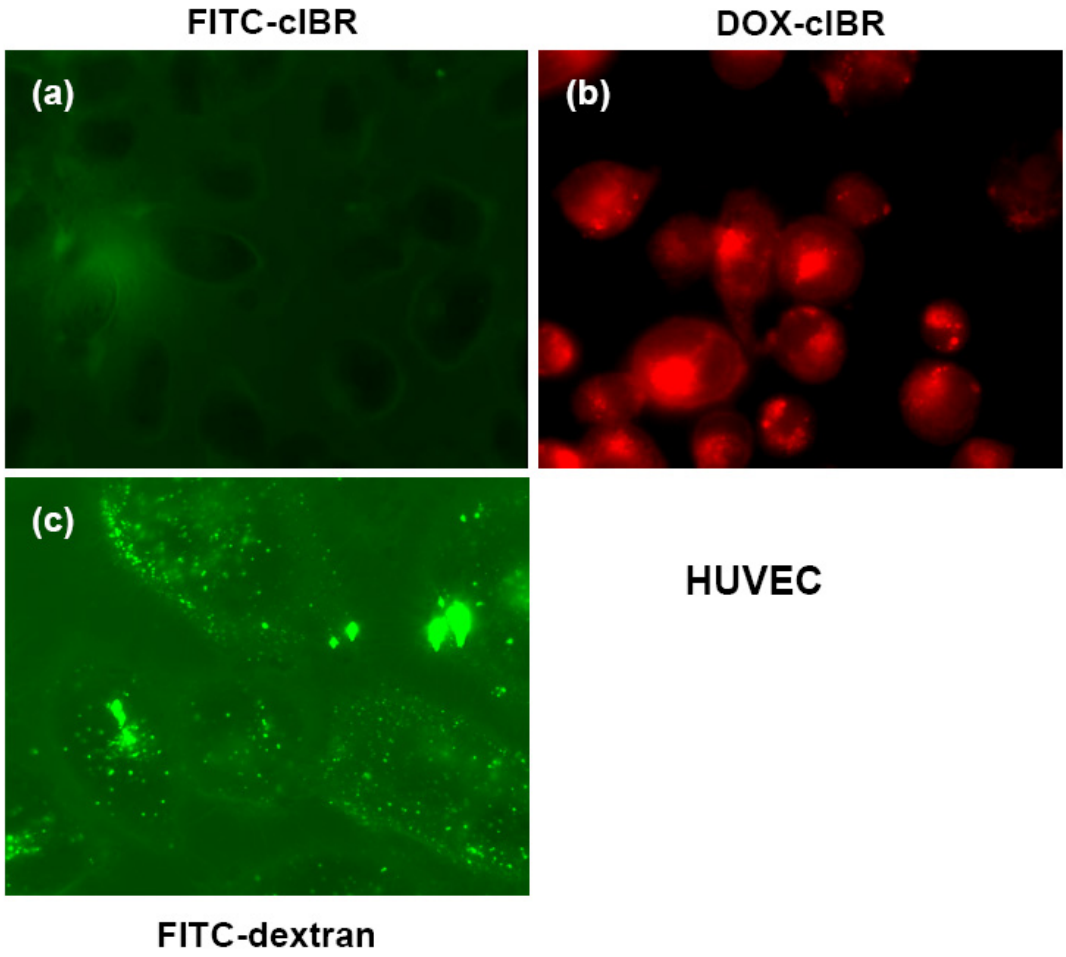

Figure 2.5(a-c) FITC-cIBR entry in HUVEC was inhibited compared to FITC-dextran and DOX-cIBR. Panel **(a)** shows the cells incubated with FITC-cIBR. Intracellular fluorescence of FITC-cIBR was low suggesting inhibited entry of the compound. The small amount of compound entering the cell might be the result of fluid phase endocytosis. Panel **(b)** shows that DOX-cIBR entered these cells as the mechanism of entry for this compound is passive diffusion. Panel **(c)** shows the cellular entry and intracellular distribution profile for FITC-dextran in HUVEC.

60 cells was due to the intact DOX-cIBR and not to its degradation products (*e.g.*, free DOX). DOX-cIBR was incubated for 24 h with HL-60 cells, and the cells were isolated and lysed with acetonitrile at different time points. After removal of the cell debris by centrifugation, the acetonitrile supernatant solution was injected into an analytical HPLC with a C18 column. The disappearance of DOX-cIBR and the appearance of new peaks due to the degradation of DOX-cIBR were monitored at 480 nm to avoid interference from the proteins derived from the medium and cells. The area under the curve from the DOX-cIBR peak was integrated as a function of time (Figure 2.6). The results showed that 11.5% degradation of DOX-cIBR was observed in the first 2 h of incubation; prolonged incubation up to 24 h produced only 15% degradation. The results suggest that that the majority of DOX-cIBR was intact during the 24-h incubation in endocytic studies and that the fluorescence stains found inside the cell are due to the DOX-cIBR.

To compare the difference in lipophilicity between FITC-cIBR and DOX-cIBR conjugates, the octanol/water distribution ratios for both compounds were determined to predict the possibility of the conjugates entering the cells via passive diffusion (Table 2.1). Normally, small molecules with high lipophilicity (Log D between 1 and 3, pH 7.4) can readily partition into cell membranes and enter cells via passive diffusion. The results show that FITC-cIBR (Log D = 0.58, pH 7.4) is more hydrophilic than DOX-cIBR (Log D = 1.14, pH 7.4) but FITC-cIBR is less hydrophilic than DOX (Log D = 0.08, pH 7.4). The high hydrophobicity of DOX-cIBR explains its effective partitioning into the cell membranes and passive

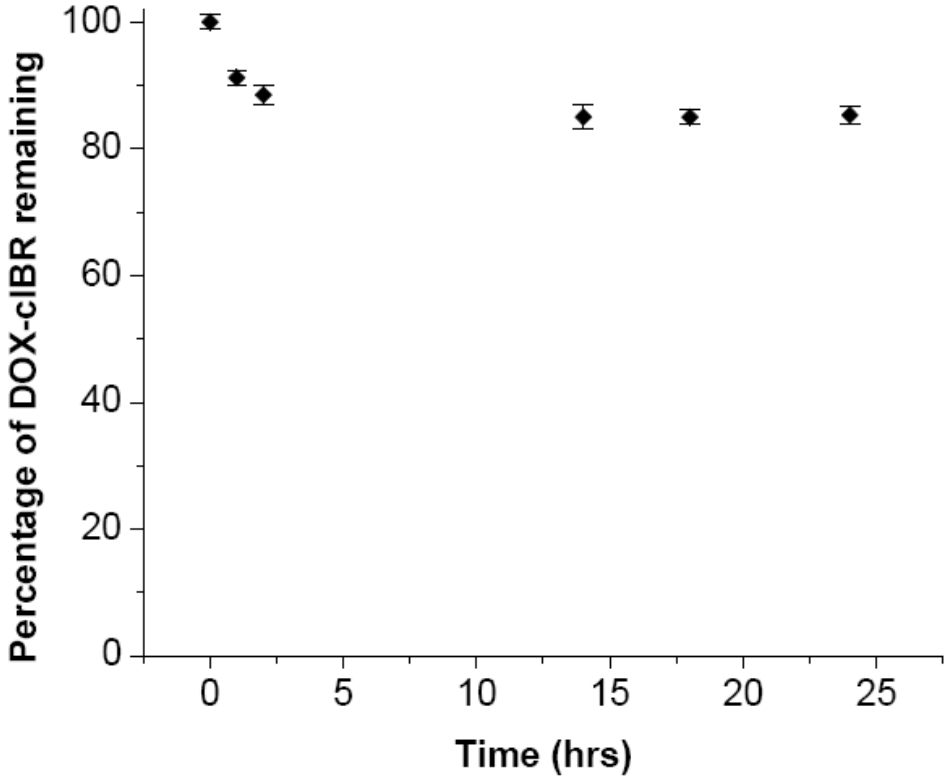

Figure 2.6 Time-dependent stability of DOX-cIBR in medium containing HL-60 cell line was determined by C18 reverse phase HPLC. The percent of DOX-cIBR remaining was determined by integrating the area under the curve for DOX-cIBR at a detection wavelength of 480 nm.

Table 2.1 Experimentally determined distribution ratio for DOX-cIBR and FITC-cIBR with 1-octanol/ aqueous buffer at pH 7.4.

Compounds	**Distribution ratio (D)**	**Log D**
DOX-cIBR	14.1	1.15
FITC-cIBR	3.8	0.58
DOX	1.2 (1.2*)	0.08
*Value in parenthesis is from reference 30		

permeation into the cell. Although FITC-cIBR is more hydrophobic than DOX, it does not partition into the membrane compared to DOX possibly due to its higher hydrogen-bonding potential with water.

2.4 Discussion

We have shown that FITC-cIBR was internalized by HL-60 via receptor-mediated endocytosis. The endocytosis may be due to the presence of LFA-1 on the HL-60 cells and binding properties of the FITC-cIBR to LFA-1, since LFA-1 receptors have been shown to be internalized and recycled by leukocytes.[25] In addition, internalization of FITC-cIBR was inhibited in the LFA-1-deficient HUVEC. FITC-cIBR peptide had been shown to bind to isolated LFA-1 and LFA-1 on the surface of T cells. This binding process could be inhibited by unlabeled cIBR peptide as well as antibodies to the I-domain of LFA-1.[14] FITC-cIBR could co-localize with anti-β_2-antibodies on the surface of T cells, suggesting that this peptide binds β_2-integrins such as LFA-1.[14] MOLT-3 and SKW T-cells could take up FITC-cIBR; however, due to the size of T cells, it was difficult to study the intracellular trafficking of FITC-cIBR in T cells compared to that in HL-60 cells.[14,16] The binding site of FITC-cIBR is at the L-site and a possible second binding site is at the MIDAS region of the LFA-1 I-domain.[15] Due to leukocyte selectivity of FITC-cIBR, the possibility of using cIBR peptide to target the anticancer drug DOX to leukemic cells (*i.e.*, HL-60 cells, MOLT-3 T cells) was investigated. DOX has been shown to be a good model drug for conjugation of carrier molecules (*i.e.*, peptides, proteins,

carbohydrates, polymers) for targeted drug delivery because its entry into the cell can be monitored by fluorescence microscopy. Thus, the endocytosis mechanism of DOX-cIBR was compared to that of FITC-cIBR with the expectation that both molecules would be internalized via a receptor-mediated endocytosis process.

It was interesting to find that DOX-cIBR passively diffused through the cell membrane of HL-60 cells, which was contrary to FITC-cIBR. The change in internalization behavior of these two conjugates may be due to many different factors. First, the high hydrophobicity of DOX-cIBR compared to FITC-cIBR (Table 2.1) may alter its mechanism of entry into the cells. It is possible that a small fraction of DOX-cIBR was internalized via a receptor-mediated process; however, due to the high fraction that partition into the cell membranes, the receptor-mediated process was overwhelmed by the passive diffusion mechanism (Figure 2.7). Secondly, the conjugation of DOX to cIBR may dramatically change the conformation of cIBR peptide compared to the conjugation of FITC to cIBR. The dramatic change in conformation of cIBR prevents the recognition of the cIBR fragment of DOX-cIBR by the receptor (*i.e.*, LFA-1) on the cell surface. Our previous studies have shown that the recognition site of cIBR peptide is at the Pro-Arg-Gly-Gly (PRGG) sequence, which resides at the N-terminus.[26] The PRGG sequence is in a stable β-turn structure as determined by NMR.[27] Conjugation of the N-terminus with another drug, methotrexate, did not change the β-turn conformation of this recognition site. Finally,

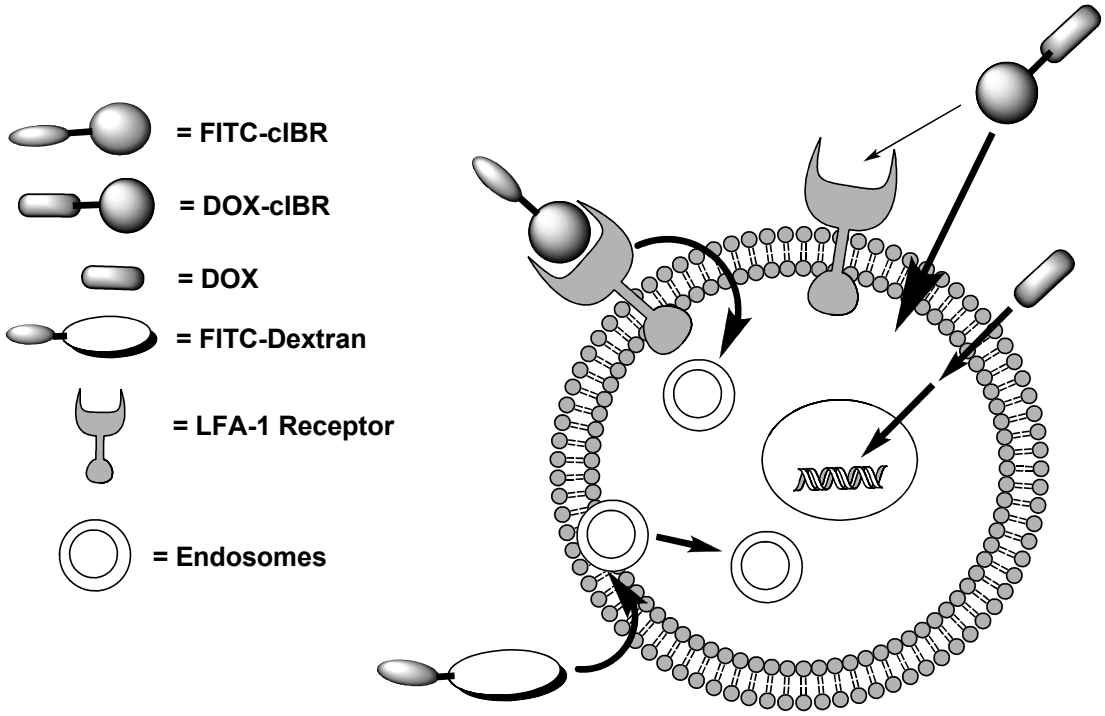

Figure 2.7. Schematic representation of the cellular entry mechanism of FITC-cIBR, FITC-dextran, DOX-cIBR, and DOX in HL-60 cells. FITC-cIBR enters the cells via a receptor-mediated process into the endosomes while FITC-dextran enters the endosomes via fluid-phase endocytosis. On the other hand, DOX-cIBR passively permeates through the cell membranes and resides in the cytoplasm, and DOX enters the cell via passive diffusion and finally resides in the nucleus.

it is also possible that the DOX fragment imposes steric hindrance on the recognition site of cIBR peptide as compared to that of the FITC fragment in FITC-cIBR. Because both DOX and FITC are conjugated to the N-terminus, there is a high probability that conjugation of a moiety to the N-terminus may interfere with the recognition of cIBR. Therefore, further structural studies will be carried out to elucidate the effect of DOX conjugation to the cIBR structure.

Normally, the passive diffusion mechanism is used by small hydrophobic drugs such as doxorubicin with molecular weights of 500 daltons following Lipinski's rules.[28] These molecules readily partition into cell membranes to cross the lipid bilayers. In contrast, large hydrophilic peptides with a high hydrogen-bonding potential are not readily partitioned into the cell membranes because it is energetically unfavorable to expel hydrogen-bonded water molecules.[28] However, DOX-cIBR has a very high octanol/water distribution ratio (pH 7.4) compared to FITC-cIBR and DOX (Table 2.1). The high distribution ratio of DOX-cIBR could explain the high propensity of DOX-cIBR to partition to cell membranes for passive diffusion. It is possible that conjugating DOX to cIBR peptide causes altered conformation of the conjugate to produce low hydrogen-bonding potential to water molecules. Based on the magnitude of the distribution ratio alone, FITC-cIBR should passively diffuse more readily than DOX alone. Instead, FITC-cIBR is internalized by a receptor-mediated process and DOX enters the cell mainly via passive diffusion. We propose that a balance exists between passive diffusion and the receptor-mediated mechanism, depending on the moiety or drug molecule that is attached to the cIBR peptide (Figure

2.7). If this is the case, the choice of drug molecule that can be conjugated to cIBR to maintain the receptor-mediated internalization properties may be limited to drugs that do not dramatically change the octanol/water distribution ratio. In other words, the distribution ratio of the conjugate should be at least similar to or lower than that of FITC-cIBR for receptor-mediated entry into the cells.

Others have conjugated DOX to peptides, proteins, oligonucleotides, and other type of carriers. A reported conjugate of DOX with a cell-penetrating peptide showed cytoplasmic distribution of the conjugate similar to that in DOX-cIBR. Unfortunately, it is not clear whether the DOX conjugate with cell-penetrating peptides enters the cell via passive diffusion or via receptor-mediated endocytosis.[29] In another study, DOX was also conjugated to a cyclic pentapeptide (CNGRC) to give DOX-CNGRC conjugate for targeting CD13 on the surface of the SK-UT-1 cell line.[30] Similar to our DOX-cIBR, the DOX-CNGRC conjugate was found in the cell cytoplasm. It has been suggested that the uptake of DOX-CNGRC is not via receptor-mediated but via passive diffusion because DOX-CNGRC has a high octanol/water distribution ratio (5.3, pH 7.4).[30] This distribution ratio is in between those of DOX-cIBR (14.1, pH 7.4) and FITC-cIBR (3.8, pH 7.4). It was also surprising to find that a DOX-transferrin conjugate was distributed in the cytoplasm and its entry into the cells could not be blocked by transferrin or lower temperature.[9,31] These results suggest that this conjugate entry was not mediated by the transferrin receptor. Because transferrin is a large molecule, it is difficult to envision that this conjugate could penetrate the cell membrane through passive diffusion. Another possible

explanation is that conjugation of the molecule to DOX may alter the conjugate physical properties and induce the formation of a molecular association that promotes partitioning into the cell membrane and permeation into the cytoplasm. Regen et al. have proposed possible mechanisms (*i.e.*, umbrella mechanism) of membrane partitioning of a conjugate between a sugar molecule and an oligonucleotide or peptide that led to cell membrane permeation.[32-34] Because DOX contains an amino sugar moiety, DOX-peptide conjugates may follow the umbrella mechanism to enter the cells via the passive route. Thus, DOX rather than the peptide becomes the important molecule for membrane partitioning; however, further studies need to be done to elucidate this possible mechanism.

The uptake of DOX-cIBR and DOX was affected by temperature; lower fluorescence intensities of these molecules were found in the cytoplasm at 4 °C than at 37 °C. It has been suggested that lower diffusion of DOX at 4 °C than 37 °C is due to the increase in self-association of DOX at 4 °C via the formation of π-interactions.[35] The effect of temperature on the uptake of DOX-cIBR could also be caused by the self-association of the conjugate at 4 °C. Alternatively, DOX-cIBR could enter the cell via a combination of passive and active transport at 37 °C but only via passive permeation at 4 °C. A similar hypothesis has been suggested for the internalization of the DOX-transferrin conjugate.[9] Due to the high octanol/water distribution ratio observed of DOX-cIBR, the passive diffusion pathway overwhelms the receptor-mediated transport of DOX-cIBR at 37 °C (Figure 2.7). As seen for FITC-cIBR, cIBR peptide did not show any cell surface staining when incubated at

4 °C, suggesting that the binding of cIBR peptide to LFA-1 was low at low temperature**.** An alternative explanation is that the cells may have a higher population of LFA-1 in a conformation with low affinity for the ligand at 4 °C. Similarly, DOX-cIBR did not show any cell surface staining at 4 °C, suggesting that it did not bind to the cell surface receptors. Unfortunately, unlike FITC-cIBR, it was difficult to differentiate between the cytoplasmic and cell surface staining when HL-60 cells are treated with DOX-cIBR in the presence of ATP inhibitors at 37 °C.

2.5 Conclusions

We have shown that FITC-cIBR peptide can be internalized via a receptor-mediated pathway, suggesting that cIBR peptide may be internalized by the LFA-1 receptor on HL-60 cells. The use of hydrophobic drugs such as DOX in the DOX-cIBR conjugate may change receptor-mediated transport to passive diffusion transport. This study has shown the importance of the physicochemical properties of the drug-peptide conjugate when considering the use of the peptide for cell-specific targeted drug delivery. We postulate that, to maintain the receptor-mediated endocytic pathway, a hydrophilic drug should be used to conjugate to cIBR peptide and that the octanol/water distribution ratio of the conjugate should be at least the same as or lower than the distribution ratio of FITC-cIBR. Another way to improve the internalization is to modify the peptide to make it more hydrophilic while retaining the binding site to the target receptor. Future work will explore this possibility by conjugating modified cIBR peptide to DOX. If a more hydrophilic conjugate of DOX

can be synthesized then it might be possible to change the internalization mechanism of DOX-peptide conjugate from an energy independent pathway to a receptor mediated process.

2.6 References

1. Garnett MC 2001.Targeted drug conjugates: principles and progress. Adv Drug Del Rev 53(2):171-216.

2. Dunehoo AL, Anderson M, Majumdar S, Kobayashi N, Berkland C, Siahaan TJ 2006.Cell adhesion molecules for targeted drug delivery. J Pharm Sci 95(9):1856-1872.

3. Lu Y, Low PS 2002.Folate-mediated delivery of macromolecular anticancer therapeutic agents. Adv Drug Del Rev 54(5):675-693.

4. Lu Y, Sega E, Leamon CP, Low PS 2004.Folate receptor-targeted immunotherapy of cancer: mechanism and therapeutic potential. Adv Drug Del Rev 56(8):1161-1176.

5. Sudimack J, Lee RJ 2000.Targeted drug delivery via the folate receptor. Adv Drug Del Rev 41(2):147-162.

6. Faulk WP, Taylor CG, Yeh CJ, McIntyre JA 1990.Preliminary clinical study of transferrin-adriamycin conjugate for drug delivery to acute leukemia patients. Mol Biother 2(1):57-60.

7. Kovar M, Strohalm J, Ulbrich K, Rihova B 2002.In vitro and in vivo effect of HPMA copolymer-bound doxorubicin targeted to transferrin receptor of B-cell lymphoma 38C13. J Drug Targeting 10(1):23-30.

8. Eavarone DA, Yu X, Bellamkonda RV 2000.Targeted drug delivery to C6 glioma by transferrin-coupled liposomes. J Biomed Mater Res 51(1):10-14.

9. Kratz F, Beyer U, Roth T, Tarasova N, Collery P, Lechenault F, Cazabat A, Schumacher P, Unger C, Falken U 1998.Transferrin conjugates of doxorubicin: synthesis, characterization, cellular uptake, and in vitro efficacy. J Pharm Sci 87(3):338-346.

10. Kratz F, Roth T, Fichiner I, Schumacher P, Fiebig HH, Unger C 2000.In vitro and in vivo efficacy of acid-sensitive transferrin and albumin doxorubicin conjugates in a human xenograft panel and in the MDA-MB-435 mamma carcinoma model. J Drug Targeting 8(5):305-318.

11. Triantafilou K, Takada Y, Triantafilou M 2001.Mechanisms of integrin-mediated virus attachment and internalization process. Crit Rev Immunol 21(4):311-322.

12. Arap W, Pasqualini R, Ruoslahti E 1998.Cancer treatment by targeted drug delivery to tumor vasculature in a mouse model. Science 279(5349):377-380.

13. Chen X, Plasencia C, Hou Y, Neamati N 2005.Synthesis and biological evaluation of dimeric RGD peptide-paclitaxel conjugate as a model for integrin-targeted drug delivery. J Med Chem 48(4):1098-1106.

14. Anderson ME, Siahaan TJ 2003.Mechanism of binding and internalization of ICAM-1-derived cyclic peptides by LFA-1 on the surface of T cells: a potential method for targeted drug delivery. Pharm Res 20(10):1523-1532.

15. Anderson ME, Tejo BA, Yakovleva T, Siahaan TJ 2006.Characterization of binding properties of ICAM-1 peptides to LFA-1: inhibitors of T-cell adhesion. Chem Biol Drug Des 68(1):20-28.

16. Gursoy RN, Siahaan TJ 1999.Binding and internalization of an ICAM-1 peptide by the surafce receptors of T cells. J Pept Res 53:414-421.

17. Potocky TB, Menon AK, Gellman SH 2003.Cytoplasmic and nuclear delivery of a TAT-derived peptide and a beta-peptide after endocytic uptake into HeLa cells. J Biol Chem 278(50):50188-50194.

18. Gong Y, Duvvuri M, Duncan MB, Liu J, Krise JP 2006.Niemann-Pick C1 protein facilitates the efflux of the anticancer drug daunorubicin from cells according to a novel vesicle-mediated pathway. J Pharmacol Exp Ther 316(1):242-247.

19. Stenbeck G, Horton MA 2004.Endocytic trafficking in actively resorbing osteoclasts. J Cell Sci 117(Pt 6):827-836.

20. Thilo L, Stroud E, Haylett T 1995.Maturation of early endosomes and vesicular traffic to lysosomes in relation to membrane recycling. J Cell Sci 108 (Pt 4):1791-1803.

21. Baravalle G, Schober D, Huber M, Bayer N, Murphy RF, Fuchs R 2005.Transferrin recycling and dextran transport to lysosomes is differentially affected by bafilomycin, nocodazole, and low temperature. Cell Tissue Res 320(1):99-113.

22. Knowles AF, Nagy AK 1999.Inhibition of an ecto-ATP-diphosphohydrolase by azide. Eur J Biochem 262(2):349-357.

23. Aft RL, Zhang FW, Gius D 2002.Evaluation of 2-deoxy-D-glucose as a chemotherapeutic agent: mechanism of cell death. Br J Cancer 87(7):805-812.

24. Decorti G, Peloso I, Favarin D, Klugmann FB, Candussio L, Crivellato E, Mallardi F, Baldini L 1998.Handling of doxorubicin by the LLC-PK1 kidney epithelial cell line. J Pharmacol Exp Ther 286(1):525-530.

25. Fabbri M, Di Meglio S, Gagliani MC, Consonni E, Molteni R, Bender JR, Tacchetti C, Pardi R 2005.Dynamic partitioning into lipid rafts controls the endo-exocytic cycle of the alphaL/beta2 integrin, LFA-1, during leukocyte chemotaxis. Mol Biol Cell 16(12):5793-5803.

26. Anderson ME, Yakovleva T, Hu Y, Siahaan TJ 2004.Inhibition of ICAM-1/LFA-1-mediated heterotypic T-cell adhesion to epithelial cells: design of ICAM-1 cyclic peptides. Bioorg Med Chem Lett 14(6):1399-1402.

27. Gursoy RN, Jois DS, Siahaan TJ 1999.Structural recognition of an ICAM-1 peptide by its receptor on the surface of T cells: conformational studies of cyclo (1,

12)-Pen-Pro-Arg-Gly-Gly-Ser-Val-Leu-Val-Thr-Gly-Cys-OH. J Pept Res 53(4):422-431.

28. Lipinski CA, Lombardo F, Dominy BW, Feeney PJ 2001.Experimental and computational approaches to estimate solubility and permeability in drug discovery and development se. Adv Drug Del Rev 46:3-26.

29. Liang JF, Yang VC 2005.Synthesis of doxorubicin-peptide conjugate with multidrug resistant tumor cell killing activity. Bioorg Med Chem Lett 15(22):5071-5075.

30. van Hensbergen Y, Broxterman HJ, Elderkamp YW, Lankelma J, Beers JC, Heijn M, Boven E, Hoekman K, Pinedo HM 2002.A doxorubicin-CNGRC-peptide conjugate with prodrug properties. Biochem Pharmacol 63(5):897-908.

31. Lai BT, Gao JP, Lanks KW 1998.Mechanism of action and spectrum of cell lines sensitive to a doxorubicin-transferrin conjugate. Cancer Chemother Pharmacol 41(2):155-160.

32. Janout V, Jing B, Regen SL 2005.Molecular umbrella-assisted transport of an oligonucleotide across cholesterol-rich phospholipid bilayers. J Am Chem Soc 127(45):15862-15870.

33. Jing B, Janout V, Herold BC, Klotman ME, Heald T, Regen SL 2004.Persulfated molecular umbrellas as anti-HIV and anti-HSV agents. J Am Chem Soc 126(49):15930-15931.

34. Jing B, Janout V, Regen SL 2003.Fully detachable molecular umbrellas as peptide delivery agents. Bioconj Chem 14(6):1191-1196.

35. Dalmark M, Storm HH 1981.A Fickian diffusion transport process with features of transport catalysis. Doxorubicin transport in human red blood cells. J Gen Physiol 78(4):349-364.

Chapter 3

Effect of modification of the physicochemical properties of ICAM-1-derived peptides on internalization and intracellular distribution in the human leukemic cell line HL-60

3.1 Introduction

Targeted drug delivery methods have been exploited to improve the delivery of cytotoxic drugs to lower their side effects. These delivery methods normally take advantage of the special features of the target cells compared to other cells in the body. One of these features is the upregulation or selective expression of certain cell surface receptors in many types of cancers compared to the normal cells.[1-3] Furthermore, certain types of cells (leukocytes) express leukocyte function-associated antigen-1 (LFA-1) receptors, which are not expressed in other cell types.[4,5] Thus, the LFA-1 receptor is an attractive target receptor for improving delivery of drugs to leukocytes. In general, peptides[6], proteins,[7,8] and antibodies[9] have been employed as carriers of many cytotoxic drugs to target a specific cell surface receptor with some success in *in vitro* and *in vivo* model systems.

Doxorubicin (DOX) is an anticancer agent with cardiotoxicity as one of its side effects. To lower side effect, DOX has been conjugated to different carrier molecules such as peptides,[10] proteins[11] and other macromolecular carriers.[12] In addition, DOX has fluorescence properties that can be used to follow the distribution of the conjugate in cells and in *in vivo* systems. The cytotoxicity of DOX is due to its intercalation of DNA in the nucleus. DOX structure can be divided into three functional domains: (1) the hydrophobic anthraquinone moiety is for DNA intercalation, (2) several substituents on the cyclohexyl ring are involved in H-bonding with the DNA bases, and (3) the daunosamine sugar moiety can bind to the minor groove of DNA.[13] DOX has been conjugated to carrier molecules through the primary amine of the

daunosamine sugar,[14] C13 ketone functionality,[15] and C14 alcoholic hydroxyl functionality.[10] Among these conjugation sites, the primary amine of the daunosamine sugar moiety has been used to conjugate DOX to many different peptides.[14,16,17]

Previously, we have conjugated DOX to cIBR peptide cyclo(1,12)PenPRGGSVLVTGC to produce DOX-cIBR conjugate. This conjugate entered into the human leukemic cell line, HL-60, in an energy-independent manner (e.g., passive diffusion) and showed a diffuse fluorescence distribution pattern in the cytosol instead the punctate distribution pattern that was expected for a molecule internalized by receptor-mediated endocytosis. The passive diffusion uptake behavior of DOX-cIBR could be due to the hydrophobicity of the conjugate because the octanol/aqueous buffer distribution ratio (pH 7.4) determination indicated that DOX-cIBR conjugate is highly hydrophobic. Therefore, we hypothesize that the hydrophobicity of the conjugate is one of the factors contributing to passive diffusion of the conjugate over the receptor-mediated entry of the conjugate.[14] A DOX conjugate with CNGRC cyclic peptide (DOX-CNGRC) for targeting CD-13 receptor has high hydrophobicity and showed a distribution similar to the DOX-cIBR.[10]

The present work is designed to test the hypothesis that increasing the hydrophilicity of the conjugates may alter the entry mechanisms of DOX-cIBR-derivatives into HL-60 cells from passive diffusion to receptor-mediated uptake. Two approaches were used to change the physicochemical properties of the conjugate. The first was to change the hydrophobicity of the peptide by eliminating the hydrophobic residue at the C-terminus of cIBR. In this case, we have modified cIBR peptide to

cIBR7 peptide (cyclo(1,8)CPRGGSVC) by eliminating four hydrophobic residues at C-terminal of cIBR and by replacing the Pen1 residue with a Cys residue (Figure 3.1a,b). It is interesting to find that cIBR7 peptide has better activity to inhibit heterotypic T-cell adhesion than that of the parent cIBR peptide, suggesting that cIBR7 binds more selectively to the I-domain of LFA-1 than does cIBR peptide.[18] The second method was to incorporate 11-amino-3,6,9-trioxaundecanate linker between DOX and cIBR7 peptide to further increase the hydrophilicity of the conjugate to give DOX-PEGcIBR7 (Figure 3.1c). Fluorescein isothiocyanate (FITC) was also conjugated to cIBR7 peptide to give FITC-cIBR7 to check for endocytic uptake as was observed for FITC-labeled cIBR (FITC-cIBR).[14] In this work, we compared the entry mechanisms and the intracellular disposition of DOX-cIBR7, DOX-PEGcIBR7, and FITC-cIBR7 in HL-60 cells. The results from these studies will allow us to test whether the changes in the physicochemical properties of the conjugates influence their entry mechanism.

3.2 Experimental

3.2.1 Cells and Chemicals

The human acute promyeloid leukemic cell line HL-60 was kindly provided by Dr. Yueshang Zhang (Arizona Cancer Center, University of Arizona). Cells were grown in RPMI 1640 medium supplemented with 10% fetal bovine serum, 100 units/mL of penicillin G sodium, 100 μg/mL of streptomycin sulfate, and 2.0 g/L of

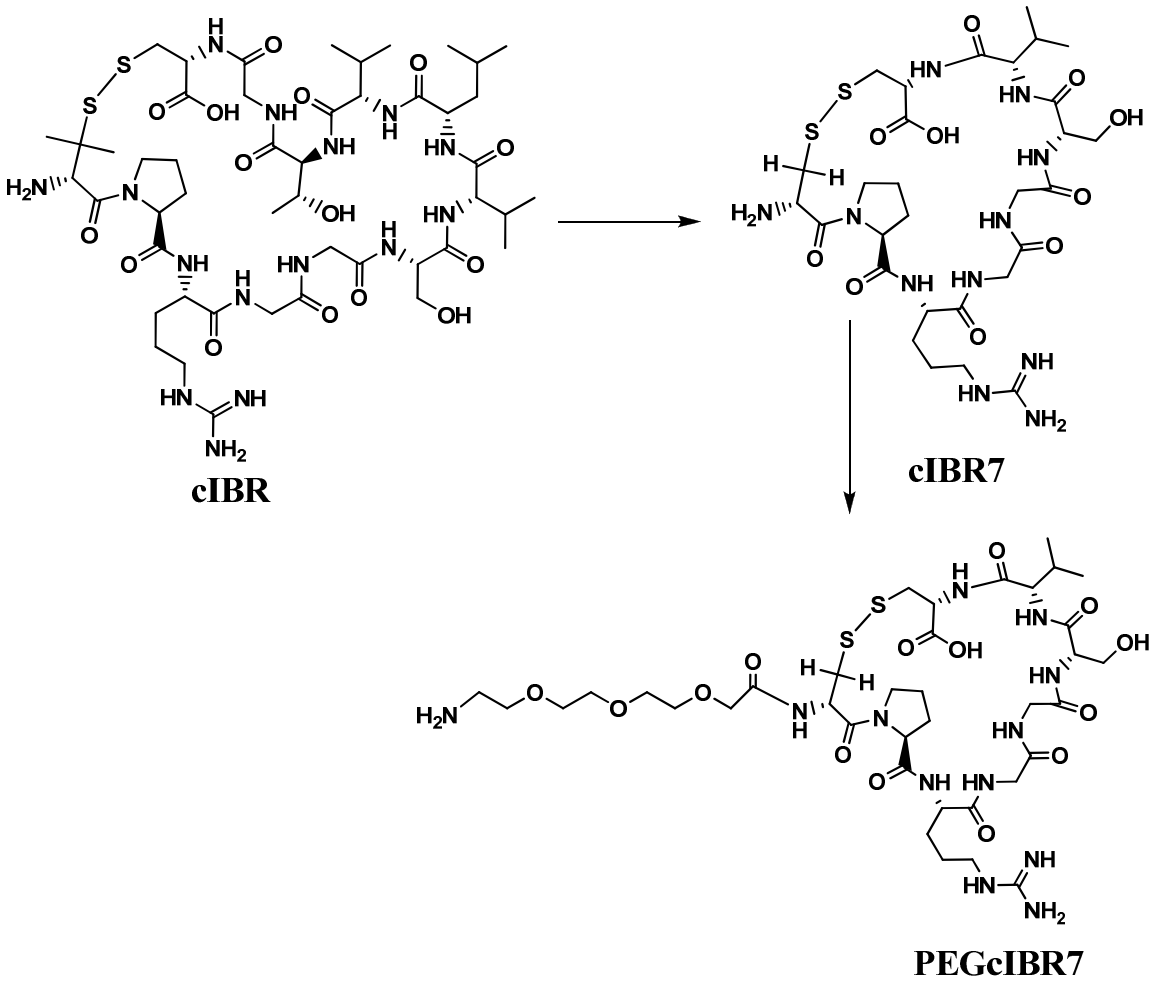

Figure 3.1 Modification of the cIBR peptide for conjugation with DOX-hemisuccinate adduct. **(a)** cIBR [cyclo(1,12)PenPRGGSVLVTGC] peptide **(b)** cIBR7 [cyclo(1,8)CPRGGSVC] peptide was synthesized by removing 'LVTG' from the C-terminal of cIBR peptide. Pen1 in cIBR was replaced by Cys1 in cIBR7 **(c)** PEGIBR7 peptide was synthesized by conjugating 11-amino-3,6,9-Trioxaundecanoic acid to the N-terminal of the IBR7 peptide by the solid phase method. PEGIBR7 was cyclized to obtain PEGcIBR7.

$NaHCO_3$. Cells were maintained at a density of 1×10^6 to 2×10^6 cells/mL at 37 °C in a humidified 5% CO_2 atmosphere. Doxorubicin hydrochloride, succinic anhydride, and diisopropylethyl amine were obtained from Sigma Chemicals (St. Louis, MO). Solvents used in peptide synthesis were of pure analytical grade. All reagents, resins, and Fmoc-protected amino acids for peptide syntheses were purchased from Peptides International (Louisville, KY), Advanced ChemTech (Louisville, KY), and Applied Biosystems (Foster City, CA). Fmoc-11-amino-3,6,9-trioxaundecanoic acid (Fmoc-mini-PEG-3™) was purchased from Peptides International (Louisville, KY) and FITC-dextran (MW 10,000) was from Molecular Probes™ (Eugene, OR).

3.2.2 Peptide Synthesis

Syntheses of linear IBR7 (CPRGGSVC) and PEGIBR7 (H_2N-$(CH_2CH_2$-O-$)_3$-CPRGGSVC) peptides were performed on a Pioneer peptide synthesizer (PerSeptive Biosystems, CA) using the standard Fmoc solid-phase strategy with O-(7-azabenzotriazole-1-yl)-N,N,N',N'-tetramethyluronium hexafluorophosphate (HATU) as the activating agent. Extended coupling cycles were employed. The resin-containing peptide was washed several times with methylene chloride and then with methanol followed by vacuum drying. A cleavage cocktail containing trifluoroacetic acid (TFA, 90%), 1,2-ethane dithiol (3%), anisole (2%), and thioanisole (5%) was used during peptide cleavage from the solid support followed by precipitation in ice-cold diethyl ether. Diethyl ether solution was allowed to stand overnight at 4 °C for maturation of the precipitate. Subsequently, the peptide precipitate was separated

from ether-containing scavengers by centrifugation. The crude linear peptides were purified by semi-preparative C18 reversed-phase HPLC. The cyclization of the linear peptides to give cIBR7 or PEGcIBR7 was carried out by bubbling air overnight into the peptide solution (0.06 mM) containing ammonium bicarbonate (0.05 M) and ammonium hydroxide at pH 8.5. The solution was lyophilized and crude cyclic peptides were purified by semi-preparative C18 reversed-phase HPLC. The molecular weights of cIBR7 (M+1 = 776.3 amu) and PEGcIBR7 (M+1 = 965.4 amu) peptides were confirmed by electrospray ionization mass spectrometry.

3.2.3 Conjugation of Doxorubicin (DOX) with cIBR7 and PEGcIBR7 Peptides

This reaction was performed according to the previously published method.[14] Briefly, the amino group in the sugar moiety of DOX was reacted with succinic anhydride in dimethyl formamide (DMF) in the presence of diisopropylethyl amine to give DOX-hemisuccinate (M+1 = 643 amu). Subsequently, DOX-hemisuccinate was reacted with the N-terminus of cIBR7 or PEGcIBR7 peptide in the presence of HBTU (O-benzotriazole-N,N,N′,N′-tetramethyl-uronium-hexafluoro-phosphate) in DMF to give DOX-cIBR7 or DOX-PEGcIBR7, respectively (Figure 3.2a,b). The progress of the reaction was monitored with C18 reversed-phase analytical HPLC. Both of the DOX-conjugates were purified using semi-preparative HPLC with a C18 column; the molecular weights of the DOX-cIBR7 (M+1 = 1401.5 amu) and DOX-PEGcIBR7 (M+1 = 1590.6 amu) were confirmed by mass spectrometry.

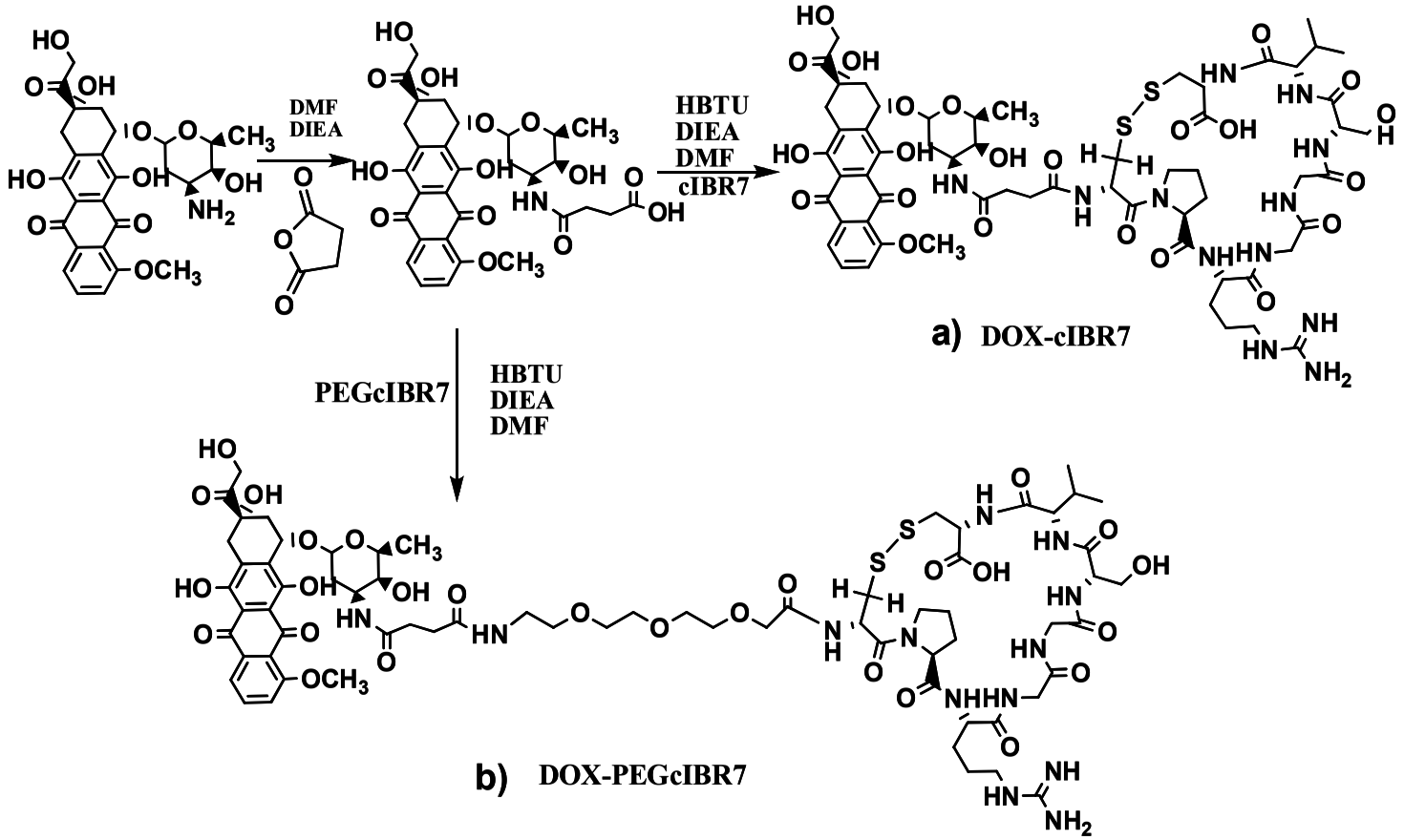

Figure 3.2 Synthesis of DOX conjugates of cIBR7 and PEGcIBR7 peptides. **(a)** DOX-cIBR7 conjugate and **(b)** DOX-PEGcIBR7 conjugate. Primary amine of the daunosamine of DOX was conjugated to succinic anhydride by amide bond to generate DOX-hemisuccinate. The N-terminal of the peptides was then conjugated to the carboxylic acid group of DOX-hemisuccinate by amide bond.

3.2.4 Conjugation of FITC with cIBR7 and cIBR Peptides

Conjugation of FITC with cIBR7 was done according to our previously published method.[14,19] Briefly, pure cIBR7 peptide (0.06 mmol) was dissolved in 5 mL of Nanopure water; 0.12 mmol fluorescein-5-isothiocyanate (Sigma) was added to the peptide solution and the pH was adjusted to 10 by addition of 1.0 N NaOH solution. After stirring for 2 h with a magnetic stirrer, the reaction mixture was neutralized by the addition of 10% v/v acetic acid solution (Figure 3.3). The solution was lyophilized and the resulting crude product of FITC-cIBR7 was purified by semi-preparative C18 reversed-phase HPLC. The pure FITC-cIBR7 was analyzed by analytical C18 reversed-phase HPLC and identified by electrospray ionization mass spectrometry (M+1 = 1165.3). Conjugation of FITC with cIBR was done in an identical manner and is described elsewhere.[14]

3.2.5 Determination of Octanol/Aqueous Buffer Distribution Ratios (pH 7.4) for DOX-cIBR7 and DOX-PEGcIBR7 Conjugates

1.0 mL of *n*-octanol (Fisher) was added to 10 mL of PBS (pH 7.4) containing 2.0 μM of DOX-cIBR7 or DOX-PEGcIBR7 in a separatory funnel and was mixed for 30 min. The two phases were allowed to equilibrate for 24 h while protected from light. The concentration of DOX-cIBR7 or DOX-PEGcIBR7 in each phase was determined using a fluorescence spectrophotometer (RF5000U, Shimadzu Inc., Kyoto, Japan). The fluorescence intensity of DOX-cIBR7 or DOX-PEGcIBR7 in aqueous buffer

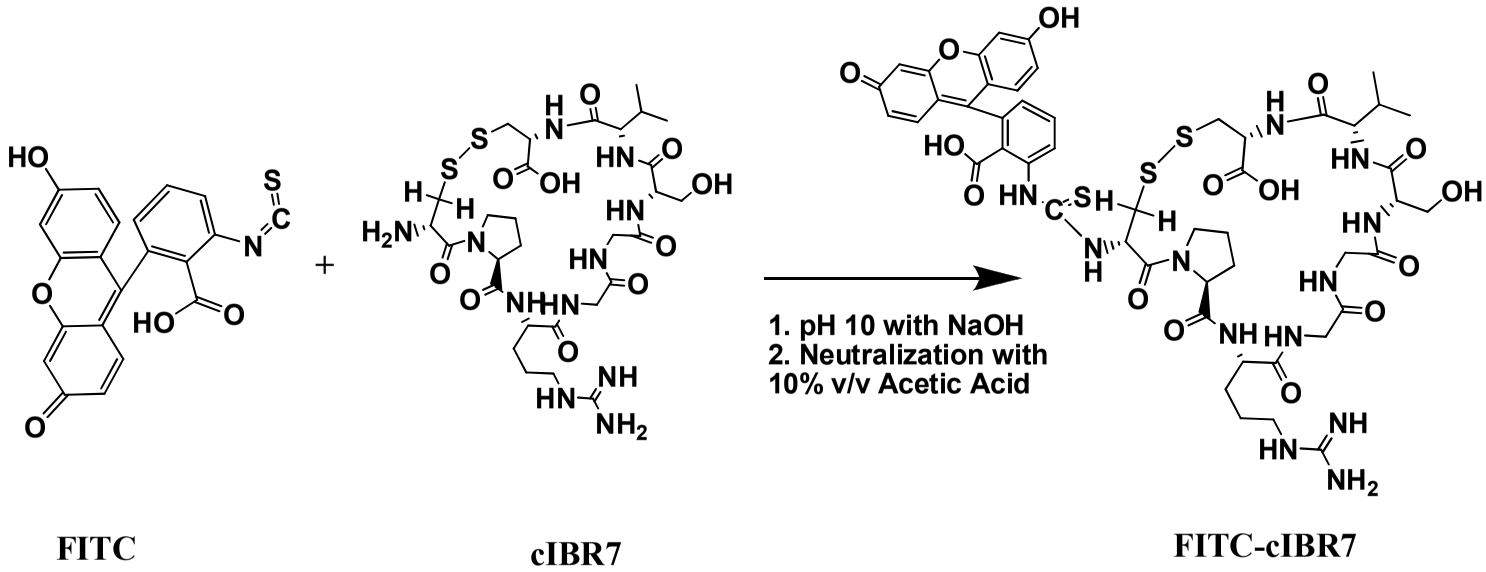

Figure 3.3 Synthesis of FITC conjugate of cIBR7 peptide. The N-terminal of the cIBR7 [cyclo(1,8)CPRGGSVC] was conjugated to the isothiocyanate group of fluorescein.

solutions (pH 7.4) was measured at different concentrations, and individual calibration curves were generated using Microcal Origin version 6.0.

3.2.6 Temperature-Dependent Internalization Studies of DOX-cIBR7, DOX-PEGcIBR7 and DOX using HL-60 Cells

HL-60 cells were centrifuged and re-suspended in RPMI 1640 medium at a concentration of 2×10^6 cells/mL. 250 µl of the cell suspension was added separately to 250 µl of a solution of DOX-cIBR7, DOX-PEGcIBR7, and DOX to reach a final conjugate or drug concentration of 10 µM. Cell viability during incubation at this concentration of the compounds was confirmed separately using Trypan Blue staining (data not shown). The cells were incubated at 37 °C and 4 °C for 1 h while protected from light, and then centrifuged at 1000 rpm for 2 min. The cells were washed three times with ice-cold phosphate-buffered saline (PBS) and suspended in 20 µL of PBS. Final cell density used for the microscopic observation was 25×10^6 cells/mL. 10 µL of the cell suspension in PBS was put on a slide for observation. A Nikon Eclipse 80*i* microscope equipped for epifluorescence was used to view the cells, and the fluorescence emissions of DOX were observed using a rhodamine filter set. Untreated cells were viewed with the same filter to check for autofluorescence. The images were captured using an Orca ER camera (Hamamatsu, Inc., Bridgewater, NJ) controlled by the Metamorph program (Version 6.2, Universal Imaging Corp., West Chester, PA).

3.2.7 Temperature-Dependent Internalization Studies of FITC-cIBR7 using HL-60 Cells

HL-60 cells were incubated in PBS at a cell density of 5×10^5 cells/mL for 10 min at 37 °C and resuspended in PBS at a cell density of 2×10^6 cells/mL. 250 µL of cell suspension was added separately to 250 µl of FITC-cIBR7 (125 µM, in PBS) and 250 µL of FITC-dextran (200 µM, in PBS). Cells were incubated at 37 °C and at 4 °C in the dark for 1 h. After the incubation, cells were treated as described above (3.2.6). Control cells without any compound were treated and prepared in the same manner. Cells were observed using a Yokugawa-type spinning disk confocal microscope. Images were captured using an EM-CCD camera (Hamamatsu) controlled by the SlideBook program (version 4.1, Intelligent Imaging Innovations, Denver, CO).

3.2.8 Colocalization Studies of FITC-cIBR and FITC-cIBR7 with Alexa 647-Dextran using HL-60 Cells

For the colocalization studies, HL-60 cells were washed with PBS and resuspended in PBS at a cell density of 2×10^6 cells/mL. 5×10^5 cells were incubated with 25 µM Alexa-647- conjugated dextran (dextran, Alexa Fluor® 647; 10,000 MW, anionic, fixable; Molecular Probes®, Eugene, OR) and 125 µM FITC-cIBR or FITC-cIBR7 for 1 h at 37 °C. At the end of the incubation, cells were washed three times with ice-cold PBS and finally resuspended in 20 µL of PBS. 10 µL of the cell suspension in PBS was placed on a slide for microscopic observation. Untreated cells were also viewed under the same conditions to check for autofluorescence. Cells were

observed using a Yokugawa-type spinning disk confocal microscope. Images were captured using an EM-CCD camera (Hamamatsu) controlled by the SlideBook program (version 4.1).

3.3 Results

3.3.1 Syntheses of DOX-cIBR7, DOX-PEGcIBR7, FITC-cIBR7 and FITC-cIBR

The linear peptides IBR7 and PEGIBR7 were synthesized by the solid phase method using Fmoc chemistry and were purified by semi-preparative HPLC. Both linear peptides were cyclized by air oxidation in high dilution conditions to give cIBR7 and PEGcIBR7. Then, cIBR7 and PEGcIBR7 cyclic peptides were conjugated to DOX-hemisuccinate to yield DOX-cIBR7 and DOX-PEGcIBR7 (Figure 3.2). FITC-cIBR7 and FITC-cIBR were also synthesized and purified using semi-preparative HPLC (Figure 3.3).

3.3.2 Determination of Octanol/Aqueous Buffer Distribution Ratios (pH 7.4) for DOX-cIBR7 and DOX-PEGcIBR7 Conjugates

The results from the octanol/aqueous buffer distribution ratio studies are presented in Table 3.1**.** It is clear that DOX-cIBR7 conjugate is more hydrophilic (distribution ratio = 4.3, pH 7.4) than DOX-cIBR (distribution ration = 14.1, pH 7.4),[14] indicating that removal of the C-terminal hydrophobic amino acid residues (i.e., LVTG) had a significant effect on the physicochemical properties of the

Table 3.1 Octanol/aqueous buffer (pH 7.4) distribution ratios for DOX-cIBR7 and DOX-PEGcIBR7 and comparison with DOX-cIBR from reference 14

Compound	**Distribution Ratio (D)**	**Log D**
DOX-cIBR7	4.3	0.63
DOX-PEGcIBR7	0.9	-0.04
DOX-cIBR	14.1	1.14

conjugate. As expected, incorporating a hydrophilic linker into DOX-PEGcIBR7 further enhanced its hydrophilicity to a distribution ratio of 0.9 at pH 7.4 (Table 3.1). As expected, the changes in the structure of the conjugates alter their physicochemical properties for high hydrophobic DOX-cIBR to a more hydrophilic DOX-PEGcIBR7 conjugate.

3.3.3 Temperature-Dependent Internalization of DOX-cIBR7, DOX-PEGcIBR7 in Comparison with DOX using HL-60 Cells

Because the receptor-mediated entry processes are energy dependent, reduction of temperature suppresses the endocytic uptake pathway. Therefore, the internalization mechanisms of DOX-cIBR7, DOX-PEGcIBR7, and DOX were evaluated at 37 °C and 4 °C. Both DOX-cIBR7 (Figure 3.4) and DOX-PEGcIBR7 (Figure 3.5) conjugates showed a diffuse fluorescence distribution pattern in the cellular cytoplasm at 37 °C (Figures 3.4a and 3.5a). There were no punctate endocytic fluorescence localization patterns inside the cells. Similar fluorescence pattern was seen for DOX-cIBR. The internalization of DOX-cIBR7 and DOX-PEGcIBR7 conjugates at 4 °C produced a diffuse fluorescence of the conjugates inside the cell cytosol (Figures 3.4b and 3.5b) without any apparent difference from the internalization at 37 °C. These results suggest that the entry of DOX-cIBR7 and DOX-PEGcIBR7 conjugates was not via endocytic pathway but via passive diffusion. As observed previously, DOX itself was localized inside the nucleus when incubated at 37 °C with the cells for 1 h (Figures 3.4c and 3.5c). Lowering the temperature

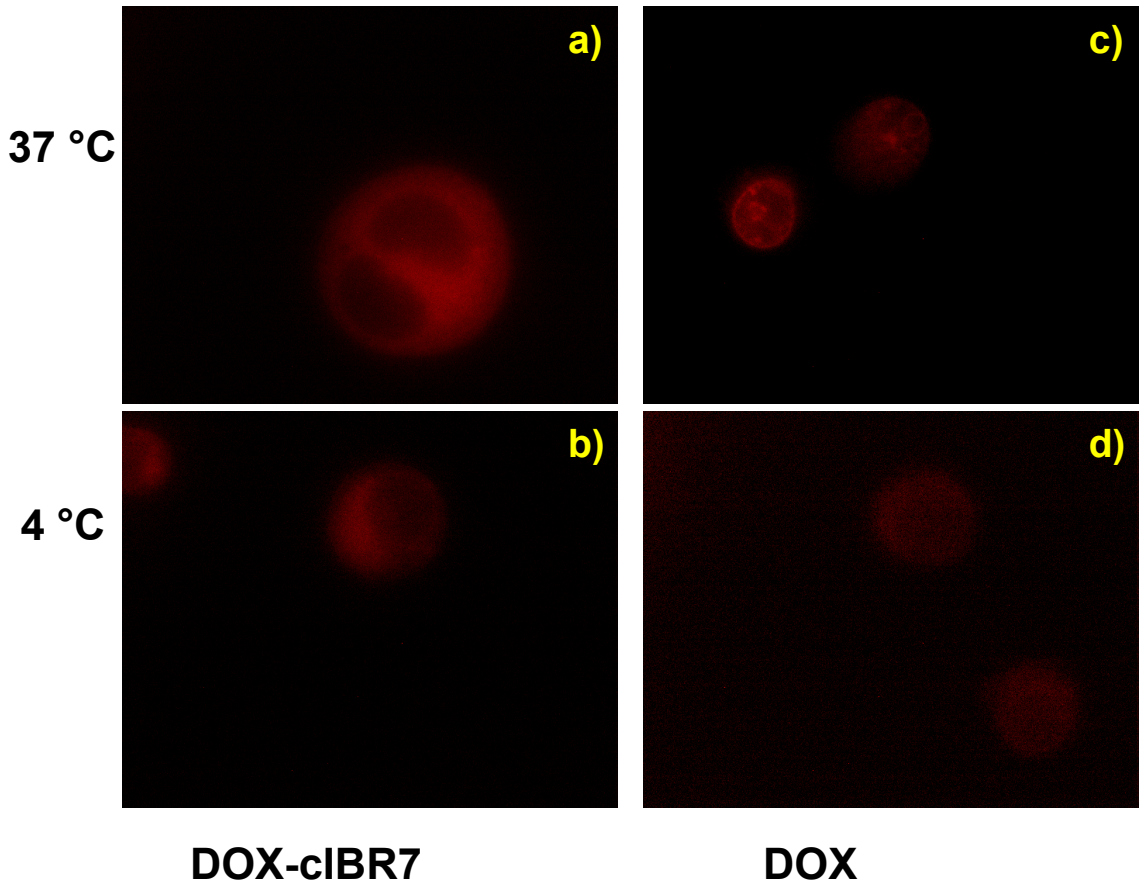

Figure 3.4 DOX-cIBR7 conjugate entry into the HL-60 cells was not affected by change in temperature. Panel (**a**) shows that DOX-cIBR7 showed diffuse fluorescence distribution in the cell cytoplasm after incubation at 37 °C. It did not show the punctate intracellular stain indicative of endocytosis. Panel (**b**) shows that incubation at 4 °C did not inhibit the conjugate entry or change the distribution pattern. For comparison, profiles of the cells incubated with DOX at 37 °C and 4 °C are shown in panels (**c**) and (**d**), respectively.

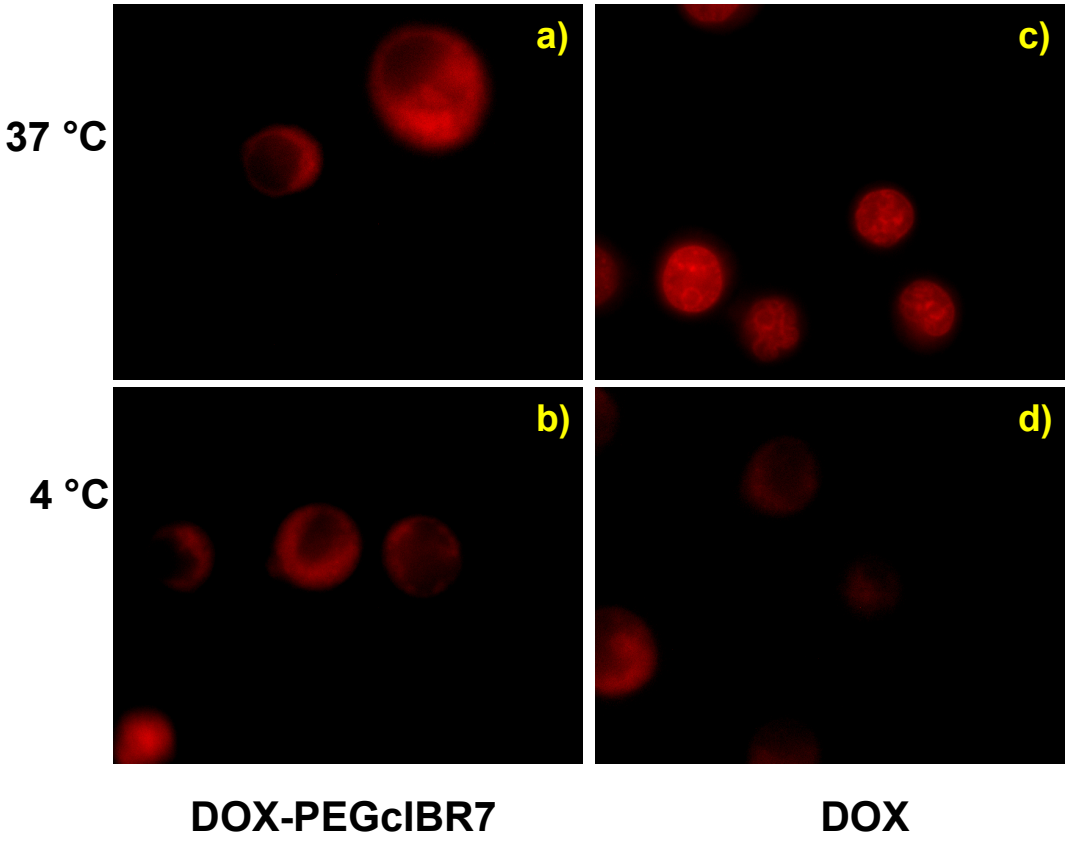

Figure 3.5 An increase in hydrophilicity of the DOX-PEGcIBR7 conjugate did not change the cellular entry mechanism or the distribution pattern compared to DOX-cIBR7 in HL-60 cells. Panel (**a**) shows cells incubated with DOX-PEGcIBR7 at 37 °C. Panel (**b**) shows cells incubated with DOX-PEGcIBR7 at 4 °C. Under both conditions, the conjugate showed a diffuse cytoplasmic fluorescence distribution patterns. Profiles of the cells incubated with DOX at 37 °C and 4 °C are shown in panels (**c**) and (**d**), respectively.

to 4 °C reduced the fluorescence intensity of DOX, indicating that the uptake of DOX was suppressed and the distribution was no longer completely localized in the cell nucleus (Figures 3.4d and 3.5d). Instead, DOX was distributed throughout the cell, including the cell cytoplasm as described previously.[14] Temperature-dependent entry of DOX has been proposed to be due to the aggregation of DOX molecules.[20] Increasing the hydrophilicity of the conjugates did not change the mode of entry of DOX-cIBR7 and DOX-PEGcIBR7 conjugates from passive diffusion to receptor-mediated endocytosis. It is possible that the DOX portion of the conjugate has more impact than the peptide fragment on the uptake behavior.

3.3.4 Temperature-Dependent Internalization of FITC-cIBR7 using HL-60 Cells

To evaluate whether cIBR7 can be internalized via a receptor-mediated pathway, FITC-cIBR7 was synthesized and evaluated for its internalization properties in a temperature-dependent manner. FITC-dextran was used as a positive control because it is known to enter the cells by fluid phase non-specific endocytosis.[21] When incubated at 37 °C for 1 h, FITC-cIBR7 localized inside the HL-60 cells in the form of punctate stains (Figure 3.6a) suggesting that it was located in the endocytic compartments. It did not show a diffuse cytoplasmic distribution pattern as did the DOX-peptide conjugates. FITC-dextran also showed endosomal punctate localization after incubation at 37 °C (Figure 3.6c). When the temperature was reduced to 4 °C, no fluorescence associated with cells incubated with FITC-cIBR7 (Figure 3.6b) or FITC-dextran (Figure 3.6d) was seen. Thus, lowering the temperature to 4 °C knocks

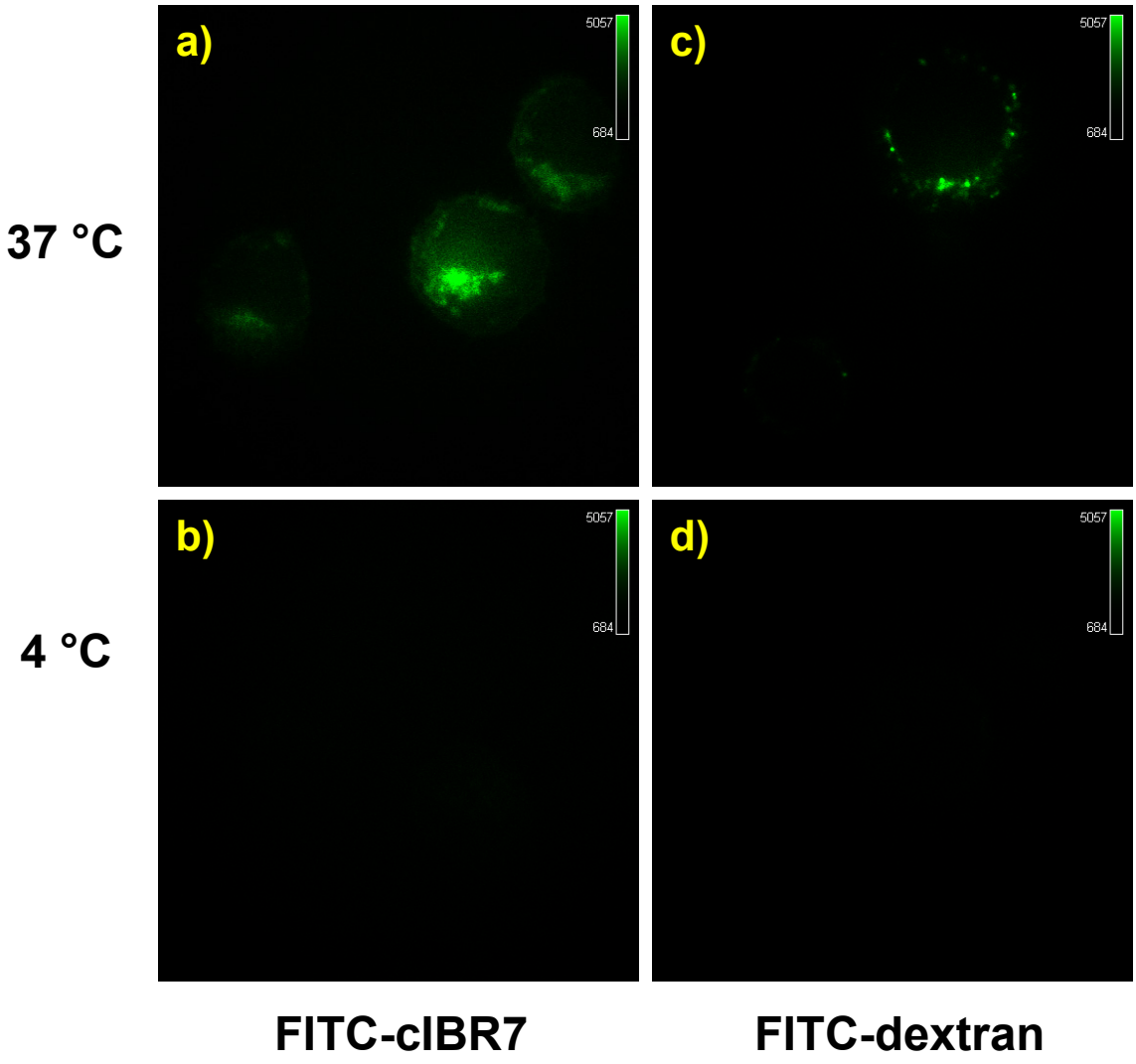

Figure 3.6 FITC-cIBR7 showed temperature-dependent internalization in HL-60 cells. Panel (**a**) shows cells incubated with FITC-cIBR7 at 37 °C. Distinct localization of FITC-cIBR7 is indicative of an endocytic uptake pathway. (**b**) Incubation of the cells at 4 °C prevented the endocytic uptake of FITC-cIBR7, suggesting that the entry was energy-dependent. As a control, FITC-dextran internalization profiles at 37 °C and 4 °C are shown in panels (**c**) and (**d**), respectively.

out the endocytic uptake pathway. These results suggested that FITC-cIBR7 entry into the HL-60 cells took place via the endocytic uptake pathway, and this entry was energy dependent.

3.3.5 Colocalization Studies of FITC-cIBR and FITC-cIBR7 with Alexa 647-Dextran using HL-60 Cells

To understand the intracellular distribution and destination of the conjugates, cells were incubated with Alexa-647-dextran and either FITC-cIBR or FITC-cIBR7. The excitation and emission maxima for FITC are at 494 nm and 521 nm, respectively, while the excitation and emission maxima for Alexa-647 are at 650 nm and 668 nm, respectively. Alexa-647-dextran was used to avoid the artifacts of bleed-through or crossover of the fluorescence emission. The endocytosis of the dextran molecules is via a non-specific, fluid-phase endocytic pathway, and these molecules move gradually through the early endosomes, the late endosomes and finally into the lysosomes after entering the cells.[21] Therefore, colocalization of the FITC-labeled peptides with dextran molecules would indicate that the FITC-labeled peptides followed a pathway similar to that of dextran into the lysosomes. The results showed that FITC-cIBR did not completely colocalize the with dextran molecules after incubation for 1 h (Figure 3.7). Even though, there was a general trend of localization of FITC-cIBR and dextran molecules in the similar areas of the individual cells, they did not completely superimpose. Differences in the uptake of these two molecules can be observed and is a possible reason for this different distribution (Figure 3.7 a,b)

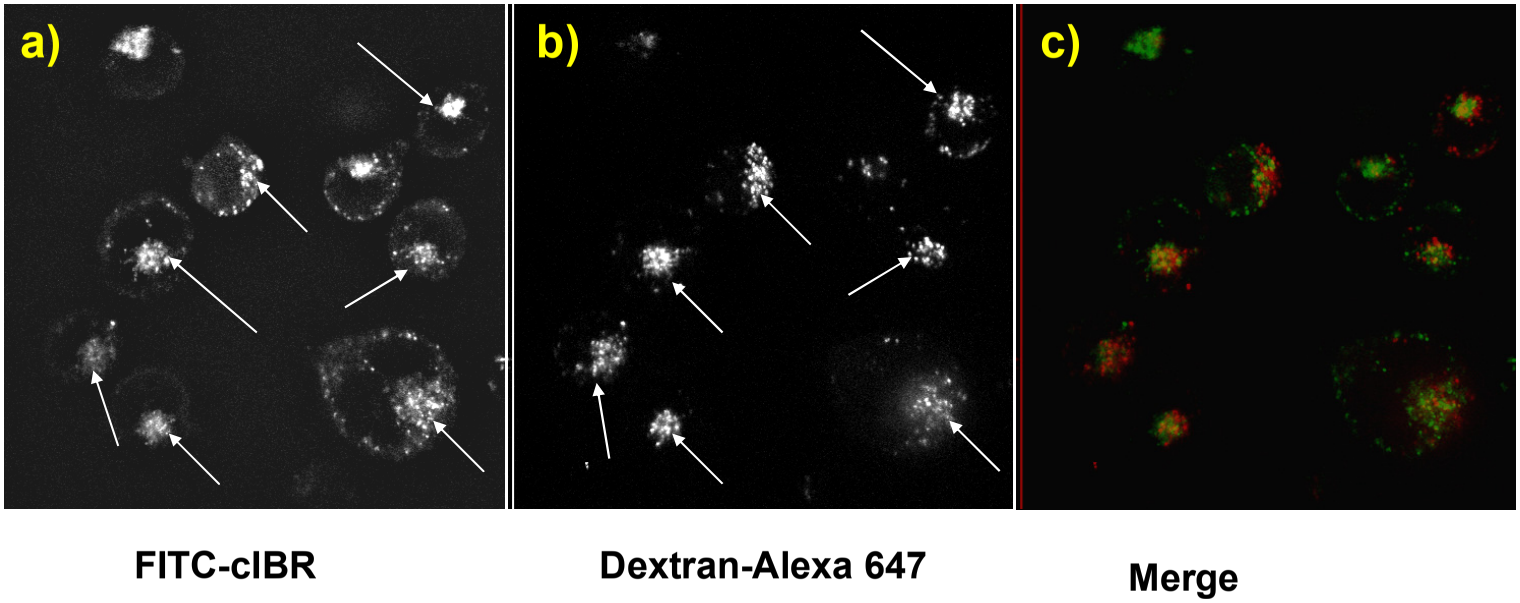

Figure 3.7 Intracellular distribution study of FITC-cIBR and Alexa 647-labeled dextran molecules after incubation for 1 h with HL-60 cells. Panel (**a**) shows the intracellular distribution for FITC-cIBR. Panel (**b**) shows the localization of the Alexa 647-labeled dextran under the same conditions. Panel (**c**) is a merge of panels (**a**) and (**b**).

It may also suggest localization of some fractions of the peptide in other cellular compartments. Distribution profile of FITC-cIBR7 with dextran molecules was similar to that between FITC-cIBR and dextran (Figure 3.8). These observations suggested that both FITC-cIBR and FITC-cIBR7 might follow a pathway different from that of dextran inside the cell. It may also indicate that 1 h time period was not enough to allow for the molecules to reach their intracellular destination.

3.4 Discussion

Previously, we have shown that FITC-cIBR conjugate enters the HL-60 and Molt-3 cells via an energy-dependent pathway.[14] In addition, FITC-cIBR colocalizes with anti-LFA-1 antibody on MOLT-3 T-cells, indicating that it binds to the I-domain of LFA-1.[22] Recently, cIBR peptide was shown (by antibody inhibition and NMR studies) to bind to the I-domain of LFA-1.[23,24] Using mutation studies, smaller linear and cyclic derivatives of cIBR peptide have been found to have similar or better activity than parent cIBR to inhibit ICAM-1/LFA-1-mediated heterotypic T-cell adhesion.[18,25] During these studies, we found that cIBR7 cyclic peptide has better activity than cIBR to inhibit heterotypic T-cell adhesion, and the binding affinity of cIBR7 to the isolated I-domain is higher than that of cIBR peptide. However, the internalization properties of cIBR7 have not been elucidated until now.

Mutation and alanine-scanning studies indicated that the recognition sequence in cIBR peptide is at the Pro-Arg-Gly-Gly (PRGG)[25] and this sequence is in a β-turn

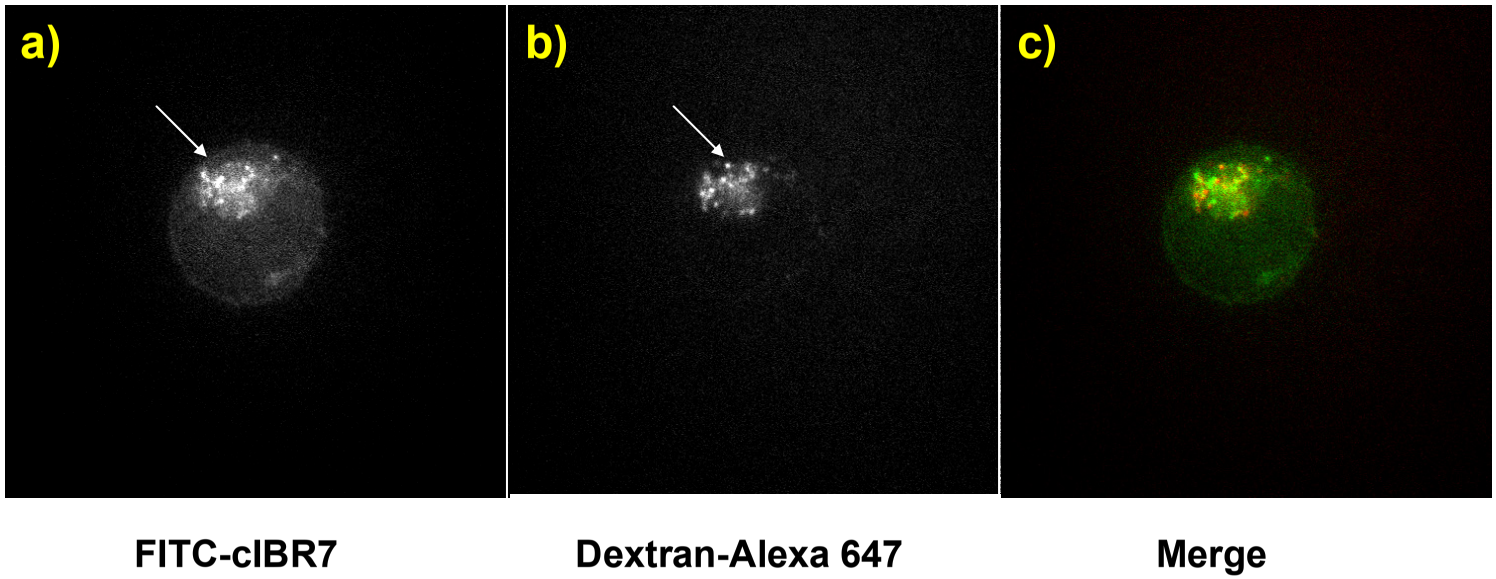

Figure 3.8 Intracellular distribution study of FITC-cIBR7 and Alexa 647-labeled dextran molecules after incubation for 1 h with HL-60 cells. Panel (**a**) shows the intracellular distribution for FITC-cIBR7. Panel (**b**) shows the localization of the Alexa 647-labeled dextran under the same conditions. Panel (**c**) is a merge of panels (**a**) and (**b**).

conformation as determined by NMR studies.[26] The importance of the "PRGG" sequence and its β-turn conformation was further demonstrated by the efficiency of linear hexapeptide LH7 (PRGGSV) in inhibiting the heterotypic T-cell adhesion to Caco-2 monolayers. LH7 peptide was cyclized (to generate CH7) using the N- and C-termini, which resulted in stabilization of the β-turn structure at the PRGG sequence. However, N- to C-terminal conjugation did not leave any suitable chemical functionality in the peptide for conjugation with drugs. In addition, introduction of the Lys5 in place of Ser5 to give cyclo(1,6)PRGGKV for providing a drug conjugation site resulted in lower peptide activity.[25] Therefore, the cyclization method was altered by using a disulfide bond to produce cIBR7 (cyclo(1,8)CPRGGSVC), which has free N- and C- termini that can be conjugated to drugs. As mentioned previously, this peptide has better binding properties to LFA-1 than the parent cIBR. In addition, due to the removal of the C-terminal hydrophobic residues ('LVTG') from the parent cIBR peptide, cIBR7 is more hydrophilic than cIBR and offers an attractive opportunity to explore the influence of the physicochemical properties on the internalization of the DOX-peptide conjugates.

To evaluate the effect of conjugate hydrophilicity on its uptake properties, we have synthesized DOX-cIBR7, DOX-PEGcIBR7, and DOX-cIBR. DOX-cIBR7 conjugate was, indeed, more hydrophilic than DOX-cIBR. Addition of a more hydrophilic linker in DOX-PEGcIBR7 produced a conjugate that was more hydrophilic than DOX-cIBR7. Unfortunately, both DOX-cIBR7 and DOX-PEGcIBR7 conjugates entered the HL-60 cells by an energy-independent pathway.

Reduction of the temperature from 37 °C to 4 °C failed to inhibit the entry of the conjugates inside the cells. In addition, the distribution profile of the conjugates inside the cell cytosol was indicative of the non-endocytic uptake pathway. The conjugates did not show localization into distinct endocytic compartments. The results indicated that the change in hydrophobicity of the DOX-peptide conjugates does not influence their internalization behavior.

There are some possible explanations for the internalization behavior of the DOX-peptide conjugates. First, there is a possibility that the DOX segment of the conjugate interacts with the DOX segments of other molecules via anthraquinone stacking to form aggregates. These aggregates can readily partition into the lipid bilayer in spite of the presence of the targeting peptide. Second, the formation of aggregates can impose steric hindrance to the recognition site of the peptide by the LFA-1 receptors on the cell surface. Third, the DOX-segment of the conjugate has a high affinity for the membrane components, which would make it difficult for the remaining part of the conjugate (i.e., peptide portion) to bind to LFA-1 and control the internalization process of the conjugate.

Aggregation of DOX molecules in aqueous solution has been observed and was proposed as the reason for the saturation kinetics and temperature-dependent entry of DOX into human red blood cells. At normal physiological pH and temperature, DOX molecules exist in both neutral and charged forms; however, only the neutral form partitions into the cell membrane. Random association of the molecules through hydrophobic interactions leads to formation of aggregates with associated charges.

Only the uncharged monomer form can permeate the cell. Reduction of temperature leads to lower permeation into the cell as it increases aggregate because of lower Brownian motion.[20] Similarly, dimer and tetramer formation for DOX and daunorubicin (DNR) in aqueous solution have also been reported. These aggregation reactions take place through self-association of the planar aromatic ring systems.[27] DNR molecules were found to dimerize below 50 nM concentration; at higher concentration the dimers were proposed to self associate leading to a much more complex association scheme.[28] The possibility of transporter-mediated uptake for DOX has also been suggested. Structural modification of anthracycline antibiotics produced tremendously different cellular entry behavior into Ehrlich ascites tumor cells. DOX, DNR, and rubidazone (RBD) showed a saturable, biphasic uptake pattern into these cell lines with the initial rate of uptake being influenced by the structural modifications. DOX, DNR, and RBD showed temperature-dependent uptake. Moreover, unlabeled DNR inhibited the uptake of [^{3}H]-DNR into these cells. All these properties are characteristics of transporter-mediated uptake.[29] Although there is no proof of any carrier-mediated transport for DOX in HL-60 cells, this idea may still be plausible for the uptake of DOX in addition to passive diffusion. It is not surprising that DOX and DNR have high affinity toward the cell membrane as there are membrane proteins with aromatic amino acids that can form molecular associations with the drug molecules through pi-electron interaction.

The aromatic doxomycinone moiety in DOX is responsible for its hydrophobic nature.[13] Similar to DOX-cIBR, DOX conjugates with other peptides could have

higher hydrophobicity than DOX itself.[10] For example, DOX-CNGRC conjugate was internalized to a similar extent into the cells with different levels of expression of the target receptor, indicating that this conjugate was not internalized via a receptor-mediated pathway.[10] DOX-cIBR also entered the HL-60 cells in the absence of energy-dependent mechanism and showed diffuse cytoplasmic distribution. Hydrophobicity of the DOX-cIBR conjugate was proposed to be the reason for its energy-independent cytosolic entry into the HL-60 cells. A similar hypothesis was proposed for the cytosolic, non-specific entry of DOX-CNGRC conjugate into the cells.[10] Our previous[14] and present studies clearly demonstrate that the hydrophobicity of the DOX-peptide conjugates is not the only factor in determining their internalization behavior. The distribution ratio for DOX-CNGRC (5.3, pH 7.4) is similar to our DOX-cIBR7 (distribution ratio 4.3, pH 7.4). DOX-PEGcIBR7 has a distribution ratio of 0.9 at pH 7.4, which is comparable to DOX (distribution ratio 1.2, pH 7.4[10,14]). However, DOX-PEGcIBR7 has internalization properties similar to the other DOX conjugates. These results suggested that the entry of DOX-peptide conjugates may not be influenced by hydrophobicity or the targeting moiety of the conjugate but may be driven by the physical properties of the DOX fragment of the conjugate. Although there are several proposals on how DOX enters the cells, there have been no systematic studies to elucidate the mechanism(s) of DOX entry into the cells.

The hypothesis that the discrepancy in the internalization behavior of the DOX-peptide conjugates was due to the properties of the DOX molecule or the final

conjugate was demonstrated by the energy-dependent uptake of FITC-cIBR7 peptide. If this were due to the properties of cIBR7 peptide, FITC-cIBR7 would also show energy-independent internalization properties. However, FITC-cIBR7 showed a temperature-dependent endocytic entry into the HL-60 cells similar to that of FITC-cIBR.[14] Similarly, FITC-labeled transferrin protein showed energy-dependent uptake into L929 cells, whereas the DOX-conjugate of transferrin protein (TRF-DOX) showed energy-independent cellular entry into the same cells. In addition, the uptake of the TRF-DOX conjugate could not be blocked by excess TRF.[8]

Colocalization study of both FITC-cIBR and FITC-cIBR7 with dextran molecules suggested the different cellular localization of the peptides compared to the dextran molecules. These peptides might take a different route inside the cells after their endocytic entry compared to dextran. It is also possible that the peptides were captured on their way to the final intracellular destination. Target receptor (LFA-1) for these peptides was shown to undergo caveolin mediated endocytosis. In human polymorphonuclear neutrophils LFA-1 receptor did not colocalize with LAMP-1 (a marker for late endosome or lysosome). In CHO cells LFA-1 never colocalized with clathrin coated pits.[30] Molecules internalized by the clathrin coat mediated pathway are often finally localized in the cellular lysosomes. Molecules internalized by caveolin mediated endocytosis are also known to be finally localized in the cellular golgi compartment.[31] All of these observations suggested that cIBR7 peptide, like cIBR peptide, has the potential to target drugs to leukocytes. Identification of the possible digestion product of the FITC-labeled peptides will help design a specific

conjugation approach to release the free drug for interaction with intracellular targets. As an alternative method to deliver DOX, this drug can be encapsulated in nanoparticles or liposomes that are decorated with targeting peptides to avoid non-specific delivery of DOX as shown above. The objective would be to prevent the formation of DOX aggregates followed by direct interaction of DOX and its aggregates with cell membranes. Decorating the surfaces of nanoparticles with cIBR or cIBR7 peptide may allow internalization of these carriers by LFA-1-expressing leukocytes to carry the loaded drugs into the cells.

3.5 Conclusions

In conclusion, we have shown that internalization of DOX-peptide conjugates is not influenced by the physicochemical properties of the conjugate. Irrespective of the size or hydrophobicity of the conjugates, they retain the energy-independent cellular entry. Unlike DOX-cIBR7 conjugates, the FITC-cIBR7 peptides showed energy-dependent cellular entry into the cells, suggesting that these two conjugates have different internalization mechanisms. The FITC-labeled peptides showed different intracellular distribution compared to dextran molecules inside the cells. Although DOX is a highly effective anticancer agent, this molecule presents a unique challenge for targeted drug delivery. Currently, we are conjugating cIBR7 peptide with anticancer drugs having different physicochemical properties (i.e., hydrophilicity) for selective delivery to leukemic cells. The hope is that the drug-cIBR/cIBR7 conjugate will enter via LFA-1-mediated endocytosis similar to the entry of FITC-cIBR/cIBR7.

3.6 References

1. Nagy A, Armatis P, Cai RZ, Szepeshazi K, Halmos G, Schally AV 1997.Design, synthesis, and in vitro evaluation of cytotoxic analogs of bombesin-like peptides containing doxorubicin or its intensely potent derivative, 2-pyrrolinodoxorubicin. Proc Natl Acad Sci USA 94(2):652-656.

2. Nagy A, Schally AV, Armatis P, Szepeshazi K, Halmos G, Kovacs M, Zarandi M, Groot K, Miyazaki M, Jungwirth A, Horvath J 1996.Cytotoxic analogs of luteinizing hormone-releasing hormone containing doxorubicin or 2-pyrrolinodoxorubicin, a derivative 500-1000 times more potent. Proc Natl Acad Sci USA 93(14):7269-7273.

3. Nagy A, Schally AV, Halmos G, Armatis P, Cai RZ, Csernus V, Kovacs M, Koppan M, Szepeshazi K, Kahan Z 1998.Synthesis and biological evaluation of cytotoxic analogs of somatostatin containing doxorubicin or its intensely potent derivative, 2-pyrrolinodoxorubicin. Proc Natl Acad Sci USA 95(4):1794-1799.

4. Anderson ME, Siahaan TJ 2003.Targeting ICAM-1/LFA-1 interaction for controlling autoimmune diseases: designing peptide and small molecule inhibitors. Peptides 24(3):487-501.

5. Dunehoo AL, Anderson ME, Majumdar S, Kobayashi N, Berkland C, Siahaan TJ 2006.Cell adhesion molecules for targeted drug delivery. J Pharm Sci 95(9):1856-1872.

6. Nagy A, Schally AV 2005.Targeting cytotoxic conjugates of somatostatin, luteinizing hormone-releasing hormone and bombesin to cancers expressing their receptors: a "smarter" chemotherapy. Curr Pharm Des 11(9):1167–1180.

7. Lu Y, Yang J, Sega E 2006.Issues related to targeted delivery of proteins and peptides. Aaps J 8(3):E466–478.

8. Lai BT, Gao JP, Lanks KW 1998.Mechanism of action and spectrum of cell lines sensitive to a doxorubicin-transferrin conjugate. Cancer chemotherapy and pharmacology 41(2):155–160.

9. Garnett MC 2001.Targeted drug conjugates: principles and progress. Adv Drug Del Rev 53(2):171–216.

10. van Hensbergen Y, Broxterman HJ, Elderkamp YW, Lankelma J, Beers JC, Heijn M, Boven E, Hoekman K, Pinedo HM 2002.A doxorubicin-CNGRC-peptide conjugate with prodrug properties. Biochem Pharmacol 63(5):897–908.

11. Kratz F, Beyer U, Roth T, Tarasova N, Collery P, Lechenault F, Cazabat A, Schumacher P, Unger C, Falken U 1998.Transferrin conjugates of doxorubicin: synthesis, characterization, cellular uptake, and in vitro efficacy. J Pharm Sci 87(3):338–346.

12. Froesch BA, Stahel RA, Zangemeister-Wittke U 1996.Preparation and functional evaluation of new doxorubicin immunoconjugates containing an acid-

sensitive linker on small-cell lung cancer cells. Cancer Immunol, Immunother 42(1):55–63.

13. Chaires JB, Satyanarayana S, Suh D, Fokt I, Przewloka T, Priebe W 1996.Parsing the free energy of anthracycline antibiotic binding to DNA. Biochemistry 35(7):2047–2053.

14. Majumdar S, Kobayashi N, Krise JP, Siahaan TJ 2007.Mechanism of internalization of an ICAM-1-derived peptide by human leukemic cell line HL-60: influence of physicochemical properties on targeted drug delivery. Mol Pharm 4(5):749–758.

15. Kruger M, Beyer U, Schumacher P, Unger C, Zahn H, Kratz F 1997.Synthesis and Stability of Four Maleimide Derivatives of the Anticancer Drug Doxorubicin for the Preparation of Chemoimmunoconjugates. Chem Pharm Bull (Tokyo) 45(2):399-401.

16. Garsky VM, Lumma PK, Feng DM, Wai J, Ramjit HG, Sardana MK, Oliff A, Jones RE, DeFeo-Jones D, Freidinger RM 2001.The Synthesis of a Prodrug of Doxorubicin Designed to Provide Reduced Systemic Toxicity and Greater Target Efficacy. J Med Chem 44(24):4216–4224.

17. Denmeade SR, Nagy A, Gao J, Lilja H, Schally AV, Isaacs JT 1998.Enzymatic Activation of a Doxorubicin-Peptide Prodrug by Prostate-Specific Antigen. Cancer Res 58(12):2537-2540.

18. Iskandarsyah, Tejo B, Tambunan USF, Verkhivker G, Siahaan TJ 2008.Structural Modifications of ICAM-1 cyclic peptides to improve the activity to inhibit T-cell heterotypic adhesion of T cells. Chem Biol Drug Design In Press.

19. Gursoy RN, Siahaan TJ 1999.Binding and internalization of an ICAM-1 peptide by the surafce receptors of T cells. J Pept Res 53:414–421.

20. Dalmark M, Storm HH 1981.A Fickian diffusion transport process with features of transport catalysis. Doxorubicin transport in human red blood cells. J Gen Physiol 78(4):349-364.

21. Baravalle G, Schober D, Huber M, Bayer N, Murphy RF, Fuchs R 2005.Transferrin recycling and dextran transport to lysosomes is differentially affected by bafilomycin, nocodazole, and low temperature. Cell Tissue Res 320(1):99-113.

22. Anderson ME, Siahaan TJ 2003.Mechanism of binding and internalization of ICAM-1-derived cyclic peptides by LFA-1 on the surface of T cells: a potential method for targeted drug delivery. Pharm Res 20(10):1523-1532.

23. Anderson ME, Tejo BA, Yakovleva T, Siahaan TJ 2006.Characterization of binding properties of ICAM-1 peptides to LFA-1: inhibitors of T-cell adhesion. Chemical biology & drug design 68(1):20-28.

24. Zimmerman T, Oyarzabal J, Sebastian ES, Majumdar S, Tejo BA, Siahaan TJ, Blanco FJ 2007.ICAM-1 peptide inhibitors of T-cell adhesion bind to the allosteric

site of LFA-1. An NMR characterization. Chemical biology & drug design 70(4):347-353.

25. Anderson ME, Yakovleva T, Hu Y, Siahaan TJ 2004.Inhibition of ICAM-1/LFA-1-mediated heterotypic T-cell adhesion to epithelial cells: design of ICAM-1 cyclic peptides. Bioorg Med Chem Lett 14(6):1399–1402.

26. Gursoy RN, Jois DS, Siahaan TJ 1999.Structural recognition of an ICAM-1 peptide by its receptor on the surface of T cells: conformational studies of cyclo (1, 12)-Pen-Pro-Arg-Gly-Gly-Ser-Val-Leu-Val-Thr-Gly-Cys-OH. J Pept Res 53(4):422-431.

27. Eksborg S 1978.Extraction of daunorubicin and doxorubicin and their hydroxyl metabolites: self-association in aqueous solution. J Pharm Sci 67(6):782-785.

28. Barthelemy-Clavey V, Maurizot J-C, Dimicoli J-L, Sicard P 1974.Self-association of daunorubicin. FEBS Lett 46(1-2):5-10.

29. Skovsgaard T 1978.Carrier-mediated transport of daunorubicin, adriamycin, and rubidazone in Ehrlich ascites tumour cells. Biochem Pharmacol 27(8):1221-1227.

30. Fabbri M, Di Meglio S, Gagliani MC, Consonni E, Molteni R, Bender JR, Tacchetti C, Pardi R 2005.Dynamic partitioning into lipid rafts controls the endo-

exocytic cycle of the alphaL/beta2 integrin, LFA-1, during leukocyte chemotaxis. Mol Biol Cell 16(12):5793-5803.

31. Razani B, Lisanti MP 2001.Caveolins and caveolae: molecular and functional relationships. Exp Cell Res 271(1):36-44.

Chapter 4

Chemical and in vitro biological stability analyses of methotrexate conjugate of cIBR peptide

4.1 Introduction

Peptides that are derived from the intercellular adhesion molecule-1 (ICAM-1) and leukocyte function-associated antigen-1 (LFA-1) receptors have been shown to inhibit ICAM-1/LFA-1-mediated homotypic and heterotypic T-cell adhesion.[1-5] Cyclic peptide cIBR, cyclo(1,12)PenPRGGSVLVTGC, has a sequence derived from the D1 domain of the ICAM-1 and is an efficient inhibitor of T-cell adhesion.[6] This peptide binds to the LFA-1 receptor on the surface of the leukocytes (i.e., T cells) and is subsequently internalized into the cell.[6,7] Antibody inhibition[8] and NMR binding[9] studies indicate that cIBR peptide binds to the I-domain of LFA-1. Because the peptide is internalized into leukocytes via a receptor-mediated process, it is an attractive molecule for selective delivery of cytotoxic drugs to the leukocytes. Utilizing cIBR peptide as a targeting molecule can be accomplished by conjugating the drug to cIBR peptide to make drug-cIBR conjugates. Thus, we have conjugated cIBR peptide to fluorescein isothiocyanate (FITC) and doxorubicin (DOX) to produce FITC-cIBR and DOX-cIBR conjugates for selective delivery of these molecules to the human leukemic cell line, HL-60.[10] It was interesting to find that FITC-cIBR entered the HL-60 cells via receptor-mediated endocytosis while DOX-cIBR entered the cells by another process.[10] As a control, the uptake of FITC-cIBR and DOX-cIBR was evaluated using human umbilical vein endothelial cells (HUVEC). The results showed that DOX-cIBR entered into HUVEC but FITC-cIBR entry was inhibited, suggesting that FITC-cIBR is internalized by LFA-1-expressing cells by a receptor-mediated pathway, but DOX-cIBR enters the cells via a non-receptor-mediated

pathway (i.e., passive diffusion).[10] Perhaps due to the hydrophobic nature of the DOX-cIBR conjugate, it entered both the LFA-1-positive (HL-60) and LFA-1-negative (HUVEC) cells via an energy-independent pathway or passive diffusion.[10]

We have conjugated the cIBR peptide to methotrexate (MTX) to produce MTX-cIBR for selective delivery of MTX to LFA-1-expressing leukocytes for treating leukemia and autoimmune diseases [i.e., rheumatoid arthritis (RA) and multiple sclerosis (MS)]. The hypothesis is that MTX-cIBR will be directed toward LFA-1-expressing cells (i.e., leukocytes) over the cells that do not express LFA-1, so the conjugate would have lower side effects than MTX alone. MTX was selected as the drug molecule because it is being used to treat leukemia at high doses[11,12] and autoimmune diseases such as rheumatoid arthritis at low doses.[13,14] The cellular uptake of MTX is mediated by reduced folate carrier (RFC) and membrane folate-binding protein (mFBP), and thus, these cellular uptake processes could occur non-selectively in different cells, which then could contribute to potential side effects.[15] MTX may also generate drug resistance due to (a) changes in RFC expression level and altered transport kinetics, and (b) increased dihydrofolate reductase (DHFR) expression with continued use of the drug. Several other reasons for MTX resistance have also been proposed in the literature.[16,17] MTX has been effectively delivered to cells using its conjugates with different carrier molecules, including peptides,[16] proteins,[18,19] and polymers.[20,21] Using target receptors other than RFC for cellular entry, the conjugate may possibly avoid cellular drug resistance. MTX-cIBR conjugate was synthesized by attaching the γ-carboxylic acid of MTX to the N-

terminal of the peptide (Figure 4.1).[22] Similar to cIBR peptide, MTX-cIBR inhibited the anti-I-domain monoclonal antibody (mAb) binding to LFA-1 in a concentration-dependent manner.[22]

In this work, we evaluated the chemical and enzymatic stability of MTX-cIBR conjugate under different conditions for optimizing the formulation and adjusting the dosing regimen of the conjugate to determine its effectiveness in *in vivo* systems. MTX-cIBR suppressed the progress of rheumatoid arthritis (RA) in the rat adjuvant model. The conjugate reduced bone loss, marrow inflammation, and paw weight in animals with RA. Although MTX-cIBR has lower toxicity compared to MTX, the conjugate had to be administered at a relatively higher dose (5 mg/kg body weight) than MTX alone to elicit RA suppressive activity. One possible explanation is that pharmacokinetics and *in vivo* stability of the conjugate may influence its biological activity. To test this hypothesis, the stability profiles of the conjugate in rat plasma and tissue homogenates were evaluated. The optimum formulation conditions were also investigated by subjecting MTX-cIBR to different solution pH conditions at elevated temperature for accelerated stability analysis. In the future, the degradation mechanisms will be used to design a more stable conjugate for *in vivo* studies.

4.2 Experimental

4.2.1 Chemical Stability Studies of MTX-cIBR

All solvents for peptide synthesis were of analytical grade. All reagents,

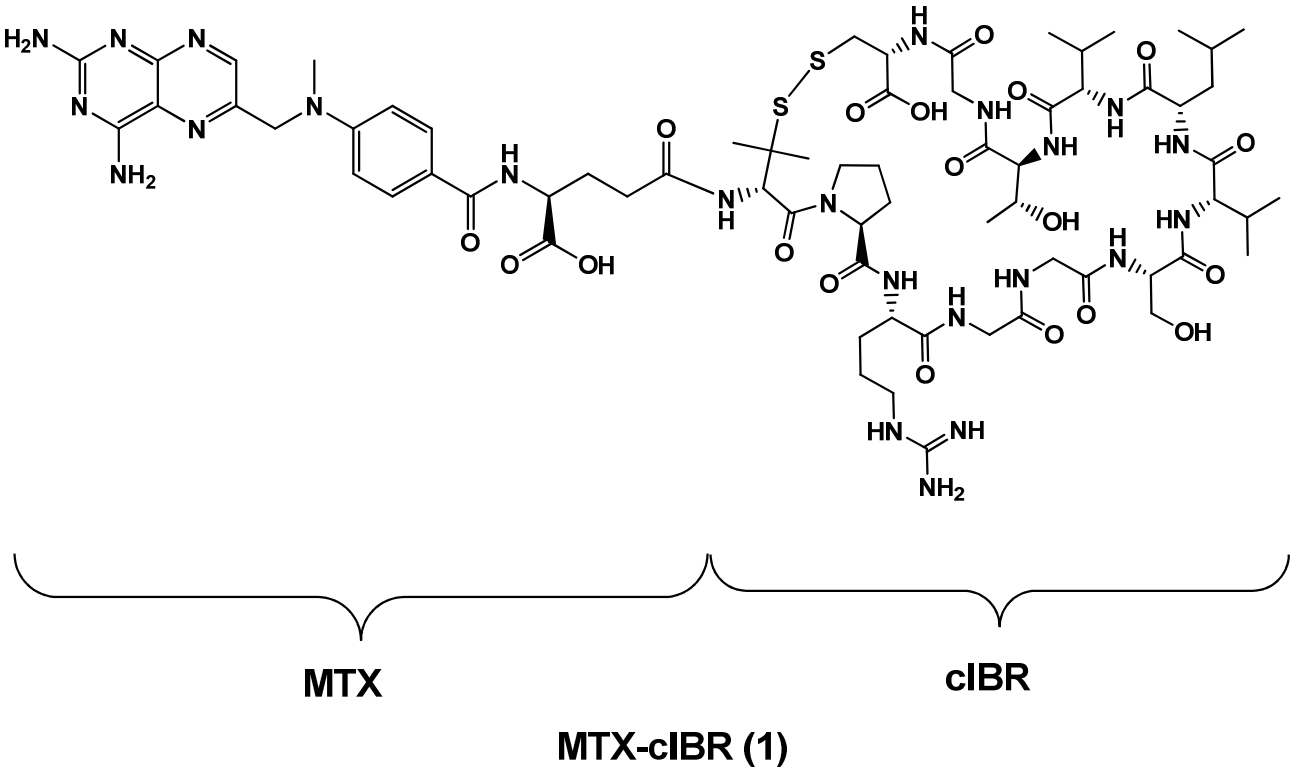

Figure 4.1 The chemical structure of MTX-cIBR conjugate.

including Fmoc-protected amino acids for peptide synthesis, were purchased from Peptides International (Louisville, KY), Advanced ChemTech (Louisville, KY) and Applied Biosystems (Foster City, CA). All the reagents for conjugation reaction were from Sigma Chemicals (St. Louis, MO). For the stability studies under different pH conditions, all the chemicals were purchased from Sigma and Fisher Chemical (Fair Lawn, NJ). Amber colored 1 mL ampoules were from WHEATON Science Products (Millville, NJ).

The stability of MTX-cIBR conjugate was determined at 70 °C. Buffers were prepared as described in Table 4.1. 100 μM of MTX-cIBR conjugate was prepared in suitable buffer and 130 μL of conjugate solution was transferred to 1 mL amber, flame-sealed ampoules. Triplicate samples were taken out of the oven and analyzed immediately at certain time points. A calibration curve was prepared for the conjugate and the concentration range for the calibration curve was kept wide enough to follow two half-lives for the degradation of the conjugate. For the calibration curve, each concentration value was determined in triplicate.

4.2.2 HPLC Analysis of MTX-cIBR Degradation

All the samples were analyzed for degradation using a Hewlett Packard 1050 reverse phase HPLC system with UV absorbance detection (220 nm). A Zorbax C18 column (2.1 × 50 mm, 5 μm particle size) was used as the stationary phase, and the column temperature was maintained constant throughout the analysis. Samples were taken out of the oven for each time point and transferred to an HPLC sample vial. 10

Table 4.1 The observed pseudo first-order rate constants and half-lives for MTX-cIBR conjugate at different pH conditions at 70 °C

pH	Buffer type	$k_{obs}(h^{-1})$	$t_{1/2}$(h)
1.0	HCl	5.25×10^{-1}	1.32
4.0	Acetate	3.2×10^{-3}	216.56
5.0	Acetate	1.3×10^{-3}	533.08
6.0	Phosphate	9×10^{-4}	770.00
7.0	Phosphate	1.2×10^{-3}	577.50
8.0	Phosphate	3.1×10^{-3}	223.55
10.0	Carbonate	2.3×10^{-2}	30.13
12.0	NaOH	7.4×10^{-2}	9.29

Ionic strengths of all the buffer solution were adjusted to 0.15 M with NaCl. 0.1 N HCl was used for pH 1; 0.01 N NaOH was used for pH 12. For all the other pH values, buffer concentration was kept at 50 mM.

μL of the sample was injected each time using a gradient program that started with 100% solvent A (95% water, 5% acetonitrile and 0.1% formic acid) and was increased to 16% solvent B (95% acetonitrile, 5% water and 0.1% formic acid) over 12 min followed by a ramp to increase the composition of solvent B to 100% by 14 min. The system was maintained at 100% B for 2 min followed by a gradient change to 100% A over 4 min. All the concentrations were converted to Log concentration (Log C). Mean and standard deviation were measured for each time point for each pH value. Plots of Log C with time (h) were generated in SigmaPlot (version 9.01, Systat Software, Inc.) and the rate constants for degradation and half-lives were calculated from the plots. A plot of k_{obs} with different pH values was used to create a pH rate profile for the conjugate at 70 °C. Ion-product of water (K_w) was calculated at 70 °C for the pH rate profile determination.

4.2.3 Identification of Degradation Products of MTX-cIBR by LC-MS

Degradation products were identified using a Q-Tof (Waters Micromass) system equipped with electrospray ionization capability. Masslynx™ (version 4.0) software was used for data collection and analysis. For the LC analysis, a Zorbax C18 column (5 cm × 1 mm, 3.5 μm, Micro-Tech Scientific) was used. Mobile phase composition was kept at 99% A (99% water, 1% acetonitrile, and 0.08% formic acid) for 1 min (flow rate 0.11 mL/min), reduced to 90% A over the next 1 min and to 80% A over the next 6 min (flow rate 0.11 mL/min). Solvent composition was changed to 95% B (99% acetonitrile, 1% water, and 0.06% formic acid) over next 7 min to flush the

column (flow rate 0.15 mL/min), and the composition was changed back to 99% A over 2 min (flow rate 0.13 mL/min). The Injection volume for each sample was kept at 5 µL.

4.2.4 MTX-cIBR Conjugate Stability in Biological Media

4.2.4.1 Stability of MTX-cIBR in Rat Plasma

The stability of MTX-cIBR was evaluated in rat plasma. MTX-cIBR solution in DMSO (100 µM) was prepared as a stock solution. 10 µL of stock solution was mixed with 990 µl of rat plasma and incubated at 37 °C in a water bath (Precision reciprocal shaking bath, Thermo Electron Corporation, Model 2870). 100 µL samples were drawn after 0, 10, 20, 30, 45, 60, 90, and 120 min of incubation. Samples were immediately treated with 500 µL of chilled acetonitrile containing internal standard Alprenolol (1 µg/mL). All samples were vortexed for 10 s and incubated in ice, followed by centrifugation at 14,000 rpm for 15 min (Eppendorf Refrigerated Microcentrifuge, Model 5417R). Aliquots (100 µL) of the supernatant were injected into the mass spectrometer. The standard curve was prepared by adding known concentrations of MTX-cIBR solution to rat plasma followed by immediate addition of cold acetonitrile containing internal standard. The solutions for the standard curve were treated in the same way as the samples. Each time point was measured in triplicate and the data are represented as percent concentration remaining at each time point.

4.2.4.2 Stability of MTX-cIBR with Homogenized Rat Heart

Tissue stability of MTX-cIBR was evaluated by incubating the conjugate with homogenized rat heart. 6.28 mL of Dulbecco's PBS (1X) solution without Ca^{2+} and Mg^{2+} (Mediatech, Inc. Cellgro®) was added to 3.18 g of rat heart tissue in a test tube. The tissues in different tubes were homogenized using a sonifier (Branson Sonifier, Branson Ultrasonic Corporation, Danbury, CT) for 3–5 min. From the stock solution of MTX-cIBR used in the plasma stability studies, 10 µl of the compound solution was mixed with 990 µl of tissue homogenate and incubated at 37 °C in a water bath. At different time points (0, 10, 20, 30, 45, 60, 90, 120 min) after incubation, triplicate samples were drawn and treated in the same way as described above for plasma stability studies.

4.2.4.3 LC-MS Analysis of MTX-cIBR Degradation in Biological Matrices

An Integrated Cohesive Technologies LX-2 series liquid chromatography system (comprised of pump, autosampler, valve interface module) coupled with a 4000 Q Trap triple quadrupole mass spectrometer (Applied Biosystems MDS-SCIEX) was used to quantify the compound extracted from the biological matrices. The mass spectrometer was equipped with a Turbo ion-spray ionization source and was operated in the positive mode. Samples were detected by multiple reaction monitoring (MRM) scan mode. For chromatographic separation, an Agilent Technologies Eclipse XDB-C18 column (4.6 × 15 mm, 3.5 µm particle diameter) was used with solvent A (10 mM ammonium formate buffer at pH 3.5) and solvent B (acetonitrile with 0.1%

formic acid) with a flow rate of 1.0 mL/min. A combination of linear and step gradients was used for the liquid chromatography separation with the following solvent composition changes: (a) 90% A to 10% A over 17 s, (b) 10% A maintained for 2 min, (c) changed to 90% A over 50 s, and (d) maintained at 90% A for 17 s.

4.3 Results

4.3.1 Chemical Stability of MTX-cIBR

Degradation of MTX-cIBR conjugate was monitored at pH values 1, 4, 5, 6, 7, 8, 10 and 12, and the degradation products at acidic and basic pH values were identified. Upon incubation at 70 °C, the samples were analyzed up to two half-lives, and the degradation profile for MTX-cIBR appeared to follow pseudo first-order kinetics at all pH values. The Log C of MTX-cIBR was plotted against time for all pH values, and the half-lives of the conjugate are shown in Table 4.1.

4.3.1.1 Degradation of MTX-cIBR at Acidic pH Conditions

MTX-cIBR conjugate degraded rapidly at pH 1.0 with a half-life of 1.32 h (Table 4.1). However, the stability of the compound increased dramatically at pH 4.0 ($t_{1/2}$ = 216.56 h). The maximum stability of the conjugate was at pH 6.0 ($t_{1/2}$ = 770 h). Further increases in pH decreased the chemical stability of the conjugate (pH 7.0, $t_{1/2}$ = 577.5 h).

The degradation products of the conjugate at acidic pH were analyzed by LC-MS. The parent MTX-cIBR (**1**, Figure 4.1) has two charges (m/z = 805.9), which are on

the side chain of the arginine residue and the tertiary amine of MTX. Because the degradation products at pH 1.0 and 4.0 were similar, only the products at pH 1.0 were identified. There are two major degradation products of the conjugate with double charges (**2**, m/z = 718.8; **3**, m/z = 711.8) as determined using the isotopic distribution profiles (Figure 4.2). Compound **2** is the cleavage product of the C–N bond between the 6-methylpteridine and phenyl rings (pathway a, Figure 4.3), and the bond cleavage may be assisted by a positively charged tertiary amine as a leaving group (Figure 4.3). Compound **2** degraded further to compound **3** by releasing the methyl group from the phenyl amine moiety (pathway b). The HPLC profile indicated that the abundance of compound 3 gradually decreased with the increase in pH value, suggesting the reaction was pH-dependent. To confirm the identity of compounds 2 and 3 when they were subjected to fragmentation, they both produced the compound 4 with m/z = 1303.6 (z = +1). This suggested that the degradation was, in fact, in the drug portion of the conjugate as the cIBR peptide was intact even in this fragmentation product (pathway c, Figure 4.3). A minor degradation product **5** (m/z = 727.8; z = +2) was derived from compound **2,** and it was the product of peptide bond hydrolysis between Gly5 and Ser6 in the cIBR portion of the conjugate (pathway a, Figure 4.4). Further hydrolysis of compound **5** gave compound **6** (m/z = 661.3; z = +2). Compound **3** degraded further via dehydration of the Ser6 residue to produce compound **7** (Figure 4.5). A similar reaction could occur for the Thr10 residue to give a dehydrated product equivalent to compound **7**.

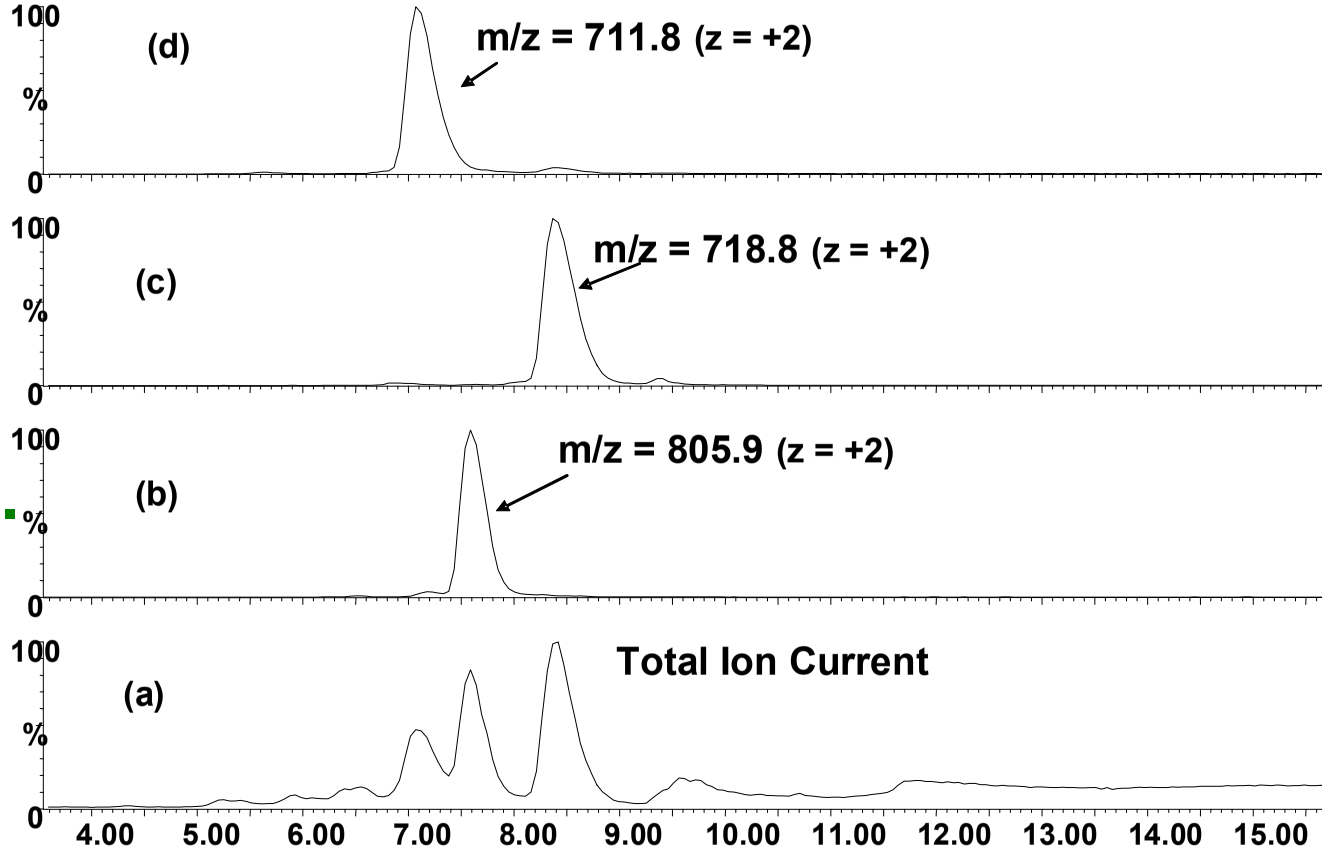

Figure 4.2 The extracted ion chromatograms (EIC) of MTX-cIBR conjugate at pH 1.0 analyzed using LC-MS. Panel **(a)** shows the total ion current chromatogram of MTX-cIBR of all the compounds. Panel **(b)** shows the major peak of m/z value 805.9 (z = +2, as determined by the isotopic distribution profile), which corresponds to the parent MTX-cIBR conjugate. Panel **(c)** shows the degradation product with m/z = 718.8 (z = +2) from the degradation of the drug fraction of the conjugate. Panel **(d)** shows the degradation product with m/z = 711.8 (z = +2), which is also produced from the degradation of the MTX fraction.

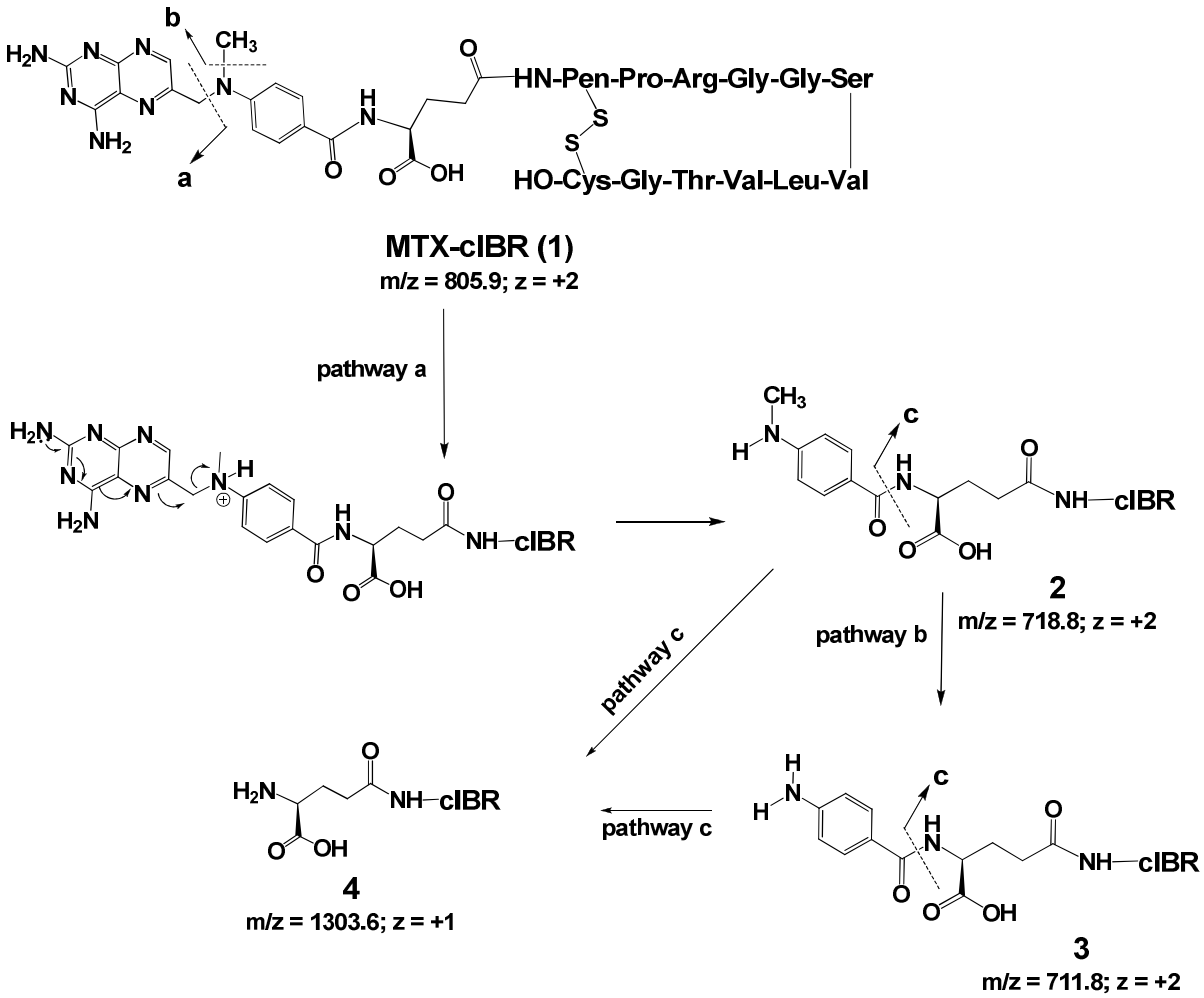

Figure 4.3 Identification of the major degradation products for MTX-cIBR at pH 1.0. Pathway **a** shows the degradation of the MTX portion of the conjugate by clipping the C-N bond between the pteridine ring and the *p*-amino-benzoyl ring to give compound **2**. Pathway **b** represents demethylation reaction of compound **2** to give degradation product **3**. Pathway **c** shows the cleavage between the *p*-amino-benzoyl group and the Glu residue of the MTX fragment of the conjugate.

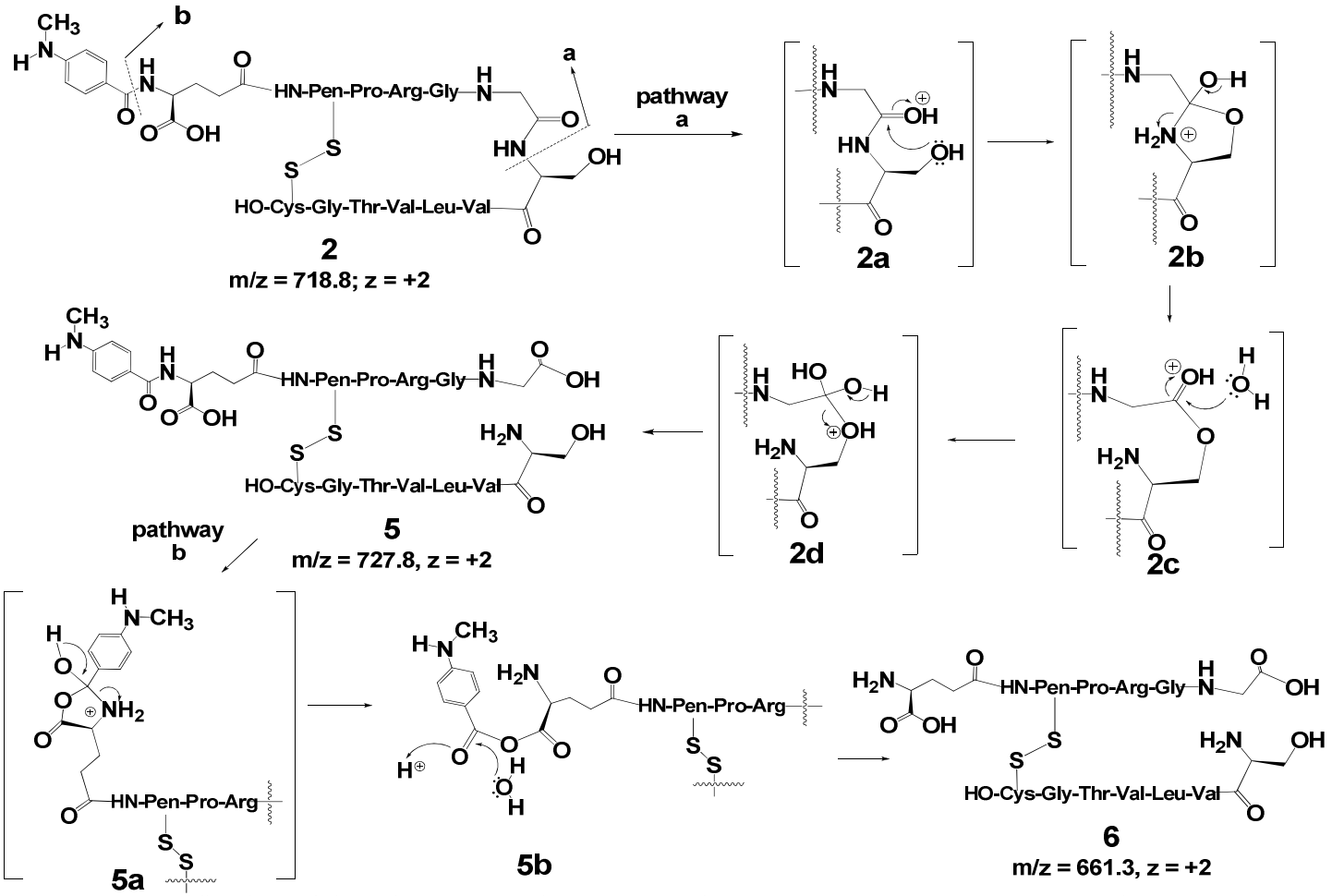

Figure 4.4 Identification of the other degradation products for MTX-cIBR at pH 1.0. Degradation product **5** is the result of peptide bond cleavage between Gly5 and Ser6 via N,O-acyl migration reaction followed by hydrolysis. Compound **6** is the product of further degradation of compound **5** to release the *p*-amino-benzoyl group.

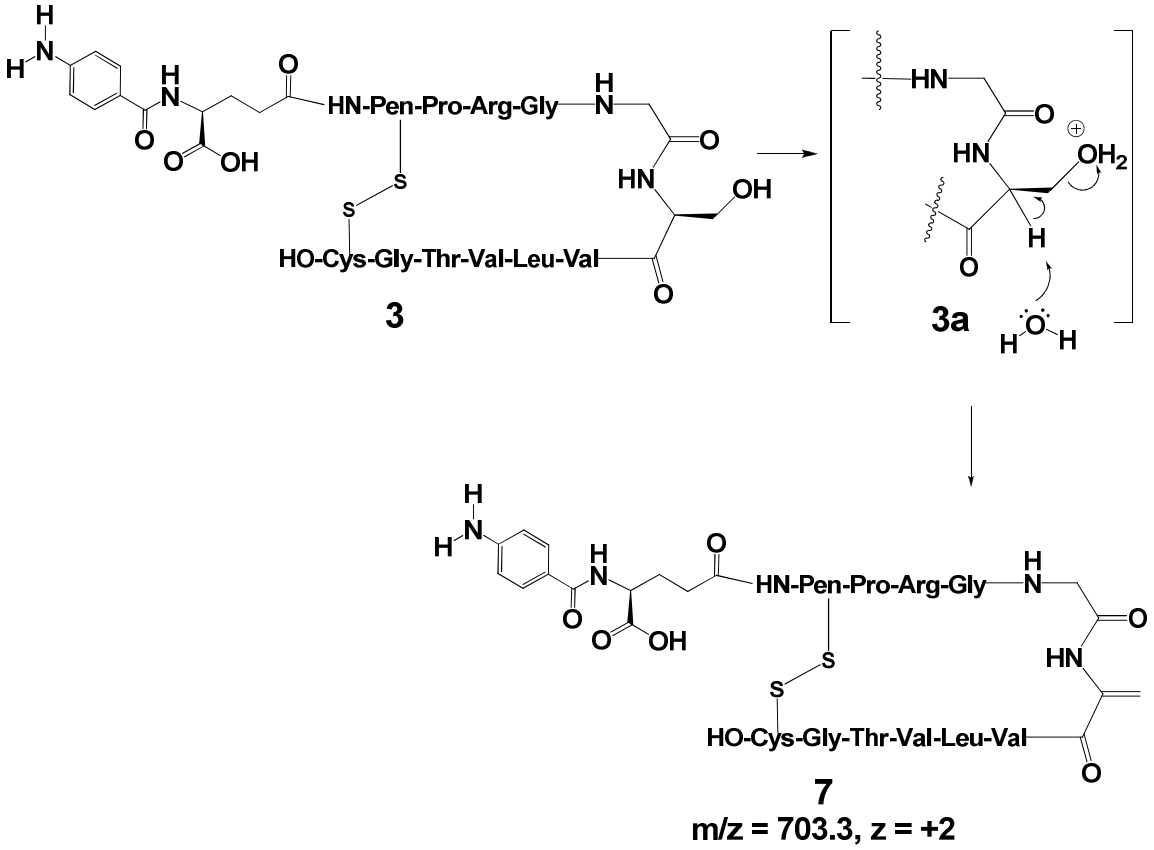

Figure 4.5 The scheme shows the mechanism of degradation of compound **3** to compound **7** via a dehydration reaction at pH 1.0.

4.3.1.2 Degradation of MTX-cIBR at Basic pH Condition

In the basic condition, as expected, the conjugate had the lowest stability at pH 12 ($t_{1/2}$ = 9.29 h, Table 4.1). The degradation characteristics at pH 10 were similar to those of at pH 12; therefore, only the degradation products at pH 12 were identified here. The parent MTX-cIBR showed a single peak before incubation at pH 12; upon incubation at pH 12, four peaks with the same molecular weight (i.e., 805.9, z = +2) appeared in the extracted ion chromatograms (Figures 4.6 and 4.7). These four products can be attributed to different amino acid stereoisomers on the peptide portion of the conjugate (e.g., compound **10**, Figure 4.8). The stereoisomers were generated by a racemization reaction, which occurred at the Ser6 or Thr10 residues. The Ser and Thr residues may undergo dehydration and rehydration reactions to racemize the α-carbon and give a mixture of L-/D-Ser or L-/D-Thr. This hypothesis is supported by the observation of four different dehydrated peaks with m/z 797.4 (z = +2) in the chromatograms (Figure 4.7), which correspond to compounds **8** and **9** and their derivatives (Figure 4.8). These dehydrated products could only be generated from the β-elimination of the hydroxyl group in Ser6 and Thr10 (Figure 4.8).

The dehydrated product **8** could undergo further degradation to form compound **15** (m/z = 721.8, z = +2, Figure 4.9). Compound **15** is a product of a combination of the dehydration reaction, disulfide bond cleavage, and C-terminal amino acid hydrolysis. It is interesting to find that compound **8** undergoes further dehydration to

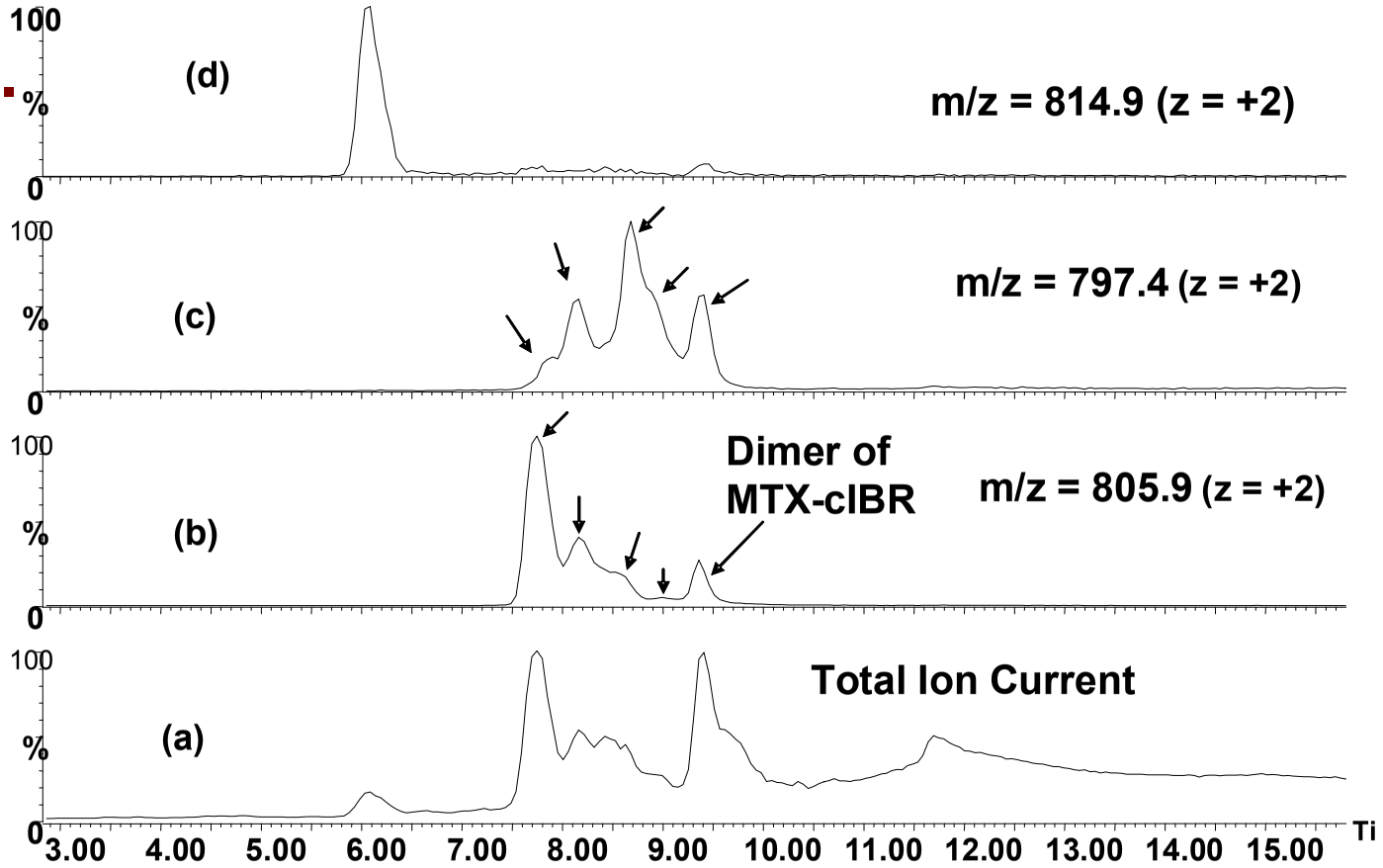

Figure 4.6 The EICs from MS experiments of MTX-cIBR conjugate at pH 12. Panel **(a)** shows the MS chromatogram of MTX-cIBR at pH 12 with the total ion current showing all the compounds together. Panels **(b)**, **(c)** and **(d)** show the EIC of the individual major peaks displayed exclusive of the other peaks. Panel **(b)** shows that there are four different peaks for the m/z value 805.9 (z = +2) with different abundances. In addition, there is also the conjugate dimer identified by its isotopic distribution pattern. All were produced by degradation of the peptide fraction. Panel **(c)** shows that there are different peaks for the dehydrated forms of MTX-cIBR that are tracking the parent conjugate peaks in panel **(b).** Panel **(d)** shows the degradation product of m/z value 814.9 (z = +2) produced by the degradation of the peptide fraction of the conjugate.

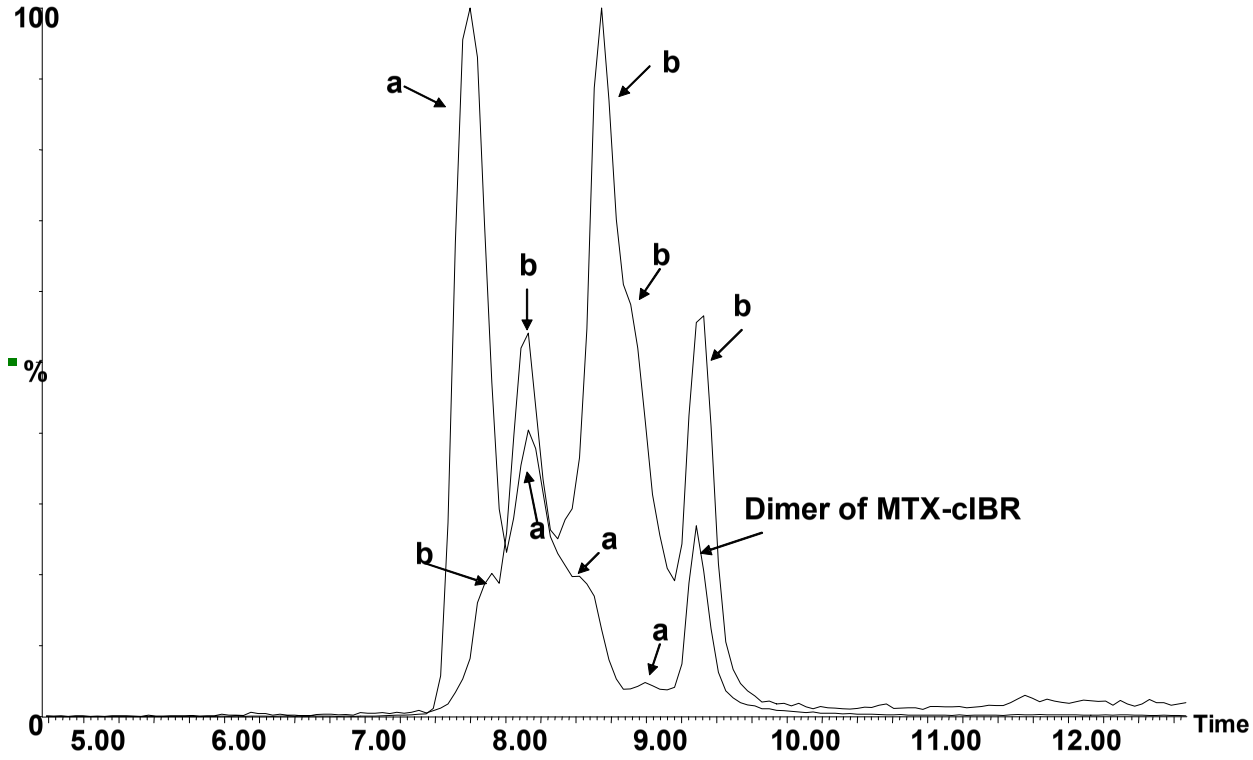

Figure 4.7 Overlay of m/z values 805.9 **(a)** and 797.4 **(b)** showing various forms of the parent molecule and the dehydrated forms. The relative abundances of these species are different. The presence of the dimer form of the MTX-cIBR is indicated in the figure.

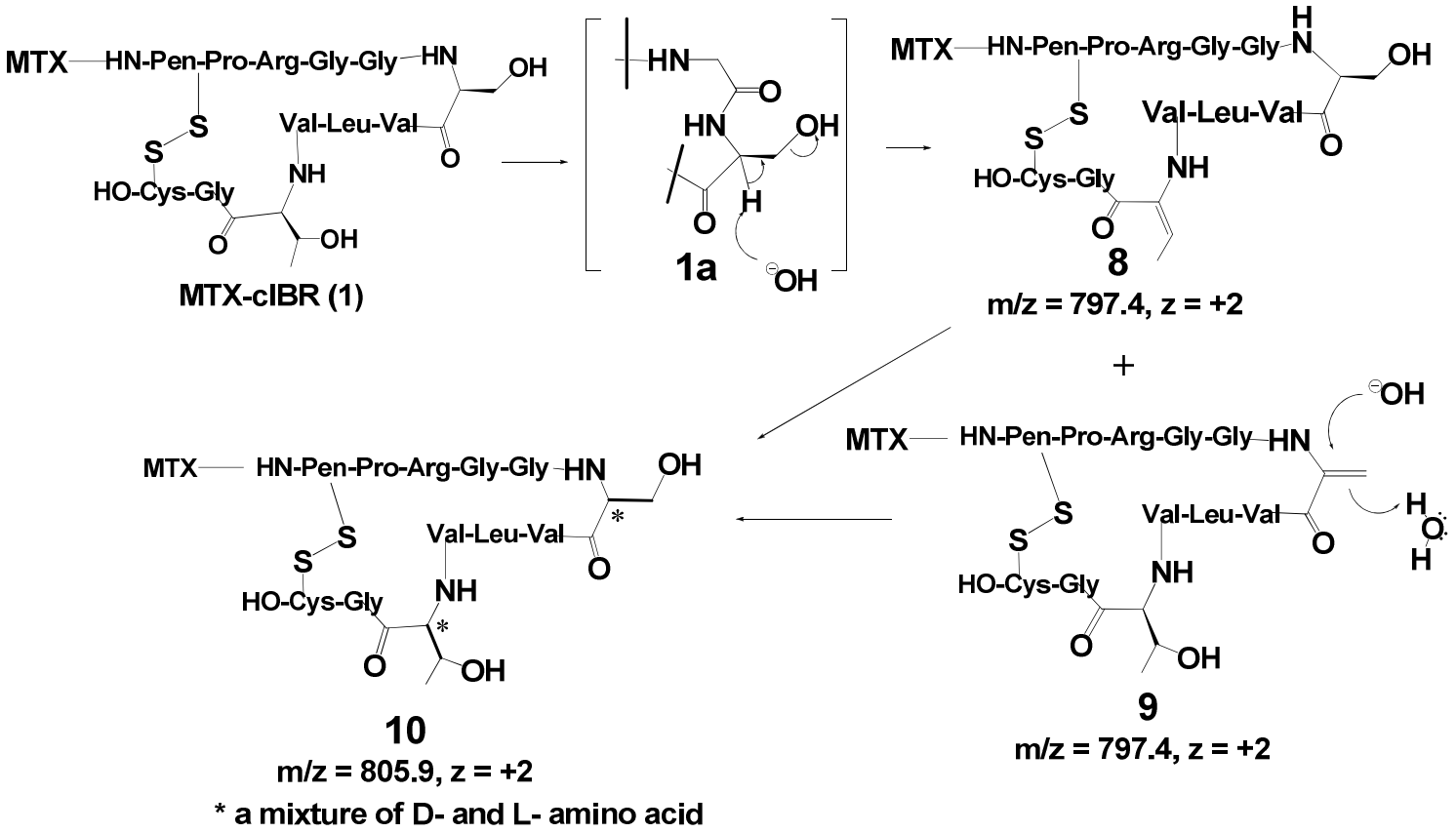

Figure 4.8 Identification of the major degradation products for MTX-cIBR at pH 12. The conjugate can undergo dehydration and racemization at the Ser6 and Thr10 residues. Compounds **8** and **9** are the representative of the dehydration reaction of the Thr10 and Ser6 residues. Subsequent attack by hydroxyl ions to the alkene groups produces the Ser6 and/Thr10 with mixed chirality (L- and D-amino acid) in compound **10**.

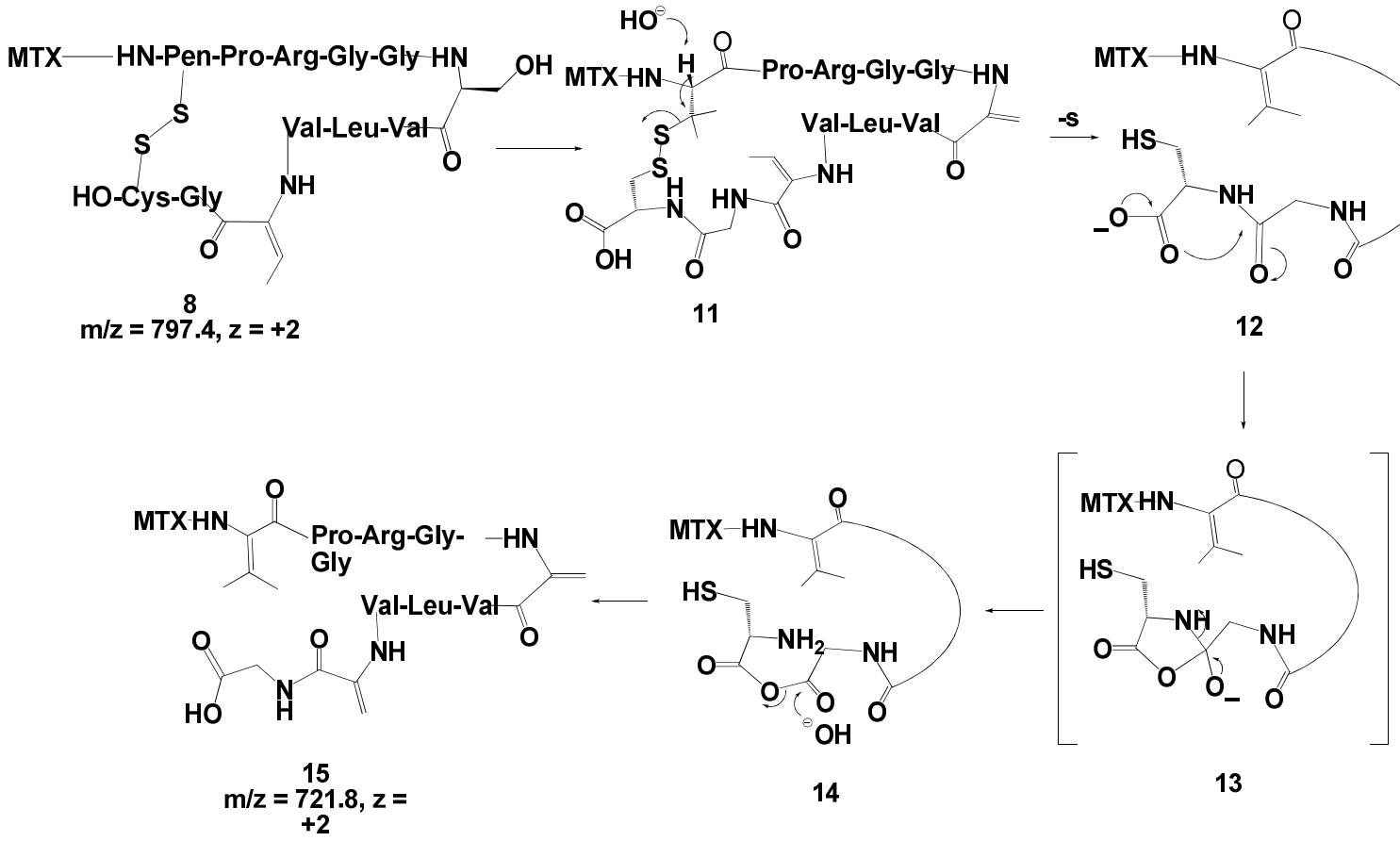

Figure 4.9 The proposed degradation mechanism of MTX-cIBR at the disulfide bond at pH 12. The hydrolysis of the disulfide bond is via β-elimination reaction initiated by attack of a hydroxyl anion on the α-carbon hydrogen of the Pen1 residue followed by ring opening to give intermediate **12**. Further degradation of intermediate 12 releases the Cy12 residue to give compound **15**.

form alkene derivatives at both Ser6 and Thr10 to give intermediate **11**. Further degradation of compound **11** via β-elimination at the Pen1 residue opened the cyclic peptide to give compound **12**. The C-terminal Cys12 was hydrolyzed from the peptide via intermediates **13** and **14** to produce compound **15**. Although it is a minor product, this product supports other observations of the degradation mechanisms of the conjugate.

Another family of products was derived from the degradation of the disulfide bond of the cyclic peptide under basic conditions (Figure 4.10). The attack of the disulfide bond by a hydroxide ion led to the opening of the disulfide bond to form a sulfenic acid and a thiol group. One of two possible products is compound **16** (m/z = 814.9, z = +2); in this case, the sulfenic acid group is at the Pen1 residue. The other possible product is the sulfenic acid group at Cys12. The thiolate group in compound **16** could further react with another molecule at the disulfide bond to give a dimer intermediate **17**. The intramolecular reaction between the thiolate and sulfenic acid groups generated a cyclic dimer **18** with m/z 805.9 and quadruple charges (Figure 4.10).

4.3.1.3 Determination of the pH Rate Profile for MTX-cIBR

To evaluate the overall stability of MTX-cIBR conjugate at various pH values, the pH-rate profile was plotted (Figure 4.11), which can be used to develop a suitable condition for the formulation of this conjugate. The pH-rate profile showed that the

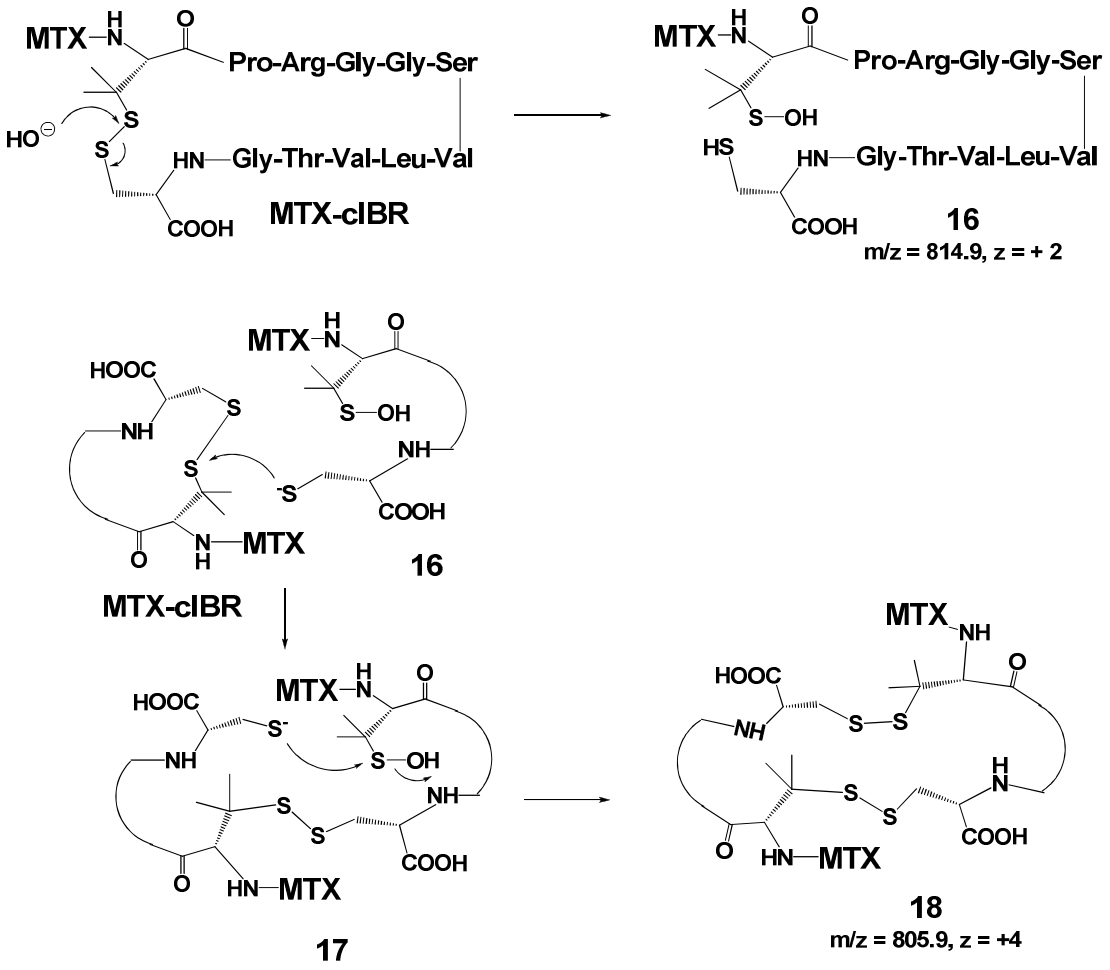

Figure 4.10 The disulfide bond degradation in MTX-cIBR at pH **12** produces thiolate-sulfenic acid **16** and cyclic dimer **17**. The disulfide bond opening is by direct attack of hydroxyl anion on the sulfur of the disulfide bond. Thiolate **16** reacts with another molecule of the conjugate to produce linear dimer **17**; intramolecular reaction of thiolate anion with the sulfur atom of sulfenic acid generates cyclic dimer **18**.

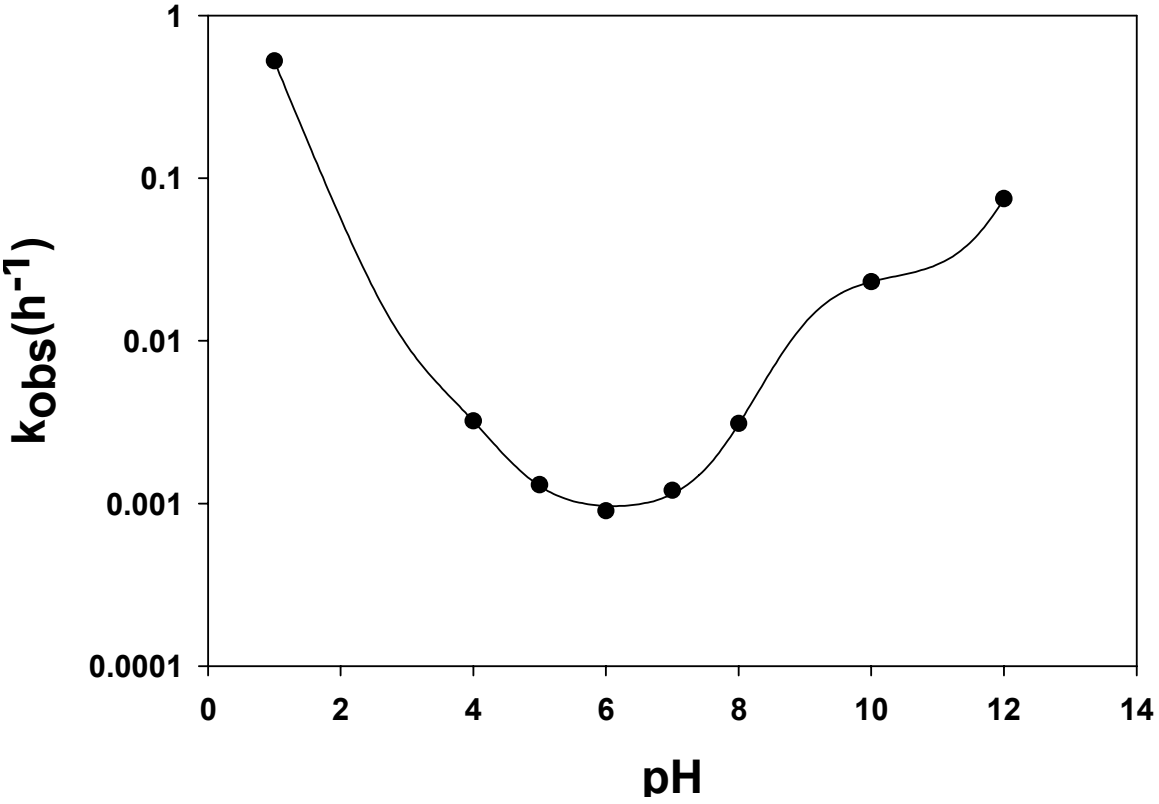

Figure 4.11 pH-rate profile for MTX-cIBR conjugate at 70 °C with buffer concentrations and ionic strength as described in the Table 4.1. Stability of the conjugate was followed at pH values 1, 4, 5, 6, 7, 8, 10 and 12. Maximum stability of the conjugate was observed at pH 6.

conjugate is most stable at pH 6.0 and two inflection points were observed at pH 3.9 and 8.9, which were due to the protonation-deprotonation of the carboxylic acid and amino groups, respectively. This pH-rate profile was constructed with the following assumptions: (a) the ionization of the two carboxylic groups occurs at the same pH, (b) the tertiary amine in the MTX can be neutral or protonated, and (c) the two amino groups on the pteridine ring are considered to be highly unreactive and their contributions are negligible. It has been reported previously that the amines in heterocyclic ring systems of methotrexate, purines, and pyrimidines are highly unreactive.[16] Thus, MTX-cIBR conjugate was treated as a molecule with three ionizable groups (a carboxylic acid, a tertiary amine, and a guanidium group). Because the guanidium group has a pKa of 12.5 and the maximum pH value studied in this experiment was 12, the system was considered to have three species with two different equilibrium constants for the dissociation, as shown in the following equation with K_{a1} and K_{a2} as the equilibrium constants, respectively:

$$H_3A^{2+} \leftrightarrow H_2A^{+} \leftrightarrow HA$$

The overall degradation kinetics for the conjugate are described by the following equation:

$$k_{obs} = (k_H[H^+]f_{H_3A^{2+}}) + (k_O f_{H_3A^{2+}}) + (k'_O f_{H_2A^+}) + (k'_{OH}[OH^-]f_{H_2A^+}) + (k''_{OH}[OH^-]f_{HA})$$

Where,

$$f_{H_3A^{2+}} = \frac{[H^+]^2}{[H^+]^2 + K_{a1}[H^+] + K_{a1}K_{a2}} \qquad f_{H_2A^+} = \frac{K_{a1}[H^+]}{[H^+]^2 + K_{a1}[H^+] + K_{a1}K_{a2}}$$

$$f_{HA} = \frac{K_{a1}K_{a2}}{[H^+]^2 + K_{a1}[H^+] + K_{a1}K_{a2}}$$

The observed rate constant shown below was obtained by substituting the values for the fraction of the individual species.

$$k_{obs} = [1/([H^+]^2 + K_{a1}[H^+] + K_{a1}K_{a2})] * [(k_H[H^+]^3) + (k_O[H^+]^2) + (k'_O K_{a1}[H^+]) + (k'_{OH} K_{a1}K_w) + (k''_{OH} K_w K_{a1}K_{a2}/[H^+])]$$

Because the study was conducted at 70 °C, the value of the ion product of water (pK_w) was calculated using the empirical relationship below.

$$pK_w = (4470.99/T) - 6.0875 + 0.01706T$$
$$= 12.80$$

From the model, the values for the constants were:

$K_{a1} = 1.3 \times 10^{-4}$, $K_{a2} = 1.3 \times 10^{-10}$, $k_H = 5.2 \times 10^6\ M^{-1}hr^{-1}$, $k_O = 0.005\ hr^{-1}$, $k'_O = 0.0009\ hr^{-1}$, $k'_{OH} = 15.6 \times 10^7\ M^{-1}hr^{-1}$, $k''_{OH} = 3.15 \times 10^5\ M^{-1}hr^{-1}$,

where, k_H is the rate constant for acid-catalyzed degradation of H_3A^{2+}, and k'_{OH} and k''_{OH} are the rate constants for the base-catalyzed degradation of H_2A^+ and HA, respectively, as shown above. k_O and k'_O are the rate constants for water-catalyzed degradation of the H_3A^{2+} and H_2A^+ species, respectively.

4.3.2 In Vitro Stability of MTX-cIBR in Plasma and Tissue Homogenate

The stability of MTX-cIBR was evaluated in rat plasma and homogenized rat tissue to determine its biological disposition (Figure 4.12). We found that MTX-cIBR conjugate has half-lives of 43.8 and 38.1 min in rat plasma and homogenized rat heart, respectively (Table 4.2). Clearly, this molecule is rapidly eliminated in the blood upon i.v. injections into the animal model of RA. This may explain the need to deliver a higher dose of the conjugate compared to the drug itself to the animals for suppressing the progress of RA. It is expected that the peptide is rapidly metabolized in plasma. The rapid peptide metabolism could be attributed to the presence of the Arg residue that makes the peptide prone to trypsin digestion. The disulfide bond in the cyclic peptide could be opened by reaction with glutathione in plasma and tissue. In addition, the MTX portion of the molecule could be metabolized to form 2,4-diamino-7-hydroxy-pteridine.[23]

4.4 Discussion

MTX is widely used to treat chronic inflammation in RA; however, due to its toxicity, this drug elicits side effects, including suppression of immune response, liver damage, anemia, and neutropenia. To lower the side effects, MTX has been conjugated to different carriers such as peptides, proteins, and polymers to improve cellular uptake.[24,25] Because RA is characterized by the activation of 'self-reactive' T-cells, it would be ideal to target MTX to activated T cells. Thus, we utilized MTX-cIBR conjugate to target MTX to activated T cells for suppressing the progress of RA

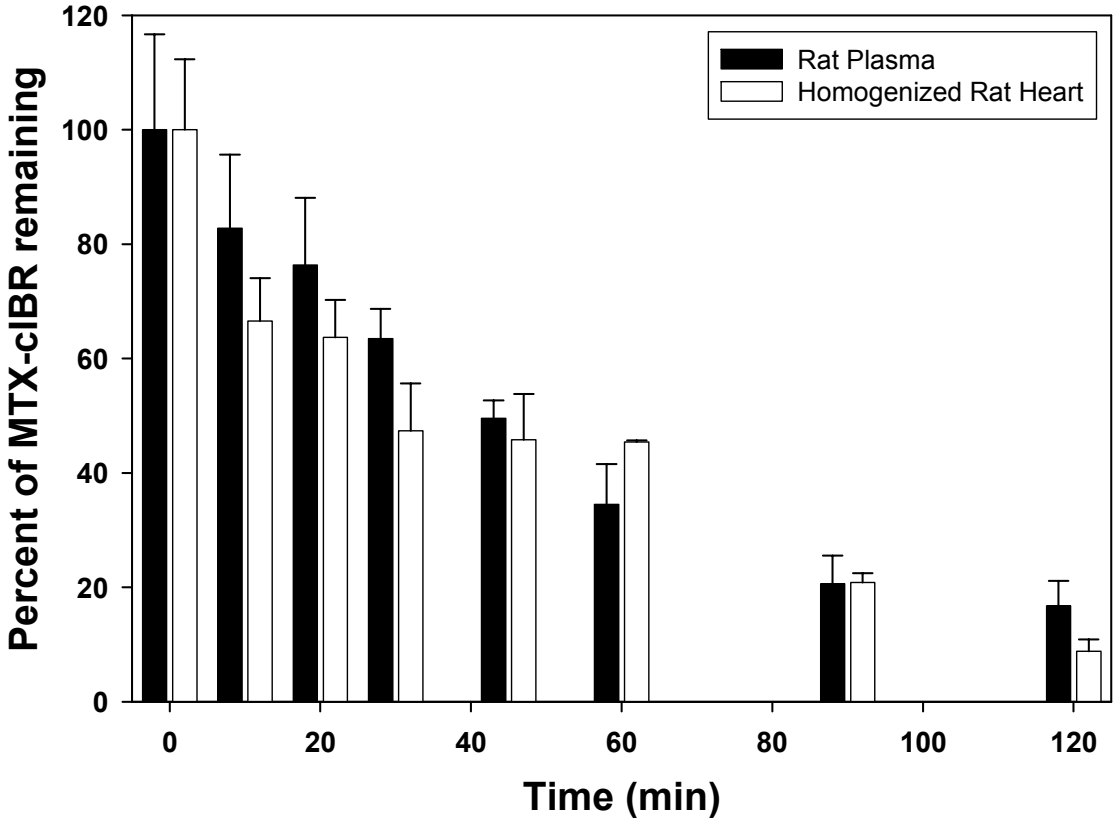

Figure 4.12 Determination of the stability of the MTX-cIBR conjugate with isolated rat plasma and homogenized rat heart tissue. Stability of the conjugate was determined over a 2-h period. Pseudo first-order plots were generated from the degradation profiles. Half-lives and rate constants for degradation are presented in Table 4.2.

Table 4.2 Rate constants and half-lives for MTX-cIBR conjugate with in vitro biological matrices		
Biological Matrix	**Rate constant for degradation (min^{-1})**	**Half-life (min)**
Rat plasma	15.8×10^{-3}	43.8
Homogenized rat heart	18.2×10^{-3}	38.1

in the rat adjuvant animal model. Upon i.v. injection of MTX-cIBR (5 mg/kg) to the rat model, the conjugate suppressed the progress of RA, and the animals had normal synovium and periarticular tissue, articular cartilage, epiphyseal bone, and distal tibia growth plate. In addition, no bone resorption was observed at the physis. In contrast, the adjuvant rats treated with vehicle had severe synovitis and periarticular inflammation due to edema and neutrophil infiltration. In addition, these animals had bone resorption across the physis with the presence of bone fragments. Unfortunately, MTX-cIBR was not effective at 1 mg/kg dose. One possible explanation is that the conjugate is not very stable in the systemic circulation. The presence of glutathione in plasma could cause the opening of the disulfide bond to convert the cyclic peptide to a linear peptide. Finally, the presence of the Arg residue in cIBR peptide makes it prone to proteolytic cleavage of C-terminal peptide bond of the Arg residue by trypsin. Thus, it is necessary to design a conjugate with higher plasma stability in the future.

It is also important to determine the chemical stability of the conjugate for future development of its formulation. Furthermore, degradation mechanisms of the conjugate can be utilized to design more stable molecules. Interestingly, the MTX portion of the conjugate is more prone to degradation in acidic conditions than in basic conditions. There are two degradation pathways of the MTX segment of the conjugate. The first degradation pathway is the release of the pteridine ring from the conjugate (pathway a, Figure 4.3) to give compound **2**. This release is due to the cleavage of the C-N bond between the pteridine ring and the *p*-amino-benzoyl ring.

This reaction is assisted by the presence of the protonated tertiary amine of the *p*-amino-benzoyl group, which acts as a good leaving group. The second major degradation product was produced by demethylation of the phenylamine moiety (pathway b, Figure 4.3) of compound **2** to give compound **3**. A second degradation pathway is the cleavage of the peptide bond connecting the *p*-aminobenzoyl group and the α-amino group of Glu residue in MTX. The reaction was observed during the conversion of degradation product **5** to product **6** (pathway b, Figure 4.4). In this case, the α-carboxylic acid group of the Glu residue of MTX attacks the carbonyl carbon of the *p*-amino-benzoyl group to form a five-membered ring intermediate **5a** (Figure 4.4.). The five-membered ring intermediate **5a** undergoes rearrangement reaction to form anhydride **5b**, which is unstable under acidic conditions to release the *p*-aminobenzoyl group to give compound **6**. Compound **6** is closely related in structure to that of compound **4** (Figure 4.3). We have previously observed a similar anchimeric assistance reaction by the C-terminal carboxylic acid group on the peptide bond hydrolysis in a cyclic pentapeptide.[26]

The major degradation sites for the peptide portion of the conjugate are at the Ser6 and Thr10 residues and at the disulfide bond. The Ser6 and Thr10 residues undergo the N,O-acyl migration reaction followed by peptide bond hydrolysis under acidic conditions. In these conditions, the degradation product **2** degrades to form compound **5** by hydrolysis of the peptide bond between the Gly5 and Ser6 residues. This reaction is initiated by protonation of the carbonyl group of Gly5 (**2a**, Figure 4.4) followed by attack on its carbonyl carbon by the hydroxyl group of Ser6 to form

a five-membered ring cyclic intermediate **2b**. Protonation of the amino group in **2b** followed by the ring opening, which produces ester intermediate **2c** as the N,O-acyl migration reaction product. Ester **2c** can be hydrolyzed under acidic conditions to form acid and alcohol that separate Gly5 and Ser6 to yield degradation product **5**.

The Ser6 and Thr10 residues also degrade via β-elimination under both acidic and basic conditions. When the conditions are acidic, the conjugate degrades via compound **3** followed by β-elimination reaction to produce compound **7** (Figure 4.5). This reaction proceeds via intermediate **3a** in which the hydroxyl group of Ser6 is protonated, followed by nucleophilic attack of the α-carbon-associated hydrogen of Ser6 to release a water molecule; this produces the dehydroalanine at position 6 (dehydro-Ala6) in compound **7**. A dehydration reaction could also occur at the Thr10 residue; at this time, we cannot distinguish at which residue the dehydration reaction occurred. In basic conditions, the dehydration reaction is also observed as the major degradation pathway of the peptide segment. After incubation in basic conditions, four peaks with the same molecular weight as the parent conjugate were observed (Figures 4.6 and 4.7). These compounds are due to the racemization at the α-carbon of Ser6 and Thr10 to give four possible conjugates with (1) L-Ser6 and L-Thr10 (the parent compound), (2) L-Ser6 and D-Thr10, (3) D-Ser and L-Thr10, and (4) D-Ser6 and D-Thr10. Racemization of the Ser residue in peptides has been observed previously in RS-26306 decapeptide and the LHRH analog histrelin.[27,28] The mechanism of racemization is supported by the presence of four different dehydration products of the conjugate (Figures 4.6 and 4.7). The dehydration products are

generated by abstraction of the α-carbon hydrogen of Ser6 and Thr10 (**1a**, Figure 4.8) followed by release of the hydroxyl anion to produce dehydro-Ala6 (compound **9**) and β-methyldehydroalanine10 (β-Me-dehydro-Ala10, compound **8**), respectively. The rehydration of the alkene group produces the racemic mixture of at Ser6 and/or Thr10. Thus, the four dehydration products are due to the presence of the following amino acids at positions 6 and 10: (1) L-Ser6 and β-Me-dehydro-Ala10, (2) D-Ser6 and β-Me-dehydro-Ala10, (3) dehydro-Ala6 and L-Thr10, and (4) dehydro-Ala6 and D-Thr10. It was not possible to identify each of these peaks individually due to the lack of separation and their co-elution with the dimer products. Our attempts to improve the separation of these molecules were unsuccessful. In addition, the fragmentation of the dehydrated species failed to yield additional information because the 6-methylpteridine-2,4-diamine ring carried most of the ion current that led to the suppression of the signal from the peptide fragments.

Another major degradation pathway of the peptide segment is via the β-elimination reaction at the Pen1 and Cys12 residues and the direct attack of the sulfur atom of the disulfide bond by hydroxide ion. The β-elimination reaction was observed in the further degradation of compound **8** to give compound **15**. During the degradation process, compound **8** is converted to compound **11** by a dehydration reaction. The abstraction of the proton from the α-carbon of Pen1 in compound **11** followed by sulfur atom extrusion generates compound **12** with the dehydro-β-dimethyl-Ala residue at position 1. It is interesting that the Cys12 residue is cleaved from compound **12**. We propose that this cleavage reaction takes place through the

formation of cyclic intermediate **13** that rearranges to form anhydride **14**, which is unstable under basic conditions. The anhydride is then rapidly hydrolyzed to give the degradation product **15**.

Finally, the disulfide bond can be cleaved directly by hydroxide ion to produce thiolate-sulfenic acid **15**, and this type of reaction has been observed previously in cyclic peptides.[26,29] The thiolate anion can attack a disulfide bond in another molecule of conjugate to produce a linear dimer **17**. The intramolecular reaction of the thiolate ion on the sulfur of sulfenic acid generates the cyclic dimer 18 and releases hydroxyl anion.

The fact that MTX-cIBR is most stable at pH 6.0 is advantageous for formulation development of the conjugate as it is close to the physiological pH (pH 7.4). Peptides and proteins with higher stability in highly acidic or alkaline pH often present a challenge in formulation development. Indications that MTX-cIBR is somewhat unstable in the presence of biological matrices combined with the identification of the chemical degradation mechanisms will help to design a more stable conjugate. Identification of the *in vivo* degradation products along with the pharmacokinetic profile will be evaluated in the future.

4.5 Conclusions

In this work, we have shown that the optimal chemical stability of MTX-cIBR conjugate occurs at pH 6.0. The major degradation mechanisms under acidic conditions involve the MTX fragment. In contrast, the major degradation mechanisms under basic conditions involve the Ser6 and Thr10 and the disulfide bond in the

peptide segment of the conjugate. The conjugate has short half-lives in plasma and tissue homogenates. These results explain why the conjugate is not effective when delivered in low doses *in vivo*. Therefore, there is a need to optimize the stability of the peptide in biological media. The effort to design more stable molecules is underway. .

4.6 References

1. Yusuf-Makagiansar H, Anderson ME, Yakovleva TV, Murray JS, Siahaan TJ 2002.Inhibition of LFA-1/ICAM-1 and VLA-4/VCAM-1 as a therapeutic approach to inflammation and autoimmune diseases. Med Res Rev 22(2):146-167.

2. Yusuf-Makagiansar H, Makagiansar IT, Hu Y, Siahaan TJ 2001.Synergistic inhibitory activity of alpha- and beta-LFA-1 peptides on LFA-1/ICAM-1 interaction. Peptides 22(12):1955-1962.

3. Yusuf-Makagiansar H, Makagiansar IT, Siahaan TJ 2001.Inhibition of the adherence of T-lymphocytes to epithelial cells by a cyclic peptide derived from inserted domain of lymphocyte function-associated antigen-1. Inflammation 25(3):203-214.

4. Tibbetts SA, Seetharama Jois D, Siahaan TJ, Benedict SH, Chan MA 2000.Linear and cyclic LFA-1 and ICAM-1 peptides inhibit T cell adhesion and function. Peptides 21(8):1161-1167.

5. Tibbetts SA, Chirathaworn C, Nakashima M, Jois DS, Siahaan TJ, Chan MA, Benedict SH 1999.Peptides derived from ICAM-1 and LFA-1 modulate T cell adhesion and immune function in a mixed lymphocyte culture. Transplantation 68(5):685-692.

6. Anderson ME, Siahaan TJ 2003.Mechanism of binding and internalization of ICAM-1-derived cyclic peptides by LFA-1 on the surface of T cells: a potential method for targeted drug delivery. Pharm Res 20(10):1523-1532.

7. Gursoy RN, Siahaan TJ 1999.Binding and internalization of an ICAM-1 peptide by the surface receptors of T cells. J Pept Res 53(4):414-421.

8. Anderson ME, Tejo BA, Yakovleva T, Siahaan TJ 2006.Characterization of binding properties of ICAM-1 peptides to LFA-1: inhibitors of T-cell adhesion. Chemical biology & drug design 68(1):20-28.

9. Zimmerman T, Oyarzabal J, Sebastian ES, Majumdar S, Tejo BA, Siahaan TJ, Blanco FJ 2007.ICAM-1 peptide inhibitors of T-cell adhesion bind to the allosteric site of LFA-1. An NMR characterization. Chemical biology & drug design 70(4):347-353.

10. Majumdar S, Kobayashi N, Krise JP, Siahaan TJ 2007.Mechanism of internalization of an ICAM-1-derived peptide by human leukemic cell line HL-60: influence of physicochemical properties on targeted drug delivery. Mol Pharm 4(5):749-758.

11. Gorlick R, Goker E, Trippett T, Waltham M, Banerjee D, Bertino JR 1996.Intrinsic and acquired resistance to methotrexate in acute leukemia. New Engl J Med 335(14):1041-1048.

12. Pui CH 1995.Childhood leukemias. New Engl J Med 332(24):1618-1630.

13. Andersson SE, Johansson LH, Lexmuller K, Ekstrom GM 2000.Anti-arthritic effect of methotrexate: is it really mediated by adenosine? Eur J Pharm Sci 9(4):333-343.

14. Williams HJ, Willkens RF, Samuelson CO, Jr., Alarcon GS, Guttadauria M, Yarboro C, Polisson RP, Weiner SR, Luggen ME, Billingsley LM, et al. 1985.Comparison of low-dose oral pulse methotrexate and placebo in the treatment of rheumatoid arthritis. A controlled clinical trial. Arthritis Rheum 28(7):721-730.

15. Westerhof GR, Rijnboutt S, Schornagel JH, Pinedo HM, Peters GJ, Jansen G 1995.Functional activity of the reduced folate carrier in KB, MA104, and IGROV-I cells expressing folate-binding protein. Cancer Res 55(17):3795-3802.

16. Kuefner U, Lohrmann U, Montejano Y, Vitols KS, Huennekens FM 1988.Chemotherapeutic potential of methotrexate peptides. Adv Enzyme Regul 27:3-13.

17. van der Heijden JW, Dijkmans BA, Scheper RJ, Jansen G 2007.Drug Insight: resistance to methotrexate and other disease-modifying antirheumatic drugs--from bench to bedside. Nature clinical practice 3(1):26-34.

18. Wolff D, Frei E, Hofmeister N, Steiner B, Kleine HD, Junghanss C, Sievert K, Terpe H, Schrenk HH, Freund M, Hartung G 2006.Methotrexate-albumin and aminopterin-albumin effectively prevent experimental acute graft-versus-host disease. Transplantation 82(4):527-533.

19. Fiehn C, Muller-Ladner U, Gay S, Krienke S, Freudenberg-Konrad S, Funk J, Ho AD, Sinn H, Wunder A 2004.Albumin-coupled methotrexate (MTX-HSA) is a new anti-arthritic drug which acts synergistically to MTX. Rheumatology 43(9):1097-1105.

20. N'Da DD, Neuse E, Nell M, Van Rensburg CEJ 2006.Carrier-bound Methotrexate. III. Antiproliferative Activity of Macromolecular MTX Conjugates Against the Human HeLa and Colo Carcinoma Cell Lines. S Afr J Chem 59:33-42.

21. Gurdag S, Khandare J, Stapels S, Matherly LH, Kannan RM 2006.Activity of Dendrimer-Methotrexate Conjugates on Methotrexate-Sensitive and -Resistant Cell Lines. Bioconj Chem 17(2):275-283.

22. Anderson ME. 2003. Utilization of ICAM-1 derived peptides for targeted drug delivery to T-cells. Pharmaceutical Chemistry, ed., Lawrence: University of Kansas.

23. Dhondt JL, Hayte JM, Millot F, Klein R, Blais JC, Pfleiderer W 1991.2,4-diamino-7-hydroxy-pteridines, a new class of catabolites of methotrexate. Eur J Biochem 200(1):237-244.

24. Ryser HJ, Shen WC 1978.Conjugation of methotrexate to poly(L-lysine) increases drug transport and overcomes drug resistance in cultured cells. Proc Natl Acad Sci USA 75(8):3867-3870.

25. Shen WC, Ryser HJ, LaManna L 1985.Disulfide spacer between methotrexate and poly(D-lysine). A probe for exploring the reductive process in endocytosis. J Biol Chem 260(20):10905-10908.

26. He HT, Gursoy RN, Kupczyk-Subotkowska L, Tian J, Williams T, Siahaan TJ 2006.Synthesis and chemical stability of a disulfide bond in a model cyclic pentapeptide: cyclo(1,4)-Cys-Gly-Phe-Cys-Gly-OH. J Pharm Sci 95(10):2222-2234.

27. Avis KE, Lieberman HA, Lachman L, edited. 1992. Pharmaceutical Dosage Forms: Parenteral Medications. 2nd ed., New York: M. Dekker. p 295.

28. Oyler AR, Naldi RE, Lloyd JR, Graden DA, Shaw CJ, Cotter ML 1991.Characterization of the solution degradation products of histrelin, a gonadotropin releasing hormone (LH/RH) agonist. J Pharm Sci 80(3):271-275.

29. Bogdanowich-Knipp SJ, Chakrabarti S, Williams TD, Dillman RK, Siahaan TJ 1999.Solution stability of linear vs. cyclic RGD peptides. J Pept Res 53(5):530-541.

Chapter 5

Summary, conclusions and future directions

5.1 Summary and Conclusions

The objective of this work was to explore the possibility of selectively delivering cytotoxic drugs to leukocytes using intercellular adhesion molecule-1 (ICAM-1)-derived cyclic peptides. Peptides derived from the D1 domain of ICAM-1 inhibited the ICAM-1/LFA-1 (leukocyte function associated antigen-1)-mediated heterotypic T-cell adhesion.[1] Among these peptides, cIBR peptide [cyclo(1,12)PenPRGGSVLVTGC] showed binding affinity to the LFA-1 receptor, and this binding was inhibited by anti-LFA-1 antibody.[2] Further, FITC-cIBR showed temperature-dependent internalization properties with MOLT-3 T-cells.[3] Interaction of cIBR peptide with its target receptor and subsequent internalization offered an attractive pathway to deliver drugs to leukocytes. This approach is advantageous for delivering highly toxic anticancer drugs such as doxorubicin (DOX), which enters the cells in a non-specific manner.[4] Drugs such as methotrexate (MTX) use ubiquitously expressed transporters like membrane folate binding protein (mFBP) and reduced folate carrier (RFC) to enter the cells; thus, MTX has side effects because it can also cause damage to the normal cells in the body.[5] Conjugation of MTX to a carrier molecule like cIBR peptide may allow it to be selectively delivered to LFA-1 expressing cells such as leukocytes.

In this work, cIBR peptide was conjugated to FITC and DOX via the N-terminal of the peptide. FITC-labeled cIBR (FITC-cIBR) showed punctate fluorescence stains inside the HL-60 (human leukemic promyelocytic cell line) cells, whereas DOX-labeled cIBR (DOX-cIBR) showed diffuse distribution throughout the

cell cytosol. Comparison of internalization was done through a) temperature-dependent internalization, b) inhibition of ATP synthesis processes using sodium azide and 2-deoxy-D-glucose and c) disruption of microtubules using nocodazole. All these studies showed that FITC-cIBR entered the HL-60 cells by an endocytic uptake pathway in an energy-dependent manner, whereas DOX-cIBR entered via an energy-independent pathway. DOX-cIBR (distribution ratio 14.1, pH 7.4) was found to be much more hydrophobic than FITC-cIBR (distribution ration 3.8, pH 7.4). The hydrophobicity of the DOX-cIBR conjugate was proposed to be one of the major reasons for its energy-independent cellular entry.[6]

As the hydrophobicity of the DOX-cIBR conjugate was proposed to be responsible for the energy-independent cellular entry into HL-60 cells, efforts were focused on understanding the contribution of this particular physicochemical property in the internalization process of the DOX-peptide conjugates. Thus, a more hydrophilic derivative of cIBR called cIBR7 (cyclo(1,8)CPRGGSVC) was used to deliver DOX and FITC molecules. cIBR7 peptide has higher binding affinity to I-domain of LFA-1 than the parent cIBR.[1] To further increase the hydrophilicity of the conjugate, a hydrophilic spacer (i.e., 11-amino-3,6,9-trioxaundecanoate) was used to link DOX to cIBR7 to produce DOX-PEGcIBR7. Octanol/aqueous buffer distribution ratios of DOX-cIBR7 and DOX-PEGcIBR7 showed that these conjugates were more hydrophilic than the parent DOX-cIBR. However, the DOX-cIBR7 and DOX-PEGcIBR7 conjugates still entered the HL-60 cells in an energy-independent manner similar to that of DOX-cIBR. Both DOX-cIBR7 and DOX-PEGcIBR7 showed

diffuse cytoplasmic fluorescence distribution pattern indicative of a non-endocytic uptake pathway. This suggests that even though hydrophobicity of the conjugate is an important property for cellular internalization, it is not the only reason for DOX-peptide conjugate entry by passive diffusion. In contrast, FITC-labeled cIBR7 (FITC-cIBR7) utilized the energy-dependent endocytic uptake mechanism. These results suggest that the entry of DOX-cIBR and its derivatives into the cell cytosol was due to the properties of DOX and not to the properties of the peptide.

To gain an insight into the endocytic migration pathway of FITC-cIBR and FITC-cIBR7 peptides inside the cell, colocalization studies were performed with fluorophore-conjugated dextran molecules. The colocalization studies showed that the both FITC-cIBR and FITC-cIBR7 followed an endocytic pathway somewhat different compared to that of dextran. Dextran molecules are known to travel through the endosomes to end up in the lysosome.[7] Lack of colocalization indicates that it might take longer than 1 h for the peptide molecules to enter the lysosome compartment. It might also indicate that the final cellular destination for these peptides is not the lysosome. This information could be used for further studying intracellular sequestration of these peptides to generate an efficient drug-peptide conjugate for intracellular release of the drug.

The methotrexate conjugate of cIBR peptide (MTX-cIBR) was synthesized by conjugating the γ-carboxylic acid of methotrexate to the N-terminal of cIBR peptide by amide bond. MTX-cIBR retained the binding affinity to the target receptor (i.e., LFA-1).[8] This conjugate also inhibited the progression of rheumatoid arthritis in the

rat adjuvant model. However, in order to be effective the conjugate had to be administered at a relatively high dose (5 mg/kg). The need to deliver a high dose of the conjugate in the *in vivo* system may be due to the instability of the conjugate in the systemic circulation. In addition, for optimizing the formulation of the conjugate, it is necessary to evaluate the chemical stability of MTX-cIBR. The accelerated chemical stability analysis of MTX-cIBR showed that MTX-cIBR conjugate was most stable at pH 6.0. The drug portion of the conjugate was unstable under the acidic conditions, while the peptide portion was unstable under the basic conditions. In acidic conditions, the major degradation product was generated by cleaving the C-N bond between the pteridine ring and the *p*-aminobenzoyl ring. Dehydration of the Ser6 and Thr10 residues along with the racemization produced the major degradation products in highly basic conditions. Disulfide bond exchange, disulfide hydrolysis, and β-elimination were the major degradation reactions in basic conditions. The half-lives of the conjugate were 38.1 min with isolated rat plasma and 43.8 min with homogenized rat heart tissue, suggesting that this is one of the reasons for the high dose needed to produce its activity *in vivo*. It is encouraging to find that MTX-cIBR did not produce undesirable side effects *in vivo,* even at higher doses. In the future, it is necessary to design conjugates that are more potent and stable in *in vivo* systems.

5.2 Future Directions

5.2.1 Delivery of DOX using cIBR and cIBR7 Peptides

Delivery of DOX has been found to be challenging using peptides and proteins. Properties of DOX (i.e., aqueous aggregation) may affect the behavior of the conjugate.[4] It is possible that it is difficult to deliver DOX using DOX-peptide conjugates irrespective of the nature of the conjugates. One possible way to deliver DOX may be protecting the drug in liposomes or nanoparticles that have been decorated with targeting peptides such as cIBR. This will ensure that DOX will enter the cells encapsulated in these particles and will not influence the selectivity of the particle delivery. We have not explored the possibility of conjugating the DOX molecule to the C-terminal cIBR peptide and its derivatives. This conjugation method may improve the recognition of the peptide segment by the LFA-1 receptor on leukocytes because the N-terminal PRGG sequence is the recognition site of the peptide.

5.2.2 Delivering Other Hydrophilic, Cytotoxic Drugs using cIBR and cIBR7

Thus far, DOX and MTX have been conjugated to the cIBR peptide while only DOX has been conjugated to cIBR7 peptide. Other cytotoxic drugs can be conjugated to these peptides to evaluate the general applicability of these peptides for targeted drug delivery. In an attempt to evaluate other drug-cIBR conjugates, melphalan has been conjugated to cIBR peptide to give Mel-cIBR. Unfortunately, Mel-cIBR conjugate was found to be highly insoluble, which precluded its use for further studies. Thus, it is important to obtain a balance between physicochemical properties and biological activity of the conjugate for its applicability in the clinical

setting. Currently, our group is exploring the effect of drug properties on the conjugate selectivity to leukocytes.

5.2.3 Understanding the Intracellular Metabolism of FITC-cIBR and FITC-cIBR7

FITC-cIBR and FITC-cIBR7 peptides have been found to be internalized by HL-60 cells via an endocytic uptake pathway. Colocalization studies have shown that FITC-cIBR and FITC-cIBR7 followed an endocytic pathway somewhat different compared to that for dextran inside the cells. Dextran is known to localize into lysosomes inside the cells. Identification of the compartment for intracellular localization of these peptides and subsequent compartment isolation will allow the identification of the possible intracellular metabolic products. The identification the metabolic product of the conjugate can be used design a better conjugate that would release the drug at the appropriate site(s) in the intracellular space.

5.2.4 Exploring the Possibility of Drug Delivery to Multidrug-Resistant Cells by using cIBR and cIBR7 Peptides

Overexpression of efflux transporters is one of the causes of drug resistance in cancer cells. Among these efflux transporters, permeability glycoprotein (Pgp) is the most widely studied. These transporters contribute to the difficulty of delivering cytotoxic drugs to the resistant cancer cells. Moreover, these transporters have an extremely diverse array of substrate specificity. Therefore, any approach to bypass

these transporters to enter the cell will be of tremendous value in cancer therapy. For this purpose, cIBR and cIBR7 peptides can be used to avoid the efflux pump for delivering cytotoxic drugs to cancer cells. Therefore, we have conjugated a Pgp substrate (i.e., rhodamine) to cIBR peptide to give Rho-cIBR. In the future, the mechanism of uptake of this conjugate may shed light on the ability of the conjugate to avoid Pgp-mediated efflux. Comparison of the internalization of Rho-cIBR to that of rhodamine in the Pgp-expressing leukemic cell line will provide information on the ability of the conjugate to evade the efflux transporters.

5.3 References

1. Anderson ME, Yakovleva T, Hu Y, Siahaan TJ 2004.Inhibition of ICAM-1/LFA-1-mediated heterotypic T-cell adhesion to epithelial cells: design of ICAM-1 cyclic peptides. Bioorg Med Chem Lett 14(6):1399-1402.

2. Anderson ME, Siahaan TJ 2003.Mechanism of binding and internalization of ICAM-1-derived cyclic peptides by LFA-1 on the surface of T cells: a potential method for targeted drug delivery. Pharm Res 20(10):1523-1532.

3. Gursoy RN, Siahaan TJ 1999.Binding and internalization of an ICAM-1 peptide by the surface receptors of T cells. J Pept Res 53(4):414-421.

4. Dalmark M, Storm HH 1981.A Fickian diffusion transport process with features of transport catalysis. Doxorubicin transport in human red blood cells. J Gen Physiol 78(4):349-364.

5. Westerhof GR, Rijnboutt S, Schornagel JH, Pinedo HM, Peters GJ, Jansen G 1995.Functional Activity of the Reduced Folate Carrier in KB, MA104, and IGROV-I Cells Expressing Folate-binding Protein. Cancer Res 55(17):3795-3802.

6. Majumdar S, Kobayashi N, Krise JP, Siahaan TJ 2007.Mechanism of internalization of an ICAM-1-derived peptide by human leukemic cell line HL-60: influence of physicochemical properties on targeted drug delivery. Mol Pharm 4(5):749-758.

7. Baravalle G, Schober D, Huber M, Bayer N, Murphy RF, Fuchs R 2005.Transferrin recycling and dextran transport to lysosomes is differentially affected by bafilomycin, nocodazole, and low temperature. Cell Tissue Res 320(1):99-113.

8. Anderson ME. 2003. Utilization of ICAM-1 derived peptides for targeted drug delivery to T-cells. Pharmaceutical Chemistry, ed., Lawrence: University of Kansas.